A Tale of Two Deaths:

Interferon Regulated Necroptosis

and

Caspase 8 Driven Pyroptosis

A thesis submitted by

Joseph Sarhan

in partial fulfillment of the requirements for the degree of

Ph.D.

in

Immunology

Tufts University

Graduate School of Biomedical Sciences

May 2020

Advisor: Alexander, Poltorak, Ph.D.

Abstract

Cell death and inflammation are intimately linked during host defense against invading pathogens. The most well studied forms of cell death include apoptosis, necroptosis and pyroptosis. In this thesis we studied the intersection of these forms of cell death. In our first study entitled “Constitutive Interferon Signaling Maintains Critical Threshold of MLKL Expression to License Necroptosis” we explore the role of type-I IFN in necroptosis. Recently, lipopolysaccharide (LPS)-induced IFN was implicated as a driver of necroptosis, a necrotic form of cell death downstream of receptor interacting protein (RIP) kinase activation and executed by mixed lineage kinase like-domain (MLKL) protein. We found that the pre-established IFN status of the cell, instead of LPS-induced IFN, is critical for the early initiation of necroptosis in macrophages. This pre-established IFN signature stems from cytosolic DNA sensing via cGAS /STING, and maintains the expression of MLKL and one or more unknown effectors above a critical threshold to allow for MLKL oligomerization and cell death. Finally, we found that elevated IFN-signaling in systemic lupus erythematosus (SLE) augments necroptosis, providing a link between pathological IFN and tissue damage during autoimmunity. In our second study entitled “Caspase-8 induces cleavage of multiple Gasdermins to elicit pyroptosis during Yersinia infection” we focus on cell death induced in the context of mitogen-activated protein kinase (MAPK) inhibition. using Yersinia pseudotuberculosis in corroboration with a simplified stimulation of lipopolysaccharide and (5Z)-7-Oxozeaenol, a small molecule inhibitor of TAK1, we show that caspase-8 activation during TAK1 inhibition leads to cleavage of both GsdmD and GsdmE in murine macrophages, resulting in pyroptosis. Loss of GsdmD delays membrane rupture,

reverting the cell death morphology to apoptosis. We found that Yersinia driven IL-1 response arises from asynchrony of macrophage death during bulk infections, and that two cellular populations are required to provide signal 1 and signal 2 for IL-1β release. Furthermore, we found that human macrophages are resistant to YopJ mediated pyroptosis, resulting in an immunologically silent infection. Ultimately, our results uncover a form of caspase-8 mediated pyroptosis and provide a plausible explanation for the increased sensitivity of humans to Yersinia infection as compared to the rodent reservoir.

Dedication

To all the mice that lost their lives for this work

Acknowledgments

Thinking back to the first-year version of myself, I find it hard to recognize any similarities. I had no idea what it meant to be a scientist at the start of graduate school. I was excited by the technical aspect of doing science but gave very little thought to experimental design, biological significance or novelty. That all changed very quickly and was re-enforced by several key mentors and peer including: Sasha Poltorak, Brigitte Huber, David Thorley-Lawson and Steve Bunnell.

By now Sasha knows me as well as my mother, all of my strengths and weaknesses. He always stood by me even when he thought I was wrong or acted irresponsibly. I have never known a scientist so devoted to the lab, work and experiments. Sasha and I struggled through publishing our first paper together in a process that started under review in Immunity in January 2017 and concluding with an acceptance at Cell Death and Differentiation in March of 2018. I started working on TAK1 induced cell death as a distraction during the long review process of the necroptosis paper. Sasha even supported me as it started to look like I was abandoning my necroptosis paper in favor of TAK1. I always overestimated my capacity to multitask and fell short on deadlines countless times. Still, Sasha always supported me, spending a non-proportional amount of time and money on my projects. There was never a collaborator, reagent, mouse or instrument that I needed which went un-fulfilled. In this way, I have been incredibly spoiled, and I am sure to have quite an adjustment for my next lab experience. I still have a lot to learn from Sasha and look forward to our continued interaction for years to come.

Steve, Brigitte and David were also critical for my development. Steve is the most knowledgeable scientist I know. His understanding of innate immunity and cell death is beyond many people actively publishing in that area. Brigitte was the first person to show me how to dissect a paper in her class and pushed me to think about science. She provided an example of a very strong and independent person who never had any interest in nonsense and always in action mode. I was fortunate to be able to collaborate with Brigitte and her student Chi Weindel on the connection we discovered between autoimmunity and necroptosis. This helped elevate the impact of our work tremendously and I learned a great deal from them! David was another critical mentor and I learned a great deal from our interactions, which started with the qualifying exam. When we were first meeting about the qualifying exam, I thought there was no pleasing him. I never read enough or had an idea that could impress him. He could poke holes in everything I suggested without even batting an eye. I foolishly thought I could get by with my usual minimal effort, which had worked wonderfully in the past. I was comparing my ideas relative to provided examples and concluded I had done an adequate job, but David saw right through this and pushed me to work to my full potential. We spent months fighting over the qualifying exam and by the time we had finished, I had begun my transformation into a scientist. He always asked the most insightful questions, not to hear himself talk, but out of genuine interest. David once asked me why in a population of cells treated with LPS+ zVAD, there are resistant and sensitive cells. I had no idea at the time, but after four years of work, I finally have the start of an answer presented in this thesis.

Of course, I have to thank the rest of my committee members Caroline Genco, Bree Aldridge and Ananda Roy who always made time to meet and give who have been

though countless meetings and seen more data than they would care to admit. The contributions of my committee members are evident in the discussion section of the thesis. The MD PhD program including Naomi Rosenberg, Jim Schwob and Gordon Huggins who accepted me into the program and always being supportive of my crazy research plans and inability to fit into a mould All of my previous scientific mentors sparked my curiosity in science including Ram Savan, Gautham Rao, Jeff Bender and Donald Lovett. Maria-Cristina Seminario for her amazing stories and for providing very useful career and life advice. My MD PhD classmates Tom Dixon, Danish Saleh, Sanna Herwald and Wenhui Zhou who have become my best friends over the past seven years and have provided countless fun times and tolerated my many flaws. My sole immunology PhD classmate Charles Torgbor, who always entertained my crazy ideas and discussions. Hayley Muendlein and Beiyun Liu made scientific contributions. Amy Tang, who started in the lab as a high school student and pleasantly surprised all of us with her intellect and superb technical abilities and is now starting her journey at Northwestern as a graduate student. Stephen Schworer who took me under his wing in his last year in the lab. I inherited many wonderful projects from Steve and learned a great deal. Chi Weindel, who became a great friend and collaborator over the years as well as our common superhero friend Brendan McDonough who is a bohemian wizard of English and patience. Dan Ram, Mike Ophir and Michael Fray who were hilarious senior students always eager to share advice and gossip. Of course, I cannot go without thanking my bay mate Irina Smirnova. She is a cloning genius and cloned MLKL for me in record time to finish the necroptosis paper. She helped tremendously with RNA isolation for that paper and we always had great conversations. Shruti and Greg who were great friends,

confidants and mentors since before the start of graduate school. All the members of the Jaharis 5th floor labs provided a stimulating and collaborative environment, with George Papadopulos standing out as an incredibly helpful and hardworking member as well as Robert Berland who was always willing to share his time. I would be remiss if I failed to mention the many great discussions about science and life with Edouard Vannier, Xudong Li and Peter Brodeur. Diana Pierce who always made me laugh and made sure I got the required things done. I have made many friends while at Tufts and cannot think of a more fun place to have spent my time doing science.

Finally, I cannot go without thanking my parents Lamis and Shakir and sisters Alia and Maysa for all their support and putting up with all my absences through these years. I hope to be able to re-gain their trust in the years to come and show them how much I care for them. Maysa shares a particular connection to my time in graduate school for all the work we collaborated on in RIPK dependent inflammation. She has done a significant number of In Vivo experiments in Austria as well as visited here to conduct more experiments to help us establish a new branch of research. I hope our collaboration will continue and medicine will not get too much in the way of scientific discoveries.

Most of this work would not be possible without our many scientific collaborators, who are authors or acknowledged in the papers presented. I would also like to thank the reviewers of my paper for reading the work and making helpful suggestions. Scientists are some of the most sharing people (post paper acceptance)! I hope to one day give back to the community from which I have taken and learned so much.

Joseph Sarhan

Table of Contents

List of Figures

List of Abbreviations

5z7	(5Z)-7-Oxozeaenol
AIM2	Absent in melanoma 2
ASC	Apoptosis associated speck-like protein containing a CARD
ATP	Adenosine triphosphate
BAL	Bronchoalveolar lavage
BMDMs	Bone marrow derived macophages
CARD	Caspase activation and recruitment domain
cFLIP	Cellular FLICE-inhibitory protein
cGAMP	Cyclic [G(2',5')pA(3',5')p
cGAS	Cyclic GMP AMP synthase
CMV	Cytomegalovirus
CXCL1	Chemokine (C-X-C motif) ligand 1
dAdT	Deoxyadenylic-deoxythymidylic
DD	Death Domain
DNA	Deoxyribonucleic Acid
ELISA	Enzyme-linked immunosorbent assay
FACS	Fluorescence-activated cell sorting
FADD	Fas-associated protein with death domain
FBS	fetal bovine serum
FPKM	Fragment per kilobase mapped
GAPDH	Glyceraldehyde-3-Phosphate Dehydrogenase
GBP	Guanylate Binding Protein
GFP	Green Fluorescent Protein
GTP	Guanosine triphosphate
HIV	Human Immunodeficiency Virus
HSV	Herpes Simplex Virus
IAP	Inhibitors of Apoptosis
IFN	Interferon
IFNAR	Type I Interferon Receptor I
IL-1	Interleukin 1
ISG	Interferon Stimulated Genes
IU	International Units
JAK	Janus Kinase
LPS	Lipopolysaccharide
M-CSF	Macrophage colony stimulating factor
MAPK	Mitogen-activated protein kinases
MAVS	Mitochondrial antiviral-signaling protein
MDM	Monocyte derived macrophages
MEF	Mouse embryonic fibroblast

MK2	MAPK-activated protein kinase 2
MLKL	Mixed Lineage Kinase Like
MOI	Multiplicity of infection
MyD88	Myeloid differentiation primary response 88
Naip5	NLR family, apoptosis inhibitory protein 5
Nec-1	Necrostatin-1
NFkB	Nuclear factor kappa-light-chain-enhancer of activated B cells
NLRC4	NLR Family CARD Domain Containing 4
NLRP3	NLR Family Pyrin Domain Containing 3
NOD	Nucleotide-binding oligomerization domain
PARP	Poly (ADP-ribose) polymerase
PBMC	Peripheral blood mononuclear cell
PI	Propidium Iodide
PITs	Pore induced intracellular traps
polyI:C	Polyinosinic-polycytidylic acid
PMA	Phorbol 12-myristate 13-acetate
PYD	Pyrin
RIG-I	Retinoic acid-inducible gene I
RIP	Receptor Interacting Protein
RNA	Ribonucleic acid
ROI	Region of Interest
STAT	Signal Transducer and Activator of Transcription
STING	Stimulator of Interferon
TAB1	TGF-beta-activated kinase 1 and MAP3K7-binding protein 1
TAB2	TGF-beta-activated kinase 1 and MAP3K7-binding protein 2
TAK	TGF-beta activated kinase 1
TGFb	Transforming growth factor beta
TLR	Toll Like Receptor
TNF	Tumor Necrosis Factor
TRADD	Tumor necrosis factor receptor type 1-associated DEATH domain
TRAF	Tumor necrosis factor receptor associated factor
TRIF	TIR-domain-containing adapter-inducing interferon-β
WGA	Wheat germ agglutinin
WT	Wild type
Y.p.	*Yersinia pseudotuberculosis*
YOP	*Yersinia* outer membrane protein
zVAD	Carbobenzoxy-valyl-alanyl-aspartyl-[O-methyl]-fluoromethylketone

List of Copyright Materials

Sarhan, J., Liu, B. C., Muendlein, H. I., Weindel, C. G., Smirnova, I., Tang, A. Y., Ilyukha, V., Sorokin, M., Buzdin, A., Fitzgerald, K. A., & Poltorak, A. (2018). Constitutive interferon signaling maintains critical threshold of MLKL expression to license necroptosis. Cell Death & Differentiation. 2019;26:332–347. doi: 10.1038/s41418-018-0122-7

Sarhan, J., Liu, B. C., Muendlein, H. I., Li, P., Nilson, R., Tang, A. Y., Rongvaux, A., Bunnell, S. C., Shao, F., Green, D. R., & Poltorak, A. (2018). Caspase-8 induces cleavage of gasdermin D to elicit pyroptosis during Yersinia infection. Proceedings of the National Academy of Sciences of the United States of America. 2018;115:E10888–E10897. doi: 10.1073/pnas.1809548115.

Chapter 1: Introduction

1.1 Cell Death

1.1.1 History

Necrosis is derived from *nekros* the Greek word for death and has been studied in medicine since at least the time of the ancient physician Hippocrates (460-370 BC). The Hippocratic corpus, a collection of ancient Greek medical texts has extensive references to tissue necrosis using the terms gangrene and sphacelus. The famous Hippocratic physician Galen of Pergamon (130-210 AD) defined gangrene as the stage of disease where the tissue is turning black and losing sensation. The necrotic tissue/ disease then becomes sphacelus when the tissue loses all feeling[1]. The dangers of necrosis have long been appreciated with effective clinical management involving debridement, and antiseptic treatment. Amputation as a treatment for necrotic tissue was reported as early as the first century AD, by the Roman encyclopaedist Aulus Cornelius Celsus[2]. Interestingly, the use of larvae to remove dead or dying tissue was noted to be beneficial for wound healing by at least the early 1500's[3]. The notion that these ancient physicians were wise enough to remove necrotic tissue makes me hopeful that they may appreciate our modern understanding of necrosis. The concept of cellular necrosis had to wait an additional two thousand years from the time of Hippocrates until the advent of the microscope and appropriate tissue preparation conditions.

The famous German biologist Lorenz Oken published an essay in 1805, 'Die Zeugung', which translates to 'The Generation' where he states that all organisms are composed of and originate from cell[4]. This idea of cellular composition was not widely accepted until the publications of Schleiden and Schwann from 1838–1842. It is believed that the work of Schleiden and Schwann inspired Carl Vogt in 1842 to describe the first

known account of cell death while studying frog development[5]. The study of cell death in the context of human pathology was first introduced by the pioneering pathologist Rudolf Virchow in 1858. Virchow was the first to develop the concept of regulated cell death which he termed necrobiosis. Necrobiosis was thought of as a natural process, compared to the violent and accidental necrosis, which was defined as mortification[6]. This distinction of cell death as accidental vs. natural or programmed continued to dominate the field of cell death until the early 2000s when programmed necrosis was discovered.

1.1.2 Apoptosis

Apoptosis as regulated cell death was formally introduced by the pathologist John Kerr, who derived the word from the Greek term meaning 'falling off, as in autumn leaves falling off a tree [7]. Ironically, the term apoptosis had been previously used by Hippocrates era physicians to describe the falling off of necrotic tissue[8,9]. Nomenclature aside, Kerr was one of the first pathologists to describe the now classic morphological features of apoptotic cells including membrane blebbing and nuclear condensation.

The next evolution in the field of cell death arrived in the 1980s by studying development in *C. elegans* worms. Researchers had found that there are 1090 cells in the C. elegans worm, and could reliably detect the death of the same 131 cells, leaving 959 nuclei in adult worms [10]. The Horvitz lab went on to characterize the molecular mechanisms of cell death using genetic screening in C. elegans. Specifically, the Horvitz lab used the mutagen ethyl methanesulfonate (EMS) to create genetic lesions in worms DNA which were screened for defects in cell death [11]. Mutant worms were selected and bred to wild type worms to create F1 and F2 (F1xF1) progeny to determine if the worms could pass on the genetic defect. Using this genetic approach, one could determine if the

gene is dominant or recessive. The modern approach to genetic mapping was well established [12] and had been previously used to find the causative genes for multiple phenotypes [13]. By screening approximately 4000 mutant of worms, Ellis and Horvitz found the proteins CED-3 and CED-4 (called CED for cell death abnormal) to be critical for the induction of cell death [14].

The Horvitz lab continued to study the cell death pathway in great detail and laid the foundation for determining the molecular components of the apoptotic cascade. Using mosaic mutant worms, they next determined that the CED-3 and CED-4 proteins act within dying cells, rather than within healthy cells to induce death in neighboring cells [15]. The next advance in the apoptosis pathway came with the discovery that CED-3 is the mammalian homologue of the protease (IL-1β) converting enzyme (ICE), now known as Caspase 1 [16]. CED-3 was later shown to be more similar to mammalian caspase 3 in substrate specificity [17]. The first anti apoptotic gene CED-9, was identified shortly after CED-3 and CED-4 and is the homologue of the Bcl-2 family member protein Bcl-x_L [18]. By this time, the connection between cancer and apoptosis had become obvious since proteins of the Bcl-2 family had been established as proto-onco genes, which are a family of genes susceptible to inactivating mutations leading to cancer. In fact, the connection of cancer had been known even before this discovery as work by Doug Green's lab had already shown that cancer cells treated with chemotherapeutics undergo apoptosis[19]. For their pioneering work on cell death and C. *elegans* development, H. Robert Horvitz, John E. Sulston and Sydney Brenner shared the 2002 Nobel Prize in Medicine.

The next major advances in mammalian apoptosis closely followed the work of Horvitz, from the labs of Xiadong Wang, Vishva Dixit, Doug Green and Jürg Tschopp.

The laboratory of Xiadong Wang developed a cell free system for studying apoptosis and found that the mitochondrial protein cytochrome c is critical for apoptosis[20]. The role for mitochondria in apoptosis thus became even clearer since there were now two mitochondrial proteins critical for apoptosis, Bcl-2 family members and Cytochrome c. The next major player in mammalian apoptosis found was Apaf-1, the homologue of *C. elegans* CED-4[21]. Specifically, they showed that cytoplasmic cytochrome c binds with Apaf-1 to induce Caspase 3 activation and cell death. Three months later, the Green, Dixit and Nuez labs simultaneously published three Science papers showing that the Bcl-2 family member Bcl-x_L interacts with and inhibits the function of Apaf-1 [22–24]. By the early 2000s, a clear picture of the apoptotic machinery began to take shape with further discovery of caspase substrates and chronology of signaling events.

The apoptotic signaling pathway initially described in C. elegans is known as the intrinsic apoptosis pathway which occurs when cells are stressed or during development. The concept of extrinsic apoptosis which is induced by death receptors was initially discovered in 1989[25], simultaneously, with the discovery of the intrinsic apoptosis pathway in *C. elegans*. The receptors responsible for extrinsic apoptosis induction were ultimately shown to include Tnfr1, Fas [CD95], Edar and the four death receptors (DR): Tramp[DR3],Trail-r1[DR4],Trail-r2[DR5], Dr6. These receptors all have an extracellular amino terminal cysteine-rich domain to determine ligand specificity and a cytosolic death domain (DD) for intracellular signaling. Upon receptor binding and oligomerization, DD interactions with the adaptor FADD[26,27] forms the death inducing signaling complex (DISC), which results in subsequent caspase 8 activation. FADD is a critical component of DISC because it has a DD responsible for interaction with DR, and a death effector

domain (DED) that is critical for caspase 8 recruitment and activation. By virtue of having these two domains, FADD facilitates association of Caspase 8 with DR, which results in subsequent oligomerization and activation of caspase 8. Because Caspase 8 is activated via self-cleavage, oligomerization is another critical event in apoptosis. An important node of regulation was found in the case of FLIP (FLICE-inhibitory protein) which interacts with FADD to inhibit caspase 8 recruitment and subsequent apoptosis[28].

No discussion on apoptosis would be complete without considering caspases and their substrates. The term caspase can be broken down into three components: "c" for cysteine protease, "asp" because the protease cleaves after aspartic acid and "ase" for enzyme[29]. The role of caspases has been studied extensively in cell death and inflammation. The apoptosis associated caspases can be distinguished into initiator (caspase 8,9, and 10) and executioner (caspase 3 and 7), which are cleaved and activated by the initiator caspases. As outlined above, the intrinsic pathway of apoptosis depends on caspase 9 for initiation, while the extrinsic death receptor pathway depends on caspase 8 and 10 for initiation. Caspase 10 is a closely related homologue to caspase 8, and exists in human but not mouse cells[30]. The inflammatory caspases are involved in IL-1 production and will be covered in detail in the section involving pyroptosis. Briefly, Caspase 1 also known as IL1 converting enzyme (ICE) was the first known caspase to have this function and has shared function between mouse and human. Mouse cells are able to activate Caspase 11 in response to intracellular LPS to initiate Caspase 1 independent IL-1 production and cell death. Humans do not have Caspase 11, but instead have the homologous Caspase 4 and 5, which have now recently been linked to similar function[31,32].

Additional, less well studied caspases include Caspase 6, 12, 13 and 14, though Caspase 13 is now known to not be functional in mouse or human[33]. Caspase 12 has had a controversial history, initially having been discovered to have a protective role in sepsis [34], but this was later attributed to the caspase 11 defect on the 129 mouse genetic background[35]. Caspase 12 was also briefly believed to be important for *Toxoplasma gondii* induced apoptosis, though this work was ultimately retracted[36]. Since this time Caspase 12 has not been studied extensively and its biological function or lack thereof remains an open question. Caspase 14 is involved in the specialized process of cornification which is cell death of keratinocytes to create skin, hair and nail[37].

Caspase 6 is also not extensively studied, but has proven more complicated to classify as it has functions of both an inflammatory caspase[38] and can induce apoptosis when over-expressed, leaving Caspase 6 in somewhere in between the classification of apoptotic and inflammatory. Caspase 6 is also unique in that it has been almost exclusively linked to neurodegenerative disorders including Alzheimer[39], Parkinson[40] and Huntington[38]. Interestingly caspase 8 (traditionally and initiator caspase for extrinsic apoptosis) is also now beginning to fall into the category of inflammatory caspase as recent work has shown it can function to induce IL-1 production. This was first shown in the context of the fungal cell wall component Dectin-1[41] and has recently been expanded to include many other stimuli[42,43]. Clearly the caspases do not easily fit into the orderly classification, though our efforts have not been futile since it can provide a conceptual framework to better understand complex biology.

The subject of caspase substrates and specificity is extremely important as this determines biological function downstream of activation. Caspase substrate specificity

was first determined using small peptides linked to fluorescent reporters which become activated upon cleavage[44]. Apoptotic executioner caspases 3 and 7 cleave various Lamin proteins to induce breakdown of the nuclear envelope, PARP-1 cleavage and inactivation of the DNA repair pathway, RIP1 cleavage to block NF-kB pro survival signals, Vimentin cleavage to destroy intermediate filaments just to name a few substrates. The list of caspase substrates is extensive and has been generated into a searchable database (The Casbah; http://bioinf.gen.tcd.ie/casbah/) [45]. Another database has been generated to include predicted caspase cleavage sites (CaspDB; http://caspdb.sanfordburnham.org)[46]. The determination of caspase substrates requires extensive biochemical investigation. The Guy Salvesen lab has published a useful set of guidelines for determining caspase substrate[47]. Briefly, one must determine if the purified protein can be cleaved by recombinant caspase, if the same cleavage products can be identified in cells, one must also generate cleavage site mutants to show ablation of cleavage of recombinant protein well as introducing the cleavage mutant into deficient cells to see if cleavage is inhibited in cells. The final recommendation is for generation of transgenic animals with mutated cleavage sites to determine biological significance. Not surprisingly very few caspase substrates have been characterized this carefully, making this area of investigation potentially fertile ground for future work. One of the best examples of a modern characterization of a caspase substrate involves the identification of Gasdermin D as a substrate for Caspase 1 cleavage and death effector for pyroptosis (this is covered in more detail in the section on pyroptosis).

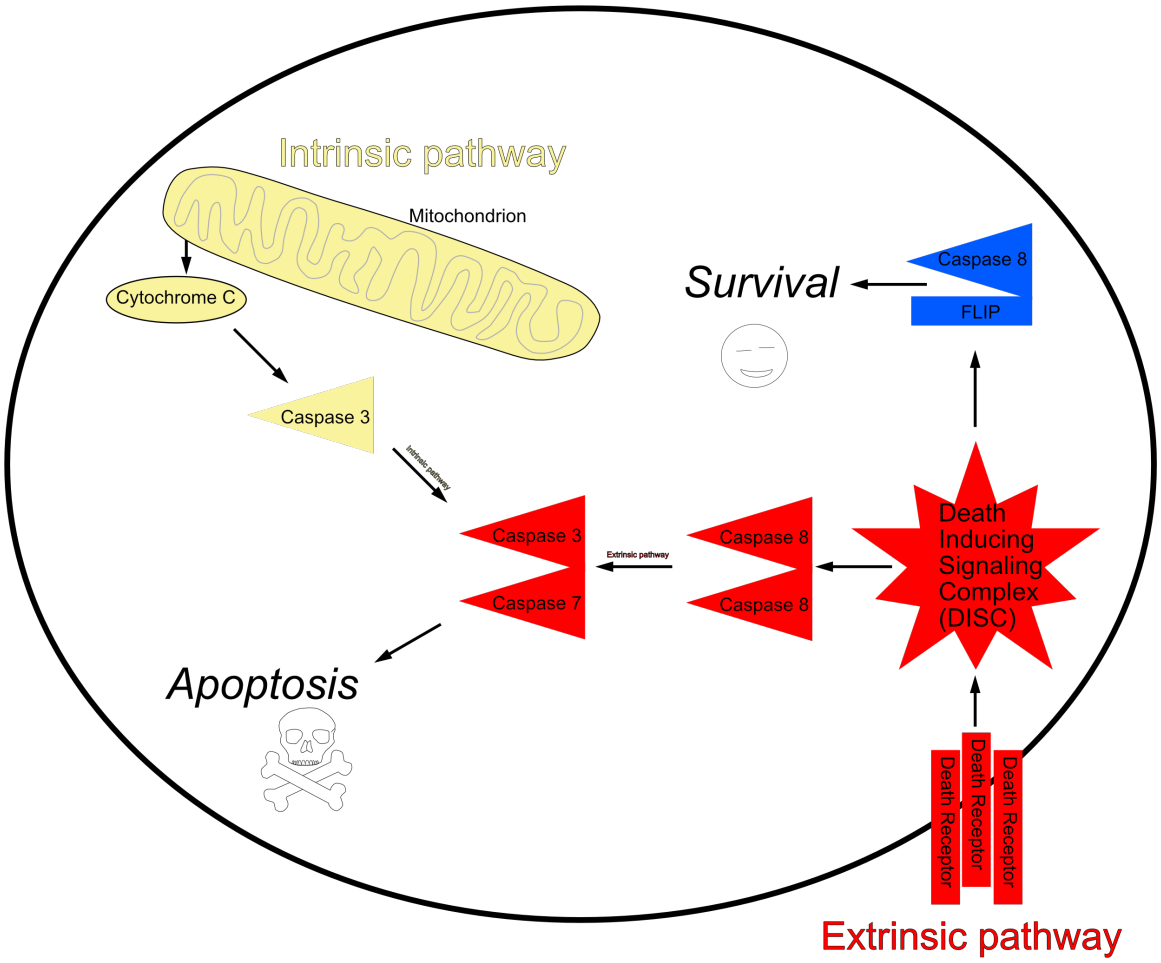

Figure 1.1: Model of intrinsic vs extrinsic apoptosis

1.1.3 Necroptosis

TNF receptor signaling engages the TNF receptor associated adaptor TRADD [48] to recruit RIP1 via death domain (DD) interactions [49], forming complex I. Complex I formation results in the activation of the MAP kinases and NFκB, which drive the production of inflammatory cytokines and pro-survival factors [50]. When MAP kinases and/or NFκB signaling is blocked, RIP1 can dissociate from TNF receptor to facilitate the formation of complex IIa by interacting with FADD and pro-Caspase-8. Complex IIa leads to caspase 8 activation and cell death [51]. What happens when cells are engaged in

Complex IIa, but caspase 8 is blocked? The cells transition to Complex IIb, which results in a potent form of cell death known as necroptosis.

While the mechanisms of apoptosis were being investigated, and the apoptotic machinery reliance on caspases was discovered, scientists began to explore what would happen to apoptosis if caspases were blocked. The breakthrough 2000 paper by Jürg Tschopp's lab did just this and they found that death receptor signaling switches to receptor-interacting protein (RIP) kinase dependent necrotic cell death in the context of caspase inhibition[52]. This was a major finding since up to this point, necrotic cell death was thought to be an un-regulated, accidental form of cell death. Necroptosis was formally introduced as caspase independent RIPK1 dependent necrotic cell death in 2005 by a now classic paper by Junying Yuan and Alexi Degterev[53]. This study involved treating U937 monocytic cells with TNF and the pan caspase inhibitor zVAD while screening the cells with a library of 15,000 small molecules. Using this approach they identified the small molecule Necrostatin-1 (Nec-1), as a potent RIP1 kinase inhibitor. They also went on to show that Nec-1 could also be beneficial in ischemic injury to the brain. The introduction of a small molecule inhibitor of necroptosis was paramount for increasing the pace of discovery ad helped show that the mechanism followed a specific program.

The next big development in necroptosis came in 2009 when the Laboratory of Francis Chan discovered the role of RIP3[54]. The Chan laboratory used an siRNA screen of 691 kinases in FADD deficient Jurkat T cells, which undergo necroptosis in response to TNF exposure. Using this approach, they identified RIP1 (which was known) and RIP3, but not any of the other RIP kinases (RIP 2,4 or 5). They went on to show that

RIP3 associates with and phosphorylates RIP1. This work was followed up by structural examination of the RIP1/RIP3 interaction showing that they form a high level oligomeric amyloid 'necrosome' protein aggregate[55].

Soon after the discovery of RIP3, the role of necroptosis in development began to take center stage. Since 1998, it had been known that Caspase 8[56] deficiency and FADD[57] deficiency result in embryonic lethality from embryonic day 10.5 to 13.5. Given that caspase-8 inhibition or FADD deficiency in vitro was now known to result in necroptosis, the role of RIP3 could now be addressed. Indeed, back to back publications in 2011 showed that RIP3 deficiency could protect both Caspase 8[58,59] deficient and FADD[60] deficient animals from embryonic lethality. This work beautifully highlights how Caspase 8 and FADD restrain necroptosis.

The next big finding in the field of necroptosis was in 2012 and involved the discovery of the cell death effector mixed lineage kinase domain-like (MLKL) protein[61,62]. The study by Xiaodong Wang's group found MLKL by treating human colon cancer HT-29 cells with TNF, smac mimetic and zVAD to induce necroptotic cell death while screening with approximately 200,000 small molecules to find an inhibitor of necroptosis, (E)-N-(4-(N-(4,6-dimethylpyrimidin-2-yl)sulfamoyl)phenyl)-3-(5-nitrothiophene-2-yl)acrylamide, otherwise known as necrosulfonamide. They were then able to show that necrosulfonamide interacts with human MLKL and additionally showed that RIP3 interacts with and phosphorylated human MLKL at threonine 357 and serine 358 residues[61]. The combined efforts of Andreas Strasser, John Silke, and Warren S. Alexander labs then generated the MLKL knockout mouse, determined the crystal structure and showed that MLKL is itself catalytically inactive and depends on RIP3 for

phosphorylation and activation before translocation of the N-terminus into the plasma membrane resulting in necroptosis[63]. They specifically showed that S345, S347 and T349 are RIPK3 phosphorylation sites in murine MLKL which corresponds to T357 and S358 in human MLKL. In quick succession, follow up work showed that MLKL forms trimers that translocates to and disrupts the plasma membrane resulting in cell death[64]. The trimers were eventually shown to be higher order complexes, likely tetramers and octamers[65] with higher order amyloid aggregates of MLKL possible[66]. Whether MLKL has additional interaction partners such as ion channels or if MLKL polymers can disrupt cellular plasma membranes directly is not yet resolved. Regardless, the work thus far on necroptosis has solidly established a mechanism for cell death with the order of events moving from RIP1 and RIP3 interaction and phosphorylation to MLKL phosphorylation followed by oligomerization and membrane insertion and cell death.

Soon after the discovery of RIP3, necroptosis also moved into the direction of additional stimuli since all of the work had focused on TNF and death receptor signaling. Indeed, Xiadong Wang's lab showed that the Toll-like receptors (TLR) can be key drivers of necroptosis. Indeed, their lab showed that both TLR4, which recognizes bacterial LPS and TLR3, which recognizes double stranded RNA, can induce necroptosis when caspases are inhibited with the pan caspase inhibitor zVAD. This work was later confirmed and expanded to show that the TLR adaptor TIR-domain-containing adapter-inducing interferon-β (TRIF) common to TLRs 3 and 4 is required for TNF independent necroptosis, while signaling via other TLRs depends on TNF and the MyD88 adaptor[67]. Knowing that TRIF is required for TLR induced production of type I IFN, Subash Sad's lab published that type I IFN receptor deficient cells are resistant to TLR3/4 mediated

necroptosis. Another paper was simultaneously published showing that type I IFN (α/β) and type II IFN (γ) can induce necroptosis via protein kinase R (PKR)[68]. Therefore, TRIF was attributed the additional role of mediating necroptosis via IFN induction. The role of interferon receptor signaling in necroptosis became the subject of our first manuscript entitled "Constitutive Interferon Signaling Maintains Critical Threshold of MLKL Expression to License Necroptosis".

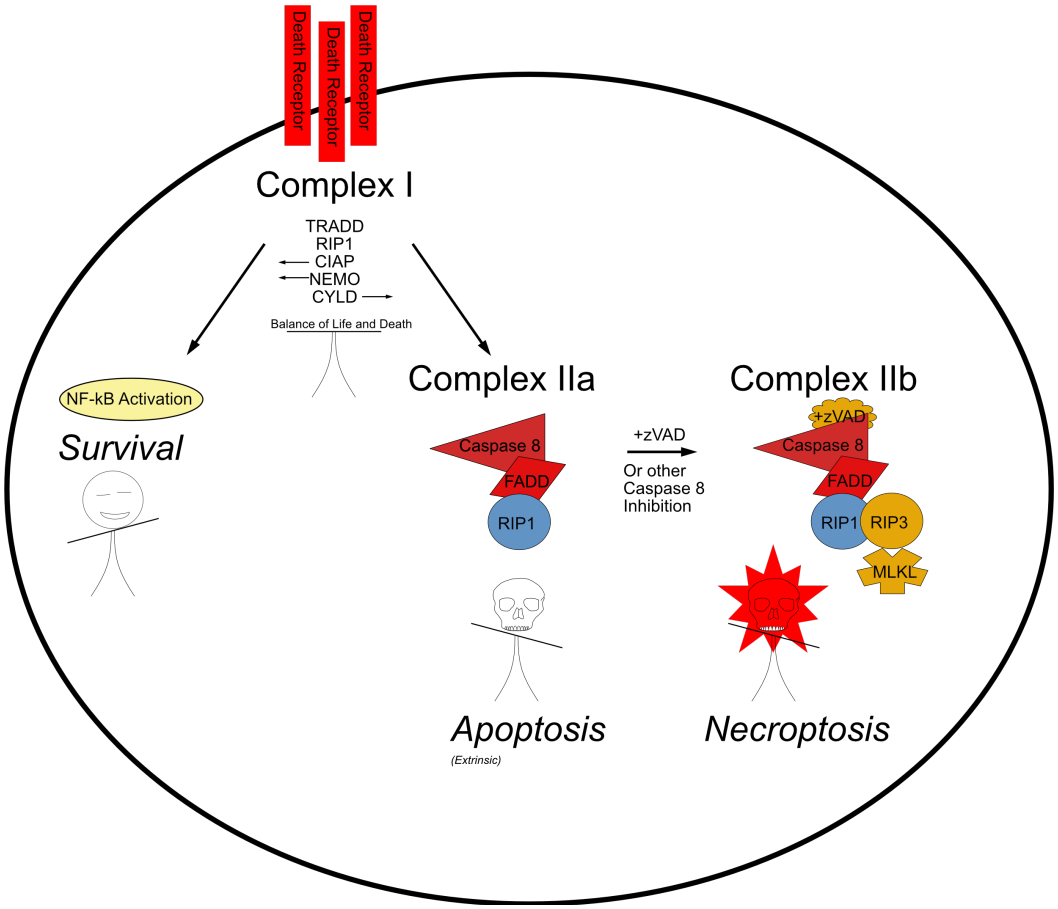

Figure 1.2: Complex I vs Complex II model

1.1.4 Pyroptosis

The term pyroptosis is derived from the Greek terms 'Pyro' meaning fire and 'ptosis' meaning falling as in leaves from a tree[69]. Pyroptosis was first used to describe

necrosis associated with Caspase 1 activation and IL1 production was proposed by Brad Cookson in 2001 back when necrosis was still widely believed to be accidental cell death[70]. This definition was inspired by the observations that *Salmonella typhimurium* infection of macrophages led to Caspase 1 dependent necrotic cell death[71]. The next big development in the field came from Jürg Tschopp and Fabio Martinon's 2002 paper describing the inflammasome, which is the molecular complex required for IL-1 maturation. There they showed that members of the NOD like receptor family (NLR) along with the adaptor protein apoptosis-associated speck-like protein containing a CARD (ASC) associate to form a molecular complex termed the inflammasome which then activates Caspase 1 to induce IL1 cleavage and release. Since this time many other inflammasome sensors have been described.

The canonical inflammasome is known to contain sensors belonging to the NLR or AIM2-like receptor (ALR) family. More specifically, these cytosolic danger sensors include NLRP3 which is activated by a wide variety of signals including pore-forming toxins, potassium efflux, ATP, uric acid, and alum[72–74] as well as the sensor absent in melanoma 2 (AIM2) which senses double stranded DNA[75–77]. These adaptors then recruit the adaptor ASC to activate Caspase 1. Additional inflammasomes include NLRP6 which is thought to react with viral RNA[78] as well as Pyrin which senses the bacterial inactivation of RhoA GTPase[79]. There are also ASC independent inflammasome sensors including NLRC4 recognizes bacterial flagellin and type III secretion system (T3SS) components via NLR family-apoptosis inhibitory proteins (NAIPs)[80]. NLRP1b functions similarly to NLRC4, which senses anthrax lethal toxin via NAIPs[81]. The common event

downstream of these sensors is Caspase 1 is activation via autocleavage, leading to cleavage of pro-IL-1 and pro-IL-18.

No discussion of pyroptosis would be complete without considering the history of IL1 family proteins, which begins in the 1943 with the search for the effector of fever[82]. These experiments involved generating sterile peritonitis in rabbits, extracting peritoneal leukocytes and taking cell free supernatant from these cells. Endotoxin free protein extracts from the supernatants of peritoneal leukocytes leukocyte were then injected into naïve rabbits resulting in rapid fever[83]. These results suggested the presence of an endogenous pyrogen, which was later identified to be IL-1[84,85]. Over time, the IL1 family was expanded to include 11 members, 7 pro-inflammatory (IL-1α, IL-1β, IL-18, IL-33, IL-36α, β, γ) and 4 anti-inflammatory (IL-1Ra, IL-36Ra, IL-37, IL38)[86]. IL-1α, IL-1β are the most potent pyrogens in humans, able to produce fever and chills at 1-10 ng/kg compared to TNF and IL-6 which require μg/ml quantities[82]. Indeed IL-1 has been implicated in driving pathogenesis in numerous categories of disease including hereditary systemic inflammatory diseases (such as familial Mediterranean fever), systemic and local inflammatory diseases (such as macrophage activation syndrome), numerous rheumatologic diseases (gout, rheumatoid arthritis and osteoarthritis), type II diabetes, myocardial infarction and now even cancer (multiple myeloma)[87,88].

Two major milestones re-defined the field of pyroptosis in recent years. The first being re-discovery of Caspase 11 in 2011 by Nobuhiko Kayagaki and Vishva Dixit[89]. Caspase 11 was initially discovered[90] and shown to interact with Caspase 1[91] by Junying Yuan's lab in the 1990s. However, with the re-discovery of Caspase 11, Vishva Dixit's group found that mice of the 129S1/SvImJ genetic background had a naturally

inactivating mutation in Caspase 11. Caspase 1 and caspase 11 are neighboring genes on chromosome 9, both located at 2.46 cM. Since the Caspase 1 deficient animals were generated using 129 embryonic stem cells and back crossed to B6, the naturally occurring defect in Caspase 11 was passed on as an unintentional 'passenger mutation'. This topic of unintended passenger mutation in genetically modified mice has recently been well discussed and should always be considered when using mice of mixed genetic background[92]. Since the re-discovery of Caspase 11, several other functions have been found, most strikingly that Caspase 11 can interact with cytosolic LPS to induce IL-1 cleavage and cell death[93–95]. Since this time, there have been many additional phenomena initially ascribed to Caspase 1 function which were re-assigned to Caspase 11, which also have unique and non-overlapping functions[96].

The next major milestone in pyroptosis research was the discovery of the effector protein Gasdermin D. This was simultaneously discovered by Vishva Dixit and Feng Shao's labs which used an N-ethyl-N-nitrosourea (ENU) mutagenesis[97] screen and a CRISPR screen[98]. These publications were quickly followed by major discoveries from the labs of Judy Lieberman, Hao Wu and Feng Shao showing that the Gasdermin D N terminus oligomerrizes to form a membrane pore which kills cells and releases IL-1 (pyroptosis)[99,100].

With the discovery that Caspase-11 drives pyroptosis via activation of pore forming protein Gasdermin D (GsdmD), the NLRP3 inflammasome was found to activate as a consequence of plasma membrane rupture and the efflux of potassium ions [101]. More recently, activation of the NLRP3 inflammasome has also been observed during

necroptosis [102,103], suggesting that inflammasome formation may be a commonality shared amongst many necrotic forms of cell death.

Recent work has shown that Gasdermin E can drive pyroptosis downstream of Caspase 1/11[104] and secondary necrosis downstream of Caspase 3[105]. Gasdermin D and Gasdermin E are the only two gasdermins known to be expressed in macrophages, though variants of other gasdermins have been implicated in various other human diseases suggesting they may play an important role in cell death pathways that will surely be the topic of future work. Given the paramount importance of gasdermins in executing pyroptosis, the Shao group has proposed the re-definition of pyroptosis as cell death mediated by gasdermin activation[106].

Recent work by the Jonathan Kagan laboratory in the field of pyroptosis has begun to re-address what it means for a cell to be dead[107]. In this paper they propose that truly dead cells release lactate dehydrogenase (LDH) and that cells with permeabilized membranes, allowing membrane impermeable nuclear dye binding (propidium iodide (PI), SYTOX, and others), but without LDH release are still alive. Membrane compromised cells were shown to be able to engulf fluorescent zymosan demonstrating phagocytic potential as well as had positive staining by Mito-tracker, suggesting that mitochondrial membrane potential is still present. Since they used immortalized cell lines to conduct the study, it would be interesting to know if membrane compromised cells (PI positive) are able to undergo cell division. Additionally, direct measurement of extracellular acidification and oxygen consumption may be warranted to determine metabolic activity. Finally, it may also be important to have a large scale low magnification (to increase cell numbers) view of the cells undergoing pyroptotic stimuli

with dual staining for live cell marker such as Calcein-AM (or total cell marker such as DiO or CFSE) coupled with a cell membrane impermeable dye such as PI. This would allow one to determine what percentage of the cell population has undergone membrane permeability. Indeed, this would help determine if there is a portion of the population that is not membrane permeable, which may account for IL-1 secretion or metabolic activity. Overall, this is a very exciting direction which has potential to completely re-define the study of cell death if cells with compromised membrane integrity are alive.

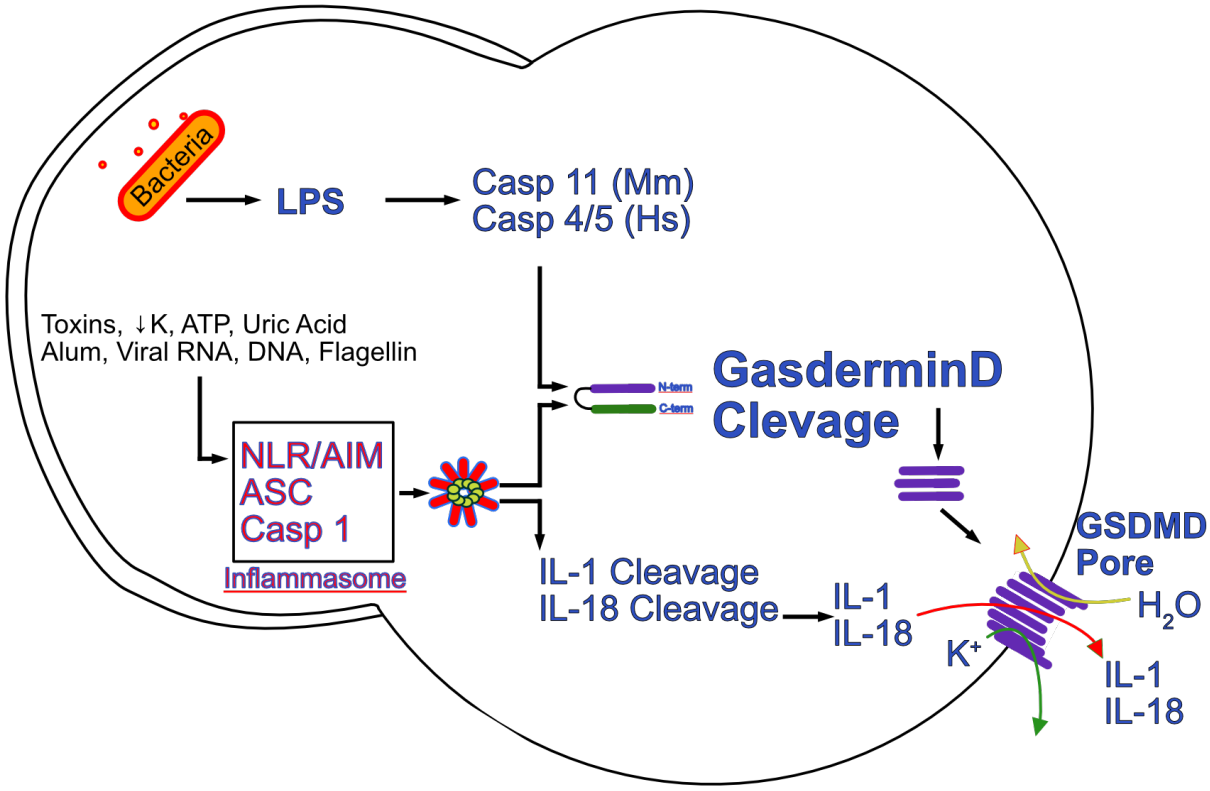

Figure 1.3: Model of Pyroptosis

1.1.5 Additional forms of cell death

There have been many other forms of cell death described, with new reports being published all the time. There is a temptation to write off these new forms of cell death as non-unique subtypes of already defined forms of death. While this may be appropriate in

certain cases, we should consider that pyroptosis was once thought to be a subset of apoptosis. Keeping this in mind, there are several additional forms of cell death that have been well characterized including ferroptosis, MPT-driven regulated necrosis, parthanos, autophagic cell death, entotic cell death, NETotic cell death, as well as microptosis.

Ferroptosis was first described in 2012 as an iron dependent, oxidative form of necrotic cell death which can be inhibited by the small molecule ferrostatin-1[108]. The process of ferroptosis has been linked to the oncogenic small molecule erastin as well as acute kidney injury[109]. Mitochondrial permeability transition (MPT)-driven regulated necrosis driven by mitochondrial rupture that is at least partially dependent on the protein Cyclophillin D (CYPD) and can be delayed by the CYPD inhibitor cyclosporin A[110,111]. MPT-driven regulated necrosis has been implicated in pathology in the case of brain ischemic injury[112] as well as kidney ischemia reperfusion injury[113]. Parthanos is a necrotic form of cell death dependen on poly(ADP-ribose) polymerase 1 (PARP1), apoptosis-inducing factor (AIF) and macrophage migration inhibitory factor (MIF)[114,115]. Parthanos has been implicated in various forms of ischemic re-perfusion injury as well as neurodegenerative disease including Alzheimer's. Autophagic cell death classically describes cell death that occurs with large autophagic vacuoles in the cytosol accompanied by a lack of nuclear condensation. Autophagy, is the process by which cells recycle organelles and is important in maintaining cellular homeostasis. This form of cell death often happens when apoptosis is blocked and could be thought of as an effort of the cell to stay alive. It is now proposed by Guido Kroemer and Beth Levine that the term autophagic cell death should be reserved to describe cell death that depends on the autophagic machinery[116]. Entotic cell death describes the engulfment and lysosome

mediated killing of viable cells by non phagogytic cells[117]. This process of cell death has been recently heavily implicated in multiple types of cancer. NETosis describes the process by which neutrophils die and extrude their nuclear contents to form extracellular traps for killing bacteria[118,119]. Microptosis describes a form of cell death that involves natural killer (NK) cells and cytolytic T lymphocytes (CTLs) killing intracellular parasites with cytotoxic granules[120]. This form of cell death resembles apoptosis in the targeted parasites and is critically important for host defense.

1.1.6 Biological relevance of cell death

The biological relevance of cell death cannot be overstated. The first instance it becomes relevant is during the process of development[121]. Some of the first studies moving on the relevance of cell death beyond development involves work showing that cytotoxic lymphocytes can induce apoptotic cell death in target cells[122]. Other landmark work includes studies showing that clonal deletion involves activation induced cell death by apoptosis to limit self-reactive T cells and autoimmunity[123]. Apoptosis is also critical for wound repair and regeneration in a process known as apoptosis-induced proliferation (AiP)[124]. Interestingly the process of AiP has also been linked to cancer growth and metastasis[125]. Caspase 9 deficient animals suffer various deformities including severe brain malformations[126], though there are also apoptosis independent functions of caspases which must be considered[127]. Additionally, apoptotic cell clearance is abundant in normal homeostasis as evidenced by a recent study tracking apoptotic cell clearing macrophages[128]. The biological relevance of apoptotic cell death cannot be overstated, and new avenues of study are found very frequently.

The functional relevance of necroptosis is less appreciated than apoptosis, perhaps because it is a process that usually requires caspase inhibition in vitro. Necroptosis is often introduced as a backup mechanism of cell death, the default mode to die when apoptosis is inhibited. Indeed, this may be one of the ancient evolutionary reasons for necroptosis, however many viral infections which are able to block caspases also have capacity to block necroptosis. This is perhaps most well documented in the case of herpes simplex virus (HSV) which has a ribonuclease component that can inhibit RIP1/RIP3 interaction and block necroptosis[129,130]. Cytomegalovirus (CMV) similarly inhibits Caspase 8 as well as the necroptosis machinery through the use of viral proteins[131]. There are many other known viral inhibitors of caspases, but only two published viral inhibitors of necroptosis (HSV and CMV) suggesting that there are either many other inhibitors of necroptosis or other forms of virus induced necroptosis that warrant study. Necroptosis may also play a significant role in the case of viral bacterial co-infection, where the virus inhibits caspase activation and bacterial LPS (from gram negative bacteria) can drive necroptosis. Limiting our discussion of necroptosis on viral infection would be reductive as perhaps the most interesting instances of biologically relevant necroptosis happens in the absence of caspase inhibition. This is the case with the proteasome inhibitors MG132 and bortezomib[132], *Staphylococcus aureus* infection[133,134], as well as in the case of many models of ischemic injury[53,135–137] as well as Alzheimer's disease[138]. The field of necroptosis is still very new and many more discoveries on the biological relevance of necroptosis are sure to come.

The relevance of pyroptosis has always been apparent in the context of host defense since pyroptosis was first described in the context of Salmonella typhimurium

infection[71]. Interestingly, pyroptosis has been shown to be protective by limiting the host replicative niche for numerous intracellular bacteria as well as by providing a potent inflammatory response via IL1 production[139]. Recent work by the Lieberman lab has also shown that the effector of pyroptosis, Gasdermin D can attack and compromise pathogenic bacteria[99]. Pyroptosis is not always positive as it was shown to be a mechanism responsible for depleting CD4 T-cells during HIV infection[140,141]. Additionally, pyroptosis has been shown to be lethal in the case of high dose endotoxemia in mice[93,94]. Pyroptosis is a powerful host defense mechanism which must be carefully regulated to avoid sepsis.

1.2 Type-I Interferon

1.2.1 Type-I Interferon receptor signaling

Interferons are a family of cytokines that were named after a phenomenon in which infection with a first virus "interferes" with the establishment of a subsequent virus in the same host[142]. There are three families of IFN cytokines, type I, II and III. Type-III interferons (IFN-λ) are represented by four genes in human (IFNL 1,2,3 and 4), while there are only two functional genes in mouse (*Ifnl2* and *Ifnl3*) as the other two genes are pseudogenes[143]. Type-III IFNs are most similar in function to Type-I IFNs despite significant sequence dissimilarity and have been implicated in various disease states including HCV infection[144,145] and intestinal inflammation[146]. Type-II IFNs are much more lonely being composed of only one member, IFNγ and is one of the most well studied. T cells, natural killer cells and natural killer T cells are the main sources for IFN□, which has been implicated in various disease processes including restriction of viral replication, atherosclerosis, autoimmune disease, and cancer[147].

Type-I interferons (IFN-I) are composed of 14 α isoforms and one β, κ, ω and δ isoform each, all of which bind a common heterodimeric receptor composed of two subunits, IFN-αR1 and IFN-αR2 (IFNAR) [148]. IFN-I regulates host response to bacterial and viral infection by binding the receptor and activating STAT 1/2 transcription factors (signal transducer and activator of transcription 1 and 2) and regulating a diverse family of genes termed Interferon Stimulated Genes (ISGs) [149]. IFN-I is best known for being induced in response to either the toll like receptors TLRs (Toll Like Receptors) or cytosolic nucleic acid (RNA and DNA)[150].

1.2.2 Type-I interferon Induction

TLRs are receptors for sensing of microbe-derived pathogen associated molecular patterns (PAMPs) at the plasma membrane and endosome[151]. TLRs are important inducers of type-I IFNs[152]. Thirteen TLRs are expressed between mice and humans (TLR1-10 in human, TLR1-9 and 11-13 in mouse) localized to either the plasma membrane or the endolysosome. A notable exception is TLR4, the receptor for LPS[153], which can signal from both the plasma membrane and the endosome following CD14-mediated endocytosis[154,155]. Other plasma membrane-associated TLRs include TLR2 which recognizes lipoteichoic acid and can form heterodimers with TLR1 or TLR6 to recognize diacyl and triacyl lipoproteins respectively. TLR 5 is another membrane associate TLR that recognizes bacterial flagellin. Finally, in mice TLR11 and TLR2 are involved in the recognition of profiling derived from *Toxoplasma gondii* infection[156]. Endosomal TLRs specialize in detecting nucleic acids. TLR3 detects virus-derived dsRNA and its synthetic analog polyinosinic polycytodylic acid (poly I:C). ssRNA is recognized by TLR7 and TLR8 whileTLR9 recognizes CpG DNA.

TLR 3 and endosomal TLR 4 are unique in that they share the common adaptor TIR-domain-containing adapter-inducing interferon-β (TRIF), while the other TLRs (and surface TLR4) all commonly use the Myeloid differentiation primary response 88 (MYD88) adaptor. The TRIF signaling TLRs are also unique in their capacity to induce IFN β[157,158], while the MYD88 signaling TLRs induce IFN α[159].

Besides TLR signaling, the other well accepted route leading to type-I IFN induction involves cytosolic nucleic acid sensing. Retinoic acid-inducible gene I (RIG-I) is a sensor of cytosolic viral RNA sensor which acts via the adaptor molecule mitochondrial antiviral-signaling protein (MAVS) to induce IRF3 activation and interferon production. Cytosolic DNA sensing via the stimulator of interferon genes (STING)/ cyclic GMP-AMP synthase (cGAS) pathway is another way to induce type-I IFN. STING is an endoplasmic reticulum (ER) resident protein that was first discovered to be a cytosolic DNA sensor involved in IFN induction in 2008 by various independent groups[160–162]. These studies overexpressed various proteins individually to screen for which could induce IFNβ. Interestingly STING does not bind to DNA directly but rather binds to cyclic dinucleotides including c-di-AMP, c-di-GMP, and 3', 5'-cGAMP[163]. A major advance in the mystery of how STING senses cytosolic DNA was made in 2013 by the Chen laboratory[164,165]. The Chen group showed that upon DNA binding, cGAS can produce an endogenous cyclic dinucleotude, 2'3'-cGAMP which will bind, dimerize and induce IFN production.

1.2.3 Constitutive Type-I IFN

With the IFN protein products being elusively small in quantity and too dilute to be detectable in healthy animals and humans, early studies turned to the hybridization of

mRNA transcripts of *Ifn* genes to measure steady-state expression. These studies found varying degree of expression in type I IFN genes in the spleen, kidney, liver, and peripheral blood leukocytes from healthy humans [166,167]. Indeed, when neutralizing antibodies against IFNγ or pan IFNα/β were injected into whole animals, blockade of these proteins enhanced tolerance to tumor grafts [168,169], indicating that *in vivo* levels of IFNs, although under the limit of protein detection, remains capable of conferring protection against malignant cells. Additionally, a recently described an IFN-β luciferase reporter which showed abundant constitutive expression In Vivo, especially in the thymus[170]. Constitutive IFN has also been well characterized in in-vitro cell lines and ex-vivo cells including mouse embryonic fibroblasts (MEFs), B cells, and macrophages [149,171]. It has been suggested that constitutive IFN sustains the expression of JAKs, STATs, and other components necessary for the IFN-I autocrine loop. Functionally, constitutive IFN-I is thought to maintain basal levels of immune-related genes to enable a rapid response to viral infection [172,173].

One of the earliest proposed sources for constitutive IFN production stems from triggering of low-levels of immune activation by commensal microorganisms. Macrophages from C3H/HeJ mice, which are hyporesponsive to LPS due to a mutation in TLR4, were found to be more supportive of vascular stomatitis virus (VSV) replication [174]. In contrast, the restriction to VSV replication by macrophages from the LPS-responsive mouse strain C3H/OuJ can be partially lifted by neutralizing antibodies against IFNα/β. Recently, oral antibiotic treatment of C57BL/6J mice was found to increase susceptibility to LCMV and influenza virus. Disruption of commensal bacterial population was associated with severe reduction in expression of *Ifn* genes as well as

genes in the IFN signaling pathway including *Stat1/2* and *Irf3/7*, and crucial ISGs involved in antiviral immunity including *Mx1/2* and *Oas* genes [172]. Commensal microbiota is thus one source of constitutive IFN production that has a protective effect against pathogens.

1.2.4 Biological significance of type-I IFN

Interferons evolved about 500 hundred millions of years ago, first appearing in vertebrates as an anti-viral defense mechanism[175]. The anti-viral effects of interferon stimulated genes have been well studied[176,177]. Various viruses are known to inhibit the host interferon response to promote viral replication[178]. Human immunodeficiency virus (HIV) inhibition of the host IFN response stands out as a well characterized example. Work by Nan Yan and Judy Lieberman showed that HIV can use the host nuclease TREX1 to digest reverse transcribed transcripts that would otherwise trigger the STING/cGAS pathway[179]. Interestingly type-I IFN in the context of bacterial infection can be either beneficial or harmful for the host[180,181]. For example *IFNb*$^{-/-}$ animals are resistant to *Salmonella typhimurium* infection[182]. Additionally IFNAR competent lymphocytes are detrimental to the host during *Listeria monocytogenes* infection[183]. In contrast IFNAR signaling is protective during *Streptococcus pyogenes* infection[184].

In contrast to the undetectable levels of IFN in healthy humans, high levels of circulating IFNα/β is a hallmark of several autoimmune diseases including Systemic Lupus Erythematosus (SLE) [185–187] and several dermatologic disorders including psoriasis [188,189], Sjögren's syndrome [190], scleroderma [191] and dermatomyositis [192]. One of the key drivers of pathology during autoimmunity is the presence of antibody toward self-antigens (autoantibodies). Notably, many of these autoantibodies target nuclear

components, supporting the hypothesis that improperly digested DNA may be triggering nucleic acid sensing pathways to induce high levels of IFN. In the case of interferonopathies including Aicardi-Goutières syndrome (RNase or DNase deficiency) and STING-associated vasculopathy with onset in infancy (SAVI) (hyperactive STING), excessive interferon directly drives disease[193,194]. Additionally, reactivation of endogenous retroelements can activate the cytosolic RNA sensing pathway RIG-I/MAVS in B cells, resulting in T-cell independent autoantibody production in addition to heightened IFN signaling [195,196]. Of note, MAVS has also been shown to be activated by reactive oxygen species from the mitochondria in a virus-independent manner [197], indicating that in addition to the their traditional pathogen recognition roles, PRRs may also function to monitor other types of cellular stress.

In a mouse model of SLE generated with TLR7 overexpression, deletion of IFNAR in these mice reduces disease severity, indicating a detrimental role for elevated IFN signaling [198]. Similarly, JAK/STAT inhibition in human patients has been shown to be protective during autoimmunity including SLE [199]. On the other end of the spectrum, a subset of MS patients display low constitutive IFN signature as defined by resting ISGs in peripheral mononuclear cells [200,201] and serum cytokine levels [202]. Recombinant IFNβ treatment in these patients restores the ISG signature to that of normal patients accompanied by ameliorated disease. Therefore, either elevated or depressed IFN levels can thus drive as well as be a product of pathology, attesting to the importance of balanced IFN signaling in homeostasis.

1.3 Mitogen-activated protein kinase (MAPK) signaling

1.3.1 Role of MAPKs in inflammation

Mitogen-activated protein kinase (MAPK) signaling is activated by numerous stimuli including TLR stimulation, growth factors, cytokines and cytosolic pathogen sensors[203]. MAPK signaling involves a sequential activation of proteins classified as level 3, 2 and 1 (MAP3K, MAP2K, and MAPK). Specifically, serine/threonine phosphorylation by MAP3Ks activates MAP2K kinases to phosphorylate and activate MAPKs. The best studied MAPKs are (ERK1/2), c-Jun NH2-terminal kinases (JNK1-3), and p38α/β. Activation MAPKs leads to phosphorylation of other kinases, transcription regulatory factors. Ultimately the major downstream consequences include transcription, mRNA stability and regulation of protein translation leading to gene expression changes[204].

Transforming growth factor beta-activated kinase 1 (TAK1) is the best-documented activator of p38 and JNK and ERK[205]. TAK1 is activated following binding of TAK1 binding partners (TAB) 1,2,3 and then can interact with ubiquitinated TNF receptor-associated factor 6 (TRAF6), which leads to phosphorylation of MAP2K, leading to p38 and JNKactivation[206]. Simultaneously, TAK1 activates the IKK complex, causing p105 degradation which together with the MAPK activation leads to cellular effects including production of pro-inflammatory cytokines, cellular differentiation, growth, survival and metabolic changes.

1.3.2 Role of MAPKs in cell death

MAPKs implicated in cell death include the MEK/ERK pathway, P38 and its substrate MK2 and the MAP3K TAK1. Early reports showed that MEK/ERK activation

is protective against growth factor deprivation induced death[207] as well as ionizing radiation induced apoptosis[208]. A group of recently published reports showed that MAPK-activated protein kinase 2 (MK2), which is a downstream target of P38 and TAK1 is required for RIP1 phosphorylation (Ser231) [209–212]. This work showed that MK2/ P38 driven RIP1 phosphorylation inhibits complex II formation and thus limits cell death.

TAK1 is the most well studied MAPK in cell death[213]. The study of TAK1 in cell death may have been initiated with the publication that whole body TAK1 deficiency results in lethality between embryonic days 9.5-10.5 [214]. The use of polyI:C, a TRIF-engaging TLR3 agonist, to induce the deletion of TAK1 resulted in rampant necrosis of the treated area along with heightened IL-1 response [215]. Similarly, the *in vivo* reduction of TAK1 using an inducible shRNA also proved difficult, since cells losing sufficient TAK1 levels likely experience tonic TNF-mediated activation of complex IIa [216]. Tissue specific ablation of TAK1 has also provided useful information including *K5-Cre* $Tak1^{flox/flox}$ animals with keratinocyte specific TAK1 ablation. Perhaps not surprisingly, TAK1 ablation in keratinocytes resulted in cell death and inflammation[217]. Recent work by the Kanneganti lab has shown that Lyz2-$Tak1^{flox/flox}$ mice dives spontaneous inflammation and myeloid proliferation[218].

Inhibition of TAK1 on the cellular level showed that TNF stimulation in the context of TAK1 deficiency leads to cell death via caspase activation and apoptosis-complex IIa. Like many other forms of caspase dependent cell death, TAK1 induced death switches to necroptosis in the case of caspase inhibition - complex IIb [219,220]. More recent work showed that TAK1 induced cell death is likely a consequence of deficient

up-regulation of pro-survival factors including Cellular FLICE-inhibitory protein (c-FLIP)[221,222]. TAK1 inhibition is also a promising target for pharmacologic inhibition in cancer and inflammatory diseases[223] to kill malignant cells and inhibit inflammatory cytokine production.

The efforts to inhibit TAK1 have culminated in the generation of multiple inhibitors, including the classically used (5Z)-7-Oxozeaenol (5z7)[224] and other inhibitors including Takinib, NG25, Resveratrol, with many others still in development[225,226]. These inhibitors have had multiple application in killing cells and inhibiting inflammation. 5z7 has been used extensively and was recently shown to sensitize cervical cancer cells to chemotherapy[227]. Takinib was shown to induce cytotoxicity in breast cancer cells[228], and similarly NG25 was also shown to induce cell death in various breast cancer cell types[229]. The inhibitor Resveratrol was shown to be protective and inhibit inflammation and fibrosis in silica induced pneumoconiosis[230]. However, caution must be used in targeting TAK1, given all the work showing that inhibiting TAK1 in vivo can have dramatically deleterious effects.

1.3.3 Yersinia, MAPK inhibition and cell death

The plague, also known as the black death is a disease caused by the gram-negative *Yersinia pestis* bacterium which was discovered by Shibasaburo Kitasato and Alexandre Yersin in 1894[231]. *Yersinia pestis* is mainly transmitted through fleas, with rodent reservoirs. When humans are infected via a tick bite, the disease will manifest in the bubonic form which causes significant skin manifestations including highly inflamed and painful superficial lymph nodes, otherwise known as bubos. The bubonic form of the disease can then evolve to the pneumonic from with bacterial outgrowth in the lungs or

rarely septicemic disease with Yersinia in the blood. If established as pneumonic disease, the bacterium can spread quickly between humans via aerosol formation[232]. Indeed, recent evidence has shown that the major plague epidemics were spread via trade routes, leading to approximately 200 million deaths[233]. With the advent of modern antibiotics, *Yersinia pestis* infection has gone from nearly 100% lethal to less than 5% if caught early before septicemic disease[234]. However, with the emergence of multi-drug resistant *Yersinia pestis*[235] and high bio-terror potential[236], a better understanding of Yersinia infection may serve quite useful.

Yersinia pestis is one of three closely related Yersinia species bacteria which are known to infect humans including *Yersinia pseudotuberculosis* and *Yersinia enterocolitica*, both of which cause gastroenteritis and are transmitted via the oral fecal route[237]. Interestingly, the more dangerous *Yersinia pestis* evolved from *Yersinia pseudotberculosis* about 6 million years ago and in the process acquired a hypoacylated TLR4 evasive LPS [238,239]. Indeed *Yersinia pestis* bacteria engineered to express E.coli LPS are potently attenuated, reducing the biocontainment classification from BSL3 to BSL2[240]. In research *Yersinia pseudotuberculosis* and *Yersinia enterocolitica* have proven exceptional models for studying host pathogen interaction without the need for BSL3 containment.

Yersinia species bacteria are known to dampen the host immune response using *Yersinia outer proteins (YOPs)* that manipulate various macrophage cytosolic processes [241]. One such protein YopJ, is known to inhibit TAK1 activation via acetylation [242], resulting in macrophage cell death [243]. Yersinia induced cell death was recently shown to be a caspase 8 dependent, RIP3 independent process. Paradoxically, while *Rip3*$^{-/-}$*Casp8*$^{-/-}$

macrophage are protected from cell death, the animals succumb to the infection, with higher bacterial burden in various solid organs [244,245]. Similarly, *Yersinia* induced macrophage cell death is strongly RIP1 kinase activity dependent, where RIP1 kinase inactive animals also show increased sensitivity to infection [246]. These studies suggest that macrophage death in the context of *Yersinia* infection is protective for the animal host. The study of MAPK inhibition and cell death in the context of bacterial infection can be expanded to other pathogens including *Bacillus anthracis* since both anthrax toxin and lethal factor inhibit MAPK activation and lead to cell death and IL1 production [247,248]. The mechanism of Caspase mediated cell death in the context of TAK1 inhibition is the central topic of investigation in our second manuscript entitled "Caspase-8 induces cleavage of multiple Gasdermins to elicit pyroptosis during *Yersinia* infection".

Chapter 2: Constitutive Interferon Signaling Maintains Critical Threshold of MLKL Expression to License Necroptosis[249]

[249] Sarhan, J., Liu, B. C., Muendlein, H. I., Weindel, C. G., Smirnova, I., Tang, A. Y., Ilyukha, V., Sorokin, M., Buzdin, A., Fitzgerald, K. A., & Poltorak, A. (2018). Constitutive interferon signaling maintains critical threshold of MLKL expression to license necroptosis. Cell Death & Differentiation.

Reprinted here with permission from publisher

2.1 Introduction

Necroptosis is a form of necrotic cell death that occurs downstream of receptor-interacting protein kinases (RIP1/RIP3) activation and the formation of plasma membrane ion channels by the pseudokinase mixed lineage kinase like-domain (MLKL)[250–252]. In the context of virus infections where apoptosis is inhibited, necroptosis engages as a secondary mode of cell death that benefits the host by limiting viral replication in infected cell[54,131]. While the virus inhibits Caspase-8 activity to subvert apoptotic cell death, necroptosis is activated when innate signaling results in RIPK1, TRIF or DAI/ZBP1 recruitment and subsequent activation of RIPK3 and MLKL. In the laboratory, the use of the small molecule pan-caspase inhibitor zVAD in conjunction with TNFα stimulation drives RIP3/MLKL dependent necroptosis[54,253]. Recently, necroptosis has been characterized to occur downstream of Toll Like Receptor (TLR) stimulation with zVAD inhibition of caspases. TLR3/4 are unique from other TLRs due to their ability to induce necroptosis via a common endosomal adaptor, TRIF (TIR-domain-containing adapter-inducing interferon-β)[67,253] independently of TNF induction. Upon engagement of TLR3/4, TRIF interacts with RIP1/RIP3 via RHIM domains, an event critical for necroptosis[253–255]. Notably, activation of TLR3/4 also induces interferon (IFN) production through TRIF[256]. With the finding that Type I IFN receptor deficient cells are resistant to TLR3/4 mediated necroptosis, TRIF was attributed the additional role of mediating necroptosis via IFN induction[257,258].

Type-I interferons (IFN-I) comprise a family of 14 α isoforms and one β, κ, ω and δ isoform each, all of which bind a common heterodimeric receptor composed of two subunits, IFN-αR1 and IFN-αR2 (IFNAR)[148]. IFNs regulate host immune responses by

binding the receptor and activating STAT1/2 transcription factors (Signal Transducer and Activator of Transcription 1 and 2) to regulate a diverse family of genes termed Interferon Stimulated Genes (ISGs)[149]. IFN-I is induced in response to cytosolic nucleic acids (RNA and DNA) or ligands of the endosomal TLRs. In contrast, constitutive IFN-I signaling in the resting state is less characterized, despite having been detected in human and mouse cells including MEFs, B cells, and macrophages[149]. It has been suggested that constitutive IFN sustains the expression of JAKs, STATs, and other components necessary for the IFN-I autocrine loop. Another function of constitutive IFN-I is to maintain basal levels of immune-related genes to enable a rapid response to viral infection[172].

Sufficient IFN signaling is critical for host defense in order to avoid potentially lethal viral and mycobacterial infections such as in STAT1 deficient individuals[259]. In contrast, excessive IFN has been linked to pathology in multiple autoimmune diseases including lupus, psoriasis, Sjogrens, dermatomyositis and type I diabetes[199]. In the case of interferonopathies including Aicardi-Goutières syndrome and STING-associated vasculopathy with onset in infancy (SAVI), IFN directly drives disease[194]. Recently, necroptosis has been linked to both IFN signaling and autoimmune disease[260,261]. Although IFNAR-deficient cells are resistant to TLR induced necroptosis, the mechanism underlying this protection as well as any connection of these findings to autoimmunity remains unclear.

In this study, we found that constitutive IFN signaling is crucial for the initiation of LPS, TNF and SMAC mimetic induced necroptosis via the endogenous activity of the cytosolic DNA sensing pathway cGAS/STING. Corroborating this finding, macrophages

from an evolutionarily divergent mouse, MOLF/Ei (MOLF), are resistant to necroptosis and deficient in resting ISG status due to an intrinsic defect in STING activation. Our findings prompt the model that constitutive IFN signaling drives the steady-state expression of MLKL to enable a rapid necroptosis response.

2.2 Results

2.2.1 Constitutive IFN signaling licenses necroptosis in macrophages

To measure cytotoxicity in mouse BMDMs, we monitored the kinetics of propidium iodide uptake in real time, which allowed us to detect cell death within the first two hours of treatment with LPS and zVAD (LZ) (Figure 2.1A). Compared to wild type cells, BMDMs from either kinase inactive RIPK1 *Rip1*$^{D138N/D138N}$, *Mlkl*$^{-/-}$ (Figure 2.1A) or RIP3 RHIM domain mutant (*Ripk3*$^{\Delta R/\Delta R}$) (Figure 2.8A) were fully resistant to LPS/ zVAD cytotoxicity, confirming necroptosis as the form of cell death.

The role of IFN in necroptosis has been studied exclusively using IFNAR-deficient animals which are unresponsive to both inducible (produced in response to stimulation) and constitutive (produced in resting cells) IFN[262]. To distinguish between inducible and constitutive IFN, we used *Ifnb*$^{-/-}$ BMDMs to establish a system that is responsive to a treatment with exogenous IFN. Like *Ifnar*$^{-/-}$ cells[257], *Ifnb*$^{-/-}$ BMDMs were completely resistant to LZ induced necroptosis (Figure 2.1B). At resting state, *Ifnb*$^{-/-}$ BMDMs exhibit reduced levels of various ISGs, including levels of STAT1 and STAT2 proteins (Figure 2.1C, Figure 2.8B), and levels of ISG15, IRF7 and MX1 mRNA (Figure 2.8C). This ISG deficiency can be rescued by the overnight treatment with a low dose (2.5 IU/ml) of recombinant IFNβ (Figure 2.1C, Figure 2.8B, C). The significant reduction of ISG expression at both the mRNA and protein level, and their responsiveness to low-dose

add-back of IFN, is consistent with *Ifnb*$^{-/-}$ mice being defective in constitutive interferon signaling. Unlike STAT1, the levels of RIP1, RIP3 and IRF3 proteins were not substantially affected by constitutive IFN status (Figure 2.1C, Figure 2.8B). In agreement with recently published work[68,262], we observed that MLKL expression is reduced in IFN-deficient BMDMs. This reduction in MLKL expression in *Ifnb*$^{-/-}$ BMDMs was rescued with a low dose (2.5 IU/ml) of recombinant IFNβ treatment overnight (Figure 2.8D).

To study the role of constitutive IFN on cell viability, we used overnight (10 hr pretreatment) or 1-hour pretreatment of cells with low dose (2.5 IU/ml) recombinant IFNβ prior to stimulation with LZ (Figure 2.1D). At 6 hours of LZ stimulation, only overnight IFNβ treatment sensitized *Ifnb*$^{-/-}$ BMDMs to necroptosis (Figure 2.1E). Since overnight treatment with 2.5 IU/ml IFNβ rescued basal ISG expression and cell death (Figure 2.1C, Figure 2.8C, Figure 2.1E), we hypothesized that one or more component(s) of the necroptotic pathway are restored in *Ifnb*$^{-/-}$ BMDMs by overnight pre-treatment with IFN. We observed gradual upregulation of *Irf7* and *Isg15* over time with IFN treatment (Figure 2.8E), further arguing that time is required for ISG status to stabilize. To study the inverse of IFN addition, we used IFNAR blocking antibody to block either stimulus-induced IFN (-1 hr Antibody pre-TX) or constitutive IFN signaling (-36 hrs Antibody) (Figure 2.1F). Both one hour and 36-hour treatment of blocking antibody inhibited STAT1 phosphorylation in B6 BMDMs when stimulated with IFNβ (Figure 2.1G). However, only 36-hours treatment with the blocking antibody decreased total STAT1 protein level (Figure 2.1G). Correspondingly, 36-hours blockade of IFNAR abolished necroptosis in B6 BMDMs (Figure 2.1H), whereas 1-hour blockade of IFNAR had no effect on cell death (Figure 2.1I). These data establish that the cellular potential for

initiating necroptosis is determined by IFN signaling that is present at steady-state, otherwise known as constitutive IFN signaling.

To extend our findings to other models of necroptosis, we treated BMDMs with TNF and zVAD (TZ). Our kinetic approach was instrumental in showing that TNF induced cytotoxicity is slower than LPS induced cell death in C57BL/6J macrophages (Figure 2.1J), suggesting that additional feedback may be required for initiation of TZ cytotoxicity. As with LZ-induced necroptosis, *Ifnb*$^{-/-}$ BMDMs were resistant to TZ induced necroptosis (Figure 2.1J). Interestingly, unlike LZ-induced necroptosis, TZ-necroptosis was sensitized by either overnight or 1 hour IFNβ pretreatment *Ifnb*$^{-/-}$ BMDMs (Figure 2.1K,L). We postulate that since TZ-induced cytotoxicity initiates later than LPS induced necroptosis (Figure 2.1J), it gives more time for IFNβ add-back concurrent with TZ stimulation to restore the missing ISG(s) during the early hours of stimulation to allow necroptosis to proceed. In support of this hypothesis, only 24 hours of IFNAR blockade was protective against TZ induced cell death, whereas 1 hour had no effect on cell death (Figure 2.8F). We also investigated the SMAC-mimetics (SM) and zVAD model of necroptosis, which unlike TNF and zVAD, resulted in the same kinetics and magnitude of cell death as LPS and zVAD treatment (Figure 2.8G). Like LZ treatment, *Ifnb*$^{-/-}$ BMDMs were resistant to SM + zVAD induced cytotoxicity and could be sensitized to necroptosis after overnight treatment with low dose IFNβ (Figure 2.8H).

To determine the relevance of our findings to necroptosis of human cells, we first confirmed that LPS and zVAD induces cell death in human monocyte derived macrophages (MDM), in a manner that is reversible with addition of Necrostatin-1 (Figure 2.8I). Next, we blocked IFN signaling with the JAK1/2 inhibitor Ruxolitinib

(Rux) in human monocyte-derived macrophages for either 1-hour prior, or 36 hours prior to LZ stimulation. Consistent with the function of constitutive IFN in maintaining ISG expression, chronic Rux treatment downregulated *Irf7* expression in resting cells (Figure 2.8J). Furthermore, 36 hr but not 1-hour Rux pretreatment downregulated total STAT1 levels, although both treatments effectively inhibited STAT1 phosphorylation in response to exogenous IFNβ (Figure 2.8K). Rux treatment did not affect MLKL levels in human cells (Figure 2.8K). Consistent with our findings in murine macrophages, we saw that chronic Jak inhibition protected human MDMs against LZ induced necroptosis (Figure 2.8L, M). Treatment of human MDMs with IFNAR blocking antibody inhibited most of the STAT1 phosphorylation in response to exogenous IFNβ (Figure 2.8N). However, 36-hour treatment with IFNAR blocking antibody did not reduce total STAT1 levels (Figure 2.8N) or IRF7 expression (Figure 2.8O). Accordingly, 36-hour IFNAR blocking antibody did not protect human MDMs from LZ treatment (Figure 2.8P). These data suggest that either the blocking antibody is not adequately blocking IFNAR signaling or there exists another IFNAR independent, JAK dependent constitutive signal in human MDMs.

Collectively, these data show that constitutive IFN signaling is required for initiation of necroptosis downstream of LPS, TNFα and SMAC-mimetic in BMDMs. The duration of signaling required for sensitization of IFN-deficient cells suggests that time is necessary to upregulate one or more effectors of necroptosis.

2.2.2 The Endosomal TLR4 adaptor TRIF initiates necroptosis independently of IFNβ induction

TRIF (encoded by*Ticam1*), a key adaptor downstream of TLR4, is required for both LPS-induced IFN (Figure 2.2A) as well as LPS/zVAD driven cell death (Figure 2.2B).

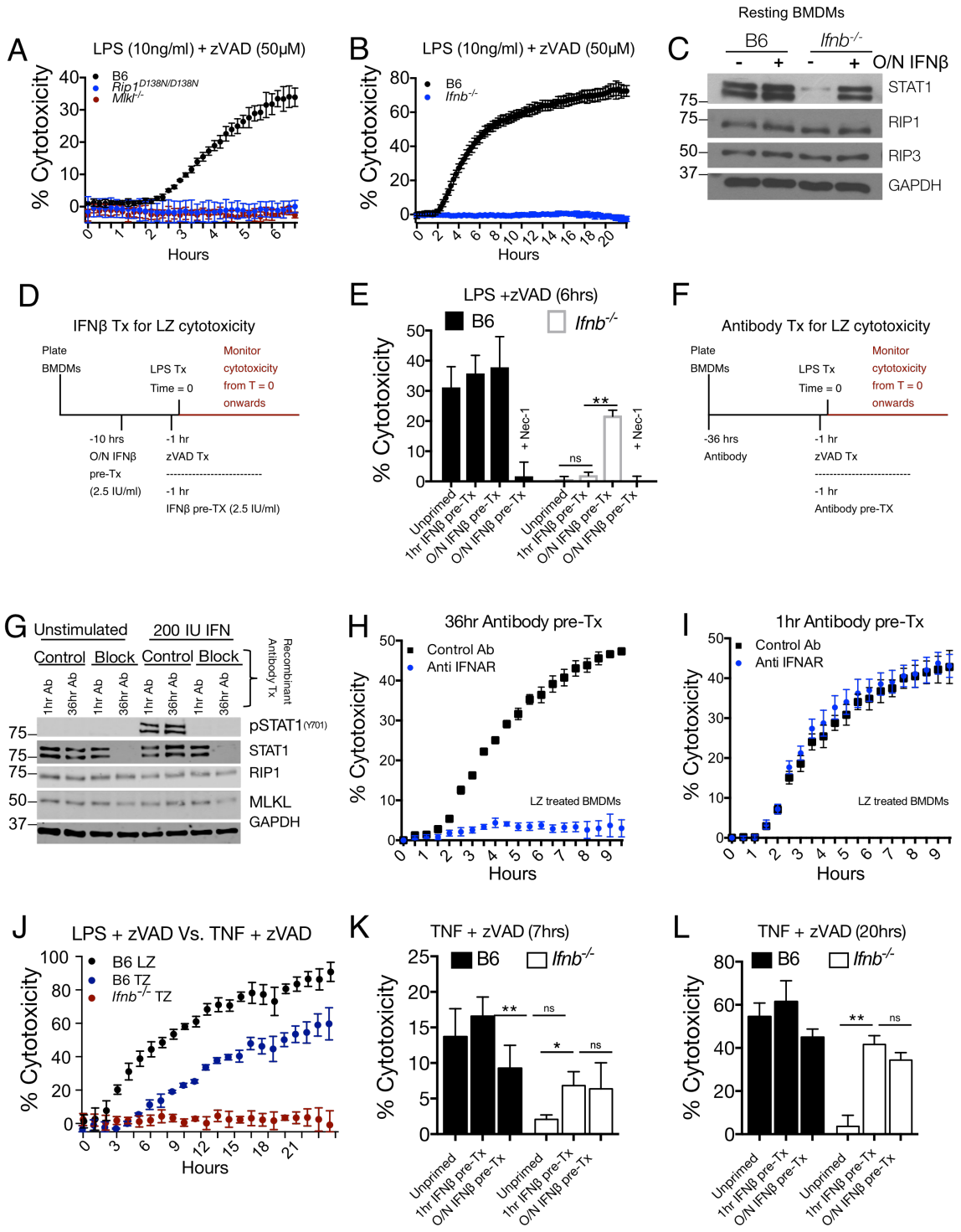

Figure 2.1: Constitutive type-I interferon (IFN-I) signaling is required for initiation of necroptosis

(A,B) Propidium iodide incorporation as a readout of cytotoxicity, measured every 15 minutes following LPS/zVAD treatment of BMDMs of indicated genotype. (C) Western

blot of indicated proteins of resting BMDMs from B6 and *Ifnb*$^{-/-}$ with or without overnight interferon treatment (2.5 IU IFNβ/ml). (D) Treatment scheme for overnight or 1hr treatment of BMDMs with 2.5 IU/ml of recombinant IFNβ. (E) Viability of B6 and *Ifnb*$^{-/-}$ BMDMs measured 6 hrs after LPS /zVAD treatment. (F) Treatment scheme for overnight or 1hr antibody treatment of B6 BMDMs. (G) Western blot for indicated proteins from B6 BMDMs treated with antibodies as in (F) before stimulation with 200 IU/ml IFNβ for 30 minutes. (H, I) Propidium iodide incorporation of B6 BMDMs treated with LZ and antibody pretreatment for 36 hour (H) or 1 hour (I) as in (F). (J) Propidium iodide incorporation over 22 hours of B6 BMDMs treated with LPS/zVAD or TNF (50 ng/ml) /zVAD (50 μM) and *Ifnb*$^{-/-}$ BMDMs treated with TNF/zVAD. (K,L) Cytotoxicity measurement at 7 hours (K) or 20 hours (L) from B6 and *Ifnb*$^{-/-}$ BMDMs treated with TNF/zVAD with IFN pre-treatment as in (D). All LPS/zVAD treatments were: LPS [10ng/ml] and zVAD [50uM/ml]. In all cases of IFNβ pre-treatment (overnight or one hour), the IFNβ is washed away before addition of experimental conditions. Time point cytotoxicity quantification +/- SD from three independent experiments compared using student two tailed t test: ns is non-significant ($p > 0.05$); *$p < 0.05$; **$p<0.01$; ***$p < 0.001$. All western blot and kinetic cytotoxicity data are representative of three or more experiments.

During LZ-induced necroptosis, TRIF has been shown to interact with RIP1/RIP3 via RHIM domain interactions[67]. Recently, the resistance of *Ticam1*$^{-/-}$ BMDMs to cell death was attributed to their inability to produce IFN upon LPS stimulation[257], leading to a model that proposes LZ-induced necroptosis to be driven by TRIF-mediated IFN autocrine signaling. In B6 BMDMs, we found that IFNβ, even when used at supraphysiologic doses of up to 4000U/ml, is not sufficient to drive necroptosis in the context of caspase inhibition (Figure 2.2C). To determine whether TRIF dependent IFN production is necessary for LPS induced necroptosis, we treated B6 and *Ticam*$^{-/-}$ BMDMs with a high dose of exogenous IFNβ (200 U/ml) concurrent with LZ stimulation. We found that 200U/ml of IFNβ with LZ stimulation did not augment cell death in B6 BMDMs, nor did it sensitize *Ticam1*$^{-/-}$ BMDMs to necroptosis (Figure 2.2D). Furthermore, we found that TRIF deficient cells were fully sensitive to the TLR-independent process of SM induced necroptosis (Figure 2.2D), indicating that the requirement for TRIF is specific to TLR-induced necroptosis pathways. *Ticam1*$^{-/-}$

BMDMs exhibited normal levels of ISGs at steady-state (Figure 2.2E), indicating that TRIF is dispensable for constitutive IFN production.

The discrepancy between our data and published reports regarding the necroptotic potential of (IFN+ zVAD) treatment may be explained by the purity grade of BSA, a carrier protein frequently used to dilute recombinant IFN. We use endotoxin Free BSA (Endotoxin level is less than 1 EU/mg) from Akron Biotech (SKU: AK8917) for re-constitution of recombinant protein. We compared re-constituted IFN in 0.1% BSA from either endotoxin free BSA (SKU: AK8917) or Fisher brand BSA (BP1600-100) to a concentration of 10 IU IFNβ/ ml. We did not observe cell death (Figure 2.9A) or TNF (Figure 2.9B) production with IFN and zVAD treatment of BMDMs with IFN re-constituted in endotoxin Free BSA. However, when IFN is diluted with Fisher brand BSA, both TNF production and necroptosis were observed and furthermore dependent on TLR4.

These data imply that TRIF promotes necroptosis in a manner independent of its IFN-inducing activities during LPS/zVAD stimulation and confirm that constitutive IFN production in macrophages is independent of TRIF signaling. Our data support the model in which TRIF associates with RIP1 and RIP3 through RHIM (Rip homotypic interaction motif) domain interactions to induce necroptosis[67].

2.2.3 The DNA sensing pathway cGAS/STING is required for constitutive interferon production

Aberrant DNA presence, either from the nucleus[263], mitochondria[264], or lysosomes[265], can activate the cytosolic DNA sensing pathway via cGAS and STING to upregulate IFN. Indeed, BMDMs lacking STING and the DNA-sensor cGAS had reduced levels of

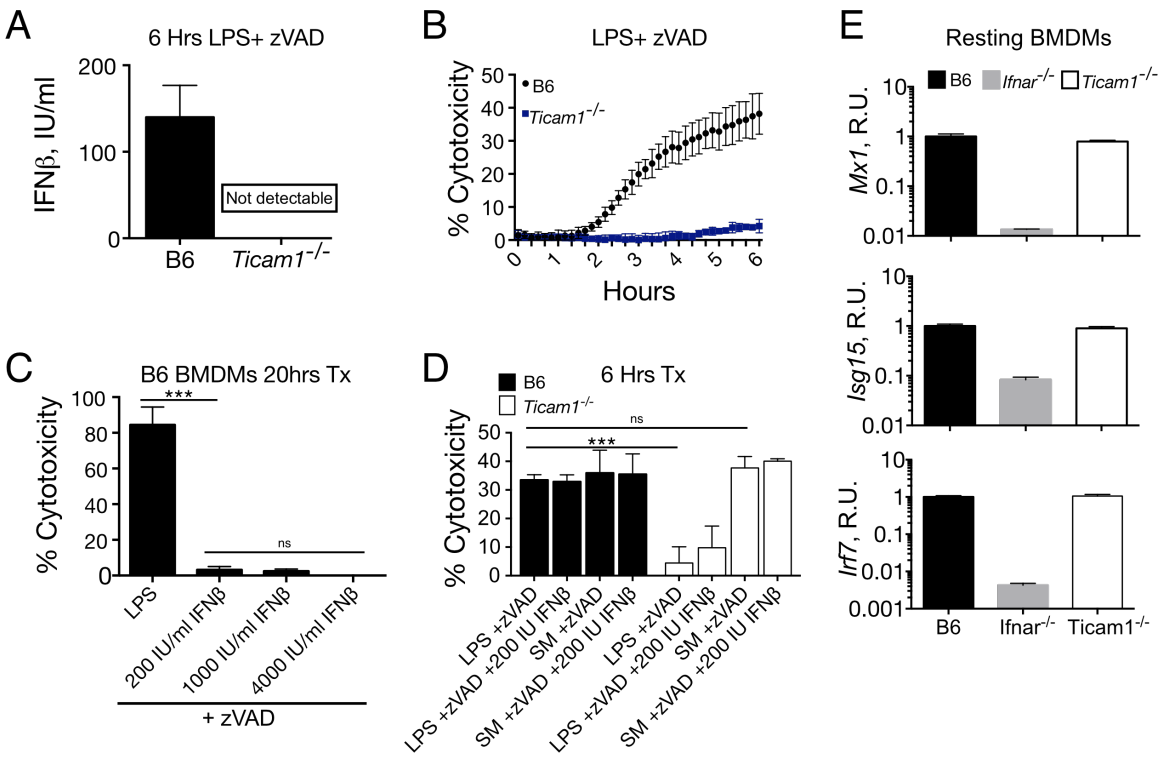

Figure 2.2: The Endosomal TLR4 adaptor TRIF initiates necroptosis independently of LPS induced IFNβ

(A) Supernatant IFNβ cytokine measured by ELISA from B6 and *Ticam1*$^{-/-}$ BMDMs stimulated with LPS/zVAD for 6 hours. (B) Propidium iodide incorporation following LPS/zVAD treatment of B6 and *Ticam1*$^{-/-}$ BMDMs as a read-out of cytotoxicity. (C) Cytotoxicity by PI incorporation of B6 BMDMs treated for 20 hours with LPS/zVAD or varying doses of IFNβ and zVAD. (D) Propidium iodide incorporation of B6 and *Ticam1*$^{-/-}$ BMDMs six hours following LPS/zVAD or SM (1nM)/zVAD treatment with or without 200 IU IFNβ. (E) Quantitative PCR of *Irf7*, *Isg15*, and *Mx1* mRNA relative to *Gapdh* from resting B6, *Ifnar*$^{-/-}$ and *Ticam1*$^{-/-}$ BMDMs. All LPS/zVAD treatments were: LPS [10ng/ml] and zVAD [50uM/ml]. Time point cytotoxicity quantification +/- SD from three independent experiments compared using student two tailed t test: ns is non-significant ($p > 0.05$); *$p < 0.05$; **$p<0.01$; ***$p < 0.001$. All qPCR and kinetic cytotoxicity data are representative of three or more experiments.

Isg15, *Irf7*, and *Mx1* mRNAs and low levels of STAT1 protein (Figure 2.3A,B; Figure 2.10A, B), indicating that the cytosolic sensing pathway could sustain constitutive IFN signaling. Consistent with the defect in ISG signature, STING- and cGAS-deficient BMDMs were resistant to LZ induced early-onset (6 hours) necroptosis (Figure 2.3C).

This resistance to cell death was reversed with overnight but not 1hr treatment with low dose (2.5 IU/ml) of exogenous IFNβ. The resistance of these IFN deficient BMDMs to necroptosis is not due to a deficiency in RIP1, RIP3 or Ticam1 expression (Figure 2.9C).

Interestingly, untreated *Sting*$^{-/-}$ BMDMs become sensitized to cytotoxicity over time, which was in sharp contrast to the complete resistance to cell death of *Ifnb*$^{-/-}$ BMDMs (Figure 2.3D). We hypothesized that LZ-induced IFNβ might sensitize *Sting*$^{-/-}$ cells to cytotoxicity over time. Indeed, we observed STAT1 phosphorylation in response to LZ treatment in *Sting*$^{-/-}$ BMDMs, despite the low STAT1 protein abundance (Figure 2.3E). To further confirm the role of LZ-induced IFN in BMDMs deficient for the DNA-sensing pathway, *Sting*$^{-/-}$ and *cGAS*$^{-/-}$ BMDMs were stimulated with LZ in the presence of IFNAR blocking antibody MAR1 or isotype control antibody (antibodies were added 1 hour prior to LZ stimulation). Blocking IFNAR during LZ stimulation protected both *Sting*$^{-/-}$ and *cGAS*$^{-/-}$ BMDMs from necroptosis, but did not affect cell death in B6 BMDMs (Figure 2.3F; Figure 2.10C). These findings strongly suggest that in cells deficient for constitutive IFN signaling, the induced IFN is able to restore the missing ISGs to sensitize cells to necroptosis. Additionally, we found that *Sting*$^{-/-}$ and *cGAS*$^{-/-}$ BMDMs were completely resistant to TNF/zVAD induced cell death (Figure 2.10E, F), consistent with the notion that TNF stimulation does not induce a potent ISG response.

Since TLR4-mediated LPS signaling engages both MyD88 and TRIF, we extended our findings to TLR3 mediated TRIF dependent necroptosis by stimulating BMDMs with polyinosinic-polycytidylic acid (pI:C) in the presence of zVAD. Consistent with our previous findings with LPS-zVAD, *Ifnar*$^{-/-}$ BMDMs were fully resistant to cell death, and *Sting*$^{-/-}$ and *cGAS*$^{-/-}$ BMDMs were kinetically delayed (Figure 2.10G).

We additionally found that IFNβ production is dampened in *Sting*$^{-/-}$ BMDMs compared to B6 macrophages in response to both LPS and LZ stimulation (Figure 2.10H, I). Priming *Sting*$^{-/-}$ BMDMs with low dose IFNβ overnight augmented the IFNβ production upon subsequent stimulation with LPS or LZ, consistent with feed forward regulation[266]. The same effect was not observed for TNF, indicating the IFN feed forward regulation may only apply to selected cytokines (Figure 2.10J, K).

2.2.4 Low IFN-signaling status confers resistance to necroptosis in MOLF/Ei macrophages

We have previously reported that resistance to necroptosis in peritoneal macrophages of the wild-derived MOLF mice is conferred by downregulation of the deubiquitinase CYLD (Cylindromatosis)[267]. Like peritoneal macrophages, MOLF BMDMs were also resistant to LZ induced necroptosis (Figure 2.10L), however CYLD expression was maintained in MOLF BMDMs (Figure 2.10M), thus indicating another mechanism for resistance to necroptosis. Recently, we characterized a hypomorphic allele of *Sting* in MOLF mice that confers low levels of IFN production in response to cytosolic DNA[268]. Since *Sting*$^{-/-}$ and *cGAS*$^{-/-}$ BMDMs were resistant to cell death due to their reduced steady-state IFN signature, we investigated if the *in natura* defect in *Sting* on the MOLF background may play a role in necroptosis via regulation of constitutive IFN signaling. Notably, we found that MOLF BMDMs were deficient for the expression of multiple ISGs at steady-state (Figure 2.3G). Nevertheless, MOLF macrophages readily underwent STAT1 phosphorylation and restored STAT1 protein levels in response to exogenous IFNβ1, suggesting that the defect in constitutive IFN signaling does not result from a defect in IFNAR function (Figure 2.10N). Like other constitutive IFN deficient cells,

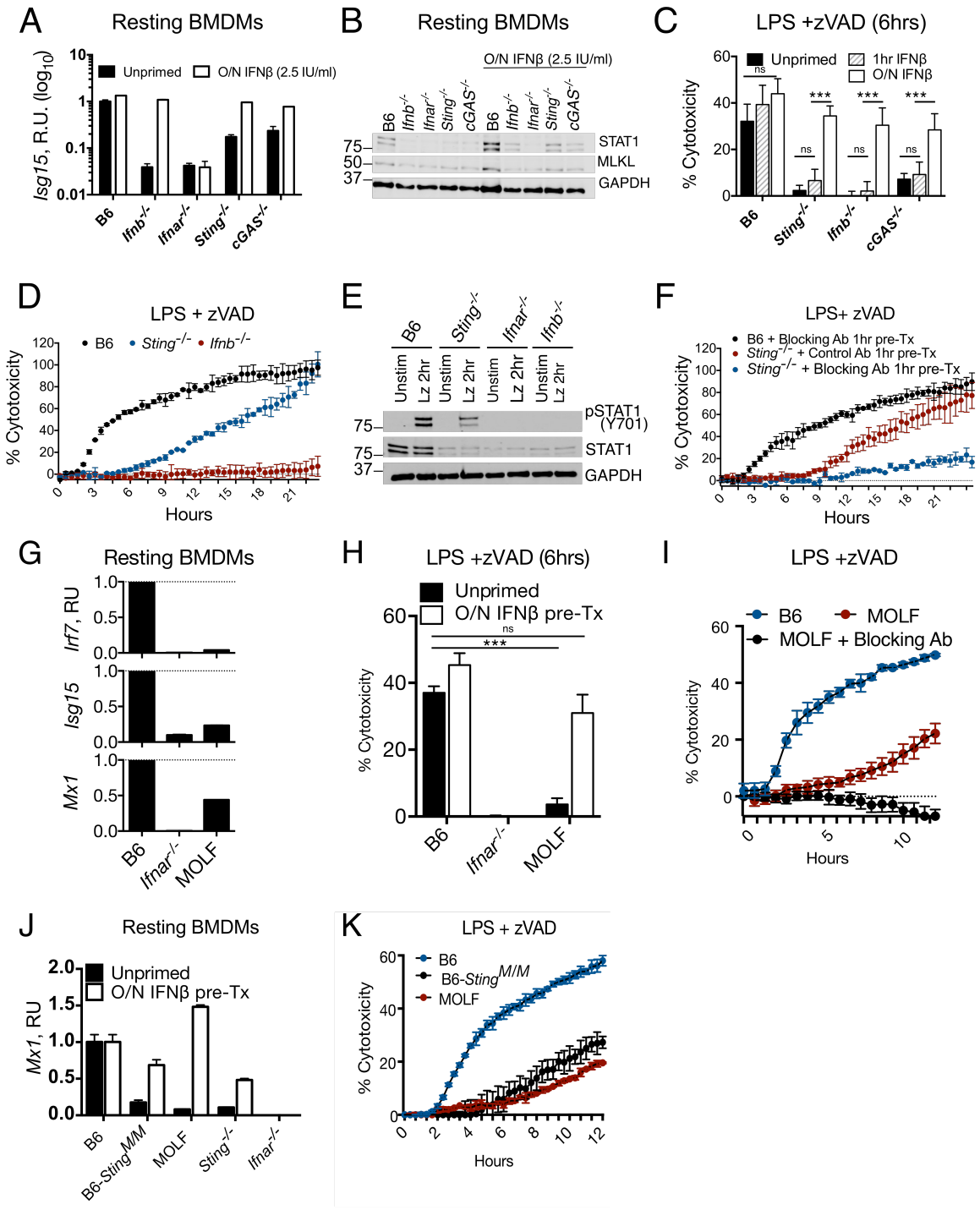

Figure 2.3: Cytosolic DNA sensing via cGAS and STING is required for constitutive interferon production

(A) Quantitative PCR of Isg15 and western blot of indicated proteins (B) from resting B6, *Ifnb*$^{-/-}$, *Ifnar*$^{-/-}$, *Sting*$^{-/-}$, and *cGAS*$^{-/-}$ BMDMs that were untreated or pre-treated with IFNβ overnight (2.5 IU IFNβ/ml). (C) Propidium iodide incorporation six hours following LPS /zVAD treatment of BMDMs, either not treated with IFN (unprimed),

pretreated with 2.5 IU IFNβ/ml overnight or 1 hour before LPS treatment. (D) 22 hrs time course of propidium iodide incorporation of B6, *Sting*$^{-/-}$, *Ifnb*$^{-/-}$, BMDMs stimulated with LPS/zVAD. (E) Western blots of pSTAT1 and STAT1 from BMDMs of indicated genotype either unstimulated or 2hrs LPS/zVAD stimulated. (F) B6 and *Sting*$^{-/-}$ BMDMs pretreated one hour with MAR1 IFNAR blocking or isotype control antibody and monitored for LPS/zVAD induced cytotoxicity. (G) Quantitative PCR of ISG mRNA relative to GAPDH mRNA from resting B6, *Ifnar*$^{-/-}$ and MOLF BMDMs. (H) Propidium iodide incorporation 6 hours following LPS /zVAD treatment of B6, *Ifnar*$^{-/-}$ and MOLF BMDMs with or without overnight interferon pre-treatment (2.5 IU IFNβ/ml). (I) Propidium iodide incorporation during 12 hours of stimulation with LZ of B6 and MOLF BMDMs with or without one hour MAR1 IFNAR blocking antibody pre-treatment. (J) Quantitative PCR of MX1 mRNA relative to GAPDH mRNA from resting BMDMs of indicated genotype without overnight 2.5 IU IFNβ/ml. (K) Propidium iodide measurement over 12 hours of LPS /zVAD treatment of B6, N10 congenic B6 *Sting*$^{MOLF/MOLF}$, and MOLF BMDMs. All LPS/zVAD treatments were: LPS [10ng/ml] and zVAD [50uM/ml]. In all cases of IFNβ pre-treatment (overnight or one hour), the IFNβ is washed away before addition of experimental conditions. Time point cytotoxicity quantification +/- SD from three independent experiments compared using student two tailed t test: ns is non-significant ($p > 0.05$); *$p < 0.05$; **$p<0.01$; ***$p < 0.001$. All western blot and kinetic cytotoxicity data are representative of three or more experiments.

MOLF BMDMs were sensitized to cytotoxicity with overnight low dose IFN priming (Figure 2.3H). Of note, MOLF BMDMs exhibited slow necroptosis kinetics that resembled that of *Sting*$^{-/-}$ and *cGAS*$^{-/-}$ BMDMs (Figure 2.3F) and similarly, IFNAR blockade during LZ stimulation prevented late time point sensitization to necroptosis in MOLF macrophages (Figure 2.3I).

To further examine the contribution of the MOLF allele of *Sting* in defective constitutive IFN signaling and necroptotic potential, we tested BMDMs from mice that are congenic for the MOLF allele of *Sting* on the C57BL/6 background (B6-*Sting*$^{M/M}$) for cell death and status of constitutive IFN signaling. Indeed, we observed low levels of constitutive IFN in B6-*Sting*$^{M/M}$ BMDMs, as exemplified by MX1 mRNA and STAT1 protein levels (Figure 2.3J; Figure 2.10O). Additionally, B6-*Sting*$^{M/M}$ BMDMs showed very similar kinetics of LZ induced necroptosis compared to parental MOLF cells, thus

confirming that MOLF *Sting* contributes to the low constitutive IFN signaling that results in resistance to necroptosis (Figure 2.3K).

2.2.5 Interferon receptor signaling is required for RIP1 and RIP3 degradation and MLKL S345 phosphorylation in BMDMs

To determine the step at which constitutive IFN is needed for LZ necroptosis, we looked at the initiating events in LPS signaling, including TLR4 endocytosis followed by engagement of TRIF and IRF3 phosphorylation[155]. Here we observed that *Ifnb*$^{-/-}$ BMDMs underwent TRIF dependent Serine 396 IRF3 phosphorylation when stimulated with LPS and LPS/zVAD, indicating that constitutive IFN is not required for the early events of TLR4 signaling leading to IRF3 activation (Figure 2.4 A; Figure 2.11A). Additionally, RIP1 modification (a molecular weight shift previously reported as phosphorylation[257] was present in *Ifnb*$^{-/-}$ BMDMs (Figure 2.4A). Interestingly, the loss of either MyD88 or TRIF individually did not impact RIP1 modification (Figure 2.4A) suggesting that a kinase activated via either MyD88 or TRIF acts on RIP1 (Figure 2.11B).

To investigate the activity of RIP1 and RIP3, we first established that LZ-induced biochemical modifications of RIP1 and RIP3 are indeed reversed by the RIP1 kinase inhibitor Nec-1. We found that RIP1 Serine 166 phosphorylation, as well as depletion of RIP1 and RIP3 total protein, were reversed by the addition of Nec1, marking these as events dependent on RIP kinase activity (Figure 2.11C). We were not able to detect LPS/zVAD-induced RIP3 modifications or significant alterations in RIP3 Serine 232 phosphorylation, previously reported as an activating modification in a model of RIPK dimerization induced necroptosis[269]. We found that *Ifnb*$^{-/-}$ BMDMs undergo RIP1 S166 phosphorylation in whole cell lysates and that overnight recombinant IFN treatment,

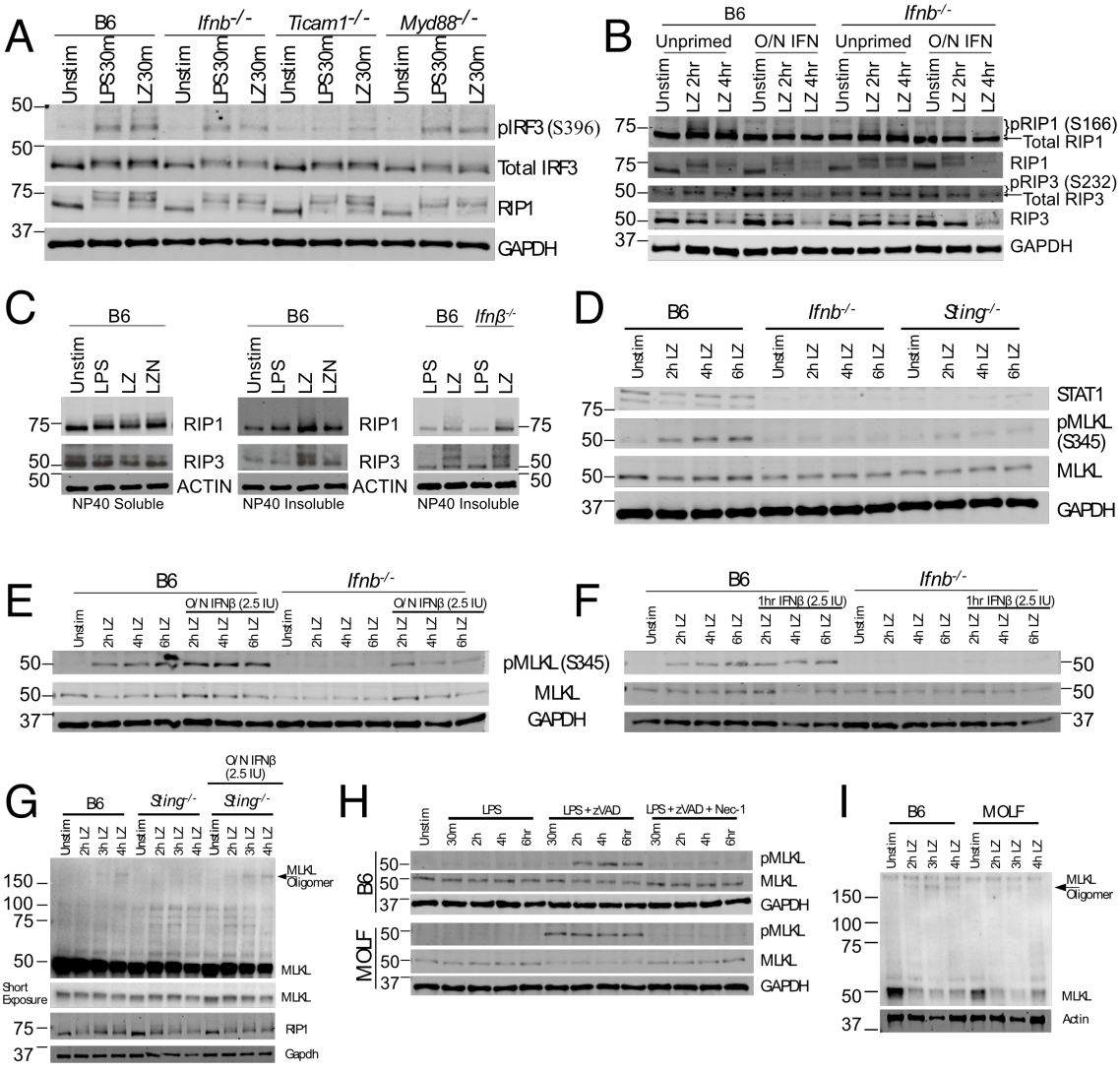

Figure 2.4: Interferon receptor signaling is required for MLKL phosphorylation in B6 BMDMs

Western blots of pIRF3 (S396), total IRF3, RIP1 and GAPDH from unstimulated, 30 minutes LPS or LPS /zVAD stimulated BMDMs from B6, *Ifnb*$^{-/-}$, *Ticam1*$^{-/-}$ and *Myd88*$^{-/-}$ mice. (B) Western blots of indicated proteins from B6 and *Ifnb*$^{-/-}$ BMDMs with or without overnight 2.5 IU/ml IFNβ treated with LPS/zVAD. (C) Western blots of RIP1 and RIP3 kinases in BMDMs of indicated genotypes in NP40 soluble or insoluble fractions. (D) Western blots of indicated proteins from B6, *Ifnb*$^{-/-}$ and *Sting*$^{-/-}$ BMDMs treated with LPS /zVAD for indicated duration of time. (E-F) Western blots of phospho MLKL (pMLKL), MLKL and GAPDH from B6 and *Infb*$^{-/-}$ BMDMs that were untreated or primed with 2.5 IU IFNβ/ml overnight. (E) or one hour (F) and treated with LPS /zVAD. (G) Non-reducing western blot featuring MLKL oligomers from B6 and *Sting*$^{-/-}$ BMDMs (with or without 2.5 IU/ml IFNβ overnight) treated with LPS /zVAD for indicated times. (H) B6 and MOLF BMDMs were treated with LPS, LPS /zVAD or LPS /zVAD/ Nec-1 for indicated durations and analyzed for indicated proteins by western blotting. Nec-1 was used at a concentration of 30μM. (I) Non-reducing western blot

featuring MLKL oligomers from B6 and MOLF BMDMs treated with LPS /zVAD for indicated times. All LPS/zVAD treatments were: LPS [10ng/ml] and zVAD [50uM/ml]. In all cases of IFNβ pre-treatment (overnight or one hour), the IFNβ is washed away before addition of experimental conditions. All western blot data are representative of three or more independent experiments.

interestingly, abolishes this S166 phosphorylation (Figure 2.4B). However, *Ifnb*$^{-/-}$ BMDMs do not undergo RIP1 and RIP3 total protein depletion unless primed overnight with recombinant IFN (Figure 2.4B). To further examine RIP1 kinase dependent processes, we utilized NP-40 detergent insoluble fraction of cellular lysates to look for RIP1 and RIP3 modifications in amyloid-like "necrosomes"[55]. Consistent with published reports on LPS/zVAD necroptosis[270], RIP1 and RIP3 modifications were present in the NP-40 detergent insoluble cellular compartments in a RIP kinase dependent manner (Figure 2.4C; 2.11D). RIP1 and RIP3 modifications in the NP-40 insoluble compartment were not reduced in *Ifnb*$^{-/-}$ BMDMs (Figure 2.4C).

Using MLKL Serine 345 phosphorylation as a read-out for LZ-stimulated cell death, we found that MLKL phosphorylation is profoundly deficient in *Ifnb*$^{-/-}$ and *Sting*$^{-/-}$ BMDMs (Figure 2.4D). Similar to the other effects of IFN re-constitution, the loss of MLKL phosphorylation in *Ifnb*$^{-/-}$ BMDMs was rescued with a low dose IFNβ treatment overnight prior to LZ stimulation (Figure 2.4E), but not when IFNβ was added at the time of LZ stimulation (Figure 2.4F). These results were in agreement with recent reports showing requirement of IFNAR-mediated signaling for MLKL phosphorylation[262]. Furthermore, we found that 36 hours - but not 1 hour - treatment with IFNAR blocking antibody reduced MLKL phosphorylation (Figure 2.11F, G). Downstream of phosphorylation, MLKL forms oligomers, which can be detected under non-reducing SDS PAGE (Figure 2.11H). Consistent with defective MLKL phosphorylation, *Sting*$^{-/-}$,

Ifnar$^{-/-}$ and *cGAS*$^{-/-}$ BMDMs were deficient in MLKL oligomerization (Figure 2.4G; Figure 2.11I,J).

On the C57BL/6 genetic background, our results indicate that constitutive IFN is required upstream of MLKL phosphorylation and oligomerization. In contrast to this, we found that MOLF BMDMs, which are resistant to necroptosis (Figure 2.3I), robustly phosphorylate MLKL, even in the absence of constitutive IFN signaling (Figure 2.4H; Figure 2.11K). Interestingly, MOLF BMDMs only weakly oligomerize MLKL (Figure 2.4I). Taken together, these findings strongly suggest the presence of a regulatory step between MLKL phosphorylation and MLKL oligomerization in MOLF BMDMs and provide rationale for further investigation of necroptosis in evolutionary divergent mouse strains.

2.2.6 Critical threshold of MLKL expression determines oligomerization

B6-*Sting*$^{M/M}$ BMDMs when compared to B6 BMDMs (Figure 2.5A). Some of these genes may play a role as an activator of necroptosis that requires constitutive IFN for expression. Additionally, we found approximately 50 genes that are significantly up-regulated in the absence of constitutive IFN (Figure 2.5B), which would be consistent with the model of IFN-signaling suppressing an inhibitor of necroptosis. Known inhibitors of necroptosis including Ppm1b[271], TRAF2[272], CHIP[273] and components of the ESCRT-I and III machinery[274] are un-altered by constitutive IFN status (Figure 2.12A,B). To our knowledge, the list of differentially expressed genes (Figure 2.5A,B) do not contain any genes that are currently thought to play a role in necroptosis, and thus could be informative for finding new component(s) of the pathway. Amongst abundantly expressed genes (FPKM >4) sorted by differential expression between B6 and *Ifnar*$^{-/-}$

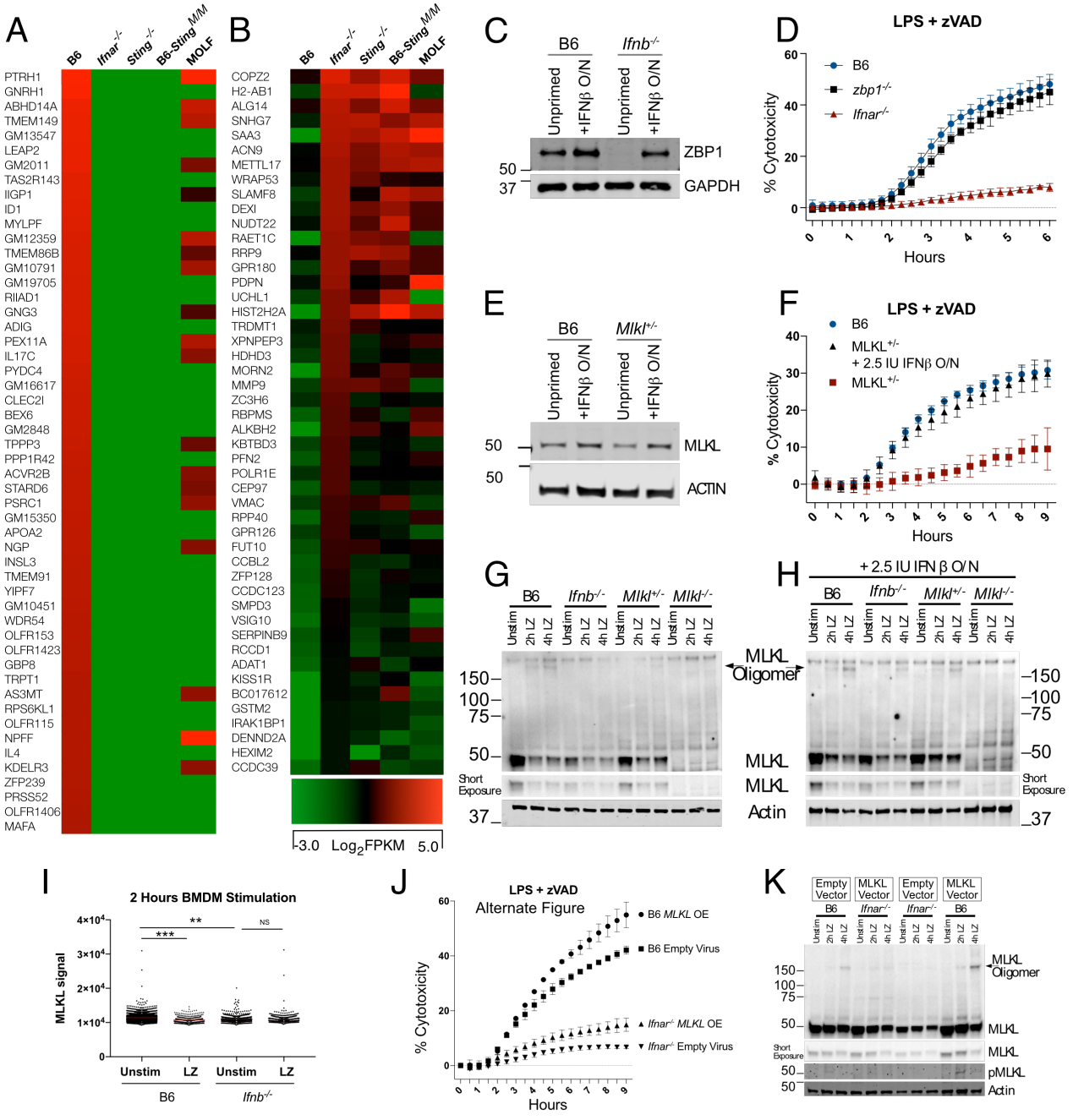

Figure 2.5: Critical threshold of MLKL expression determines oligomerization potential

(A) RNA sequencing of resting BMDMs showing genes downregulated in *Ifnar*$^{-/-}$, *Sting*$^{-/-}$, *Sting*$^{MOLF/MOLF}$ and MOLF compared to B6 (B) and significantly higher in expression compared to B6. (C) Western blot of ZBP1 in non-treated or O/N 2.5 IU/ml IFNβ treated B6 and *Ifnb*$^{-/-}$ BMDMs. (D) 6 hrs time-course of viability of LPS/zVAD treated B6, *Zbp1*$^{-/-}$, and *Ifnar*$^{-/-}$ BMDMs. (E) Western blot of MLKL in non-treated or O/N 2.5 IU/ml

IFNβ treated B6 and *Mlkl*$^{+/-}$ BMDMs. (F) 9 hrs time-course of viability of LPS/zVAD treated B6 and *MLKL*$^{+/-}$ BMDMs. (G,H) Non-reducing western blot featuring MLKL oligomers from BMDMs of indicated genotype treated with LPS /zVAD either non IFNβ primed (G) or treated overnight with 2.5 IU/ml IFNβ (H). (I) High content imaging of endogenous MLKL in PFA fixed B6 and *Ifnb*$^{-/-}$ BMDMs treated two hours with LPS/zVAD. (J,K) B6 and *Ifnar*$^{-/-}$ BMDMs transduced with either empty virus or MLKL over expressing virus and analyzed for LZ induced cytotoxicity (J) and non-reducing western blots for MLKL oligomerization and phosphorylation (K). All LPS/zVAD treatments were: LPS [10ng/ml] and zVAD [50uM/ml]. In all cases of IFNβ pre-treatment (overnight or one hour), the IFNβ is washed away before addition of experimental conditions. MLKL signal compared using student two tailed t test: ns is non-significant ($p > 0.05$); *$p < 0.05$; **$p<0.01$; ***$p < 0.001$. All western blot and kinetic cytotoxicity data are representative of three or more experiments.

BMDMs was *Zbp1* (Figure 2.12C), which encodes a protein product (ZBP1/DAI) capable of interacting with RIP3 to induce necroptosis during development[275,276] and in response to influenza A virus infection[277]. We observed that ZBP1 protein levels depended on constitutive IFN signaling (Figure 2.5C). However, *Zbp1*$^{-/-}$ BMDMs were not protected from LPS induced necroptosis (Figure 2.5D) or MLKL phosphorylation (Figure 2.12D). We also checked the ISG expression status in resting *Zbp*$^{-/-}$ cells since ZBP1 was initially characterized as a cytosolic DNA sensor[278], and found no defect in the basal expression of multiple ISGs in *Zbp1*$^{-/-}$ BMDMs (Figure 2.12D).

MLKL also appears within our genome wide analysis comparing resting gene expression in constitutive IFN deficient BMDMs (Figure 2.12E). Additionally, we have seen lower baseline expression of MLKL in multiple instances in (Figure 2.1G, 2.3B, 2.4D,E,F and Figure 2.8D, 2.11F). We found BMDMs from MLKL hemizygous animals (*Mlkl*$^{+/-}$) to be defective in baseline levels of MLKL (Figure 2.5E). Interestingly, *Mlkl*$^{+/-}$ BMDMs were resistant to both LPS + zVAD (FIgure 2.5F) and SM-164 + zVAD (Figure 2.12F) induced necroptosis. We found that *Mlkl*$^{+/-}$ BMDMs were not deficient in MLKL

phosphorylation (Figure 2.12G), but were deficient in MLKL oligomerization (Figure 2.5G), which can be rescued with low dose IFNβ priming (Figure 2.5H).

Further evidence for the critical role of basal MLKL expression in determining cell death potential comes from high content imaging of endogenous MLKL. As expected, there is a gradient of expression in resting cells, which is significantly lower in *Ifnb*$^{-/-}$ compared to B6 BMDMs (Figure 2.5I). Interestingly, we observed selective loss of cells expressing higher levels of MLKL in B6 BMDMs post LPS+zVAD treatment, indicative of necroptosis in MLKL-sufficient cells (Figure 2.5I; Figure 2.12H).

We over-expressed MLKL in IFNAR deficient BMDMs to see if MLKL alone is sufficient to restore cell death. There was limited re-sensitization towards cell death (Figure 2.5J; Figure 2.12I) or oligomerization, even though resting expression of MLKL was restored in *Ifnar*$^{-/-}$ BMDMs (Figure 2.5K). Together these results show that while adequate MLKL expression is a critical for cell death, adequate MLKL in cells that are otherwise deficient for IFNAR signaling is not sufficient for necroptosis. Therefore, there exist other unidentified ISGs regulating necroptosis.

2.2.7 Elevated Steady-state IFN Predispose Cells to Necroptosis

Serum of patients with autoimmunity is marked by elevated levels of circulating IFN[186]. With our finding that pre-established IFN status determines necroptotic potential, we wanted to investigate if elevated IFN signaling, especially in the context of autoimmunity, would increase sensitivity to necrotic stimuli. First, we pre-treated B6 BMDMs with increasing doses of IFNβ prior to LZ stimulation to observe that the magnitude of cell death showed a dose-dependent increase, although the kinetics were unaffected (Figure 2.6A, B). In contrast, exposure to these same doses of exogenous

IFNβ one hour prior to LZ stimulation did not have any effect on LZ induced cytotoxicity (Figure 2.6C, D). Additionally, MLKL expression and oligomerization was significantly enhanced during overnight priming with increased concentration of 20 IU/ml IFNβ (Figure 2.6E), while RIP1 and RIP3 seemed unaffected. Next, we utilized a well-established mouse model of lupus, in which overexpression of TLR7 transgene (TLR 7.1) results in an IFN-abundant system[279]. We decided to use resident peritoneal cells to more closely capture the in vivo autoimmune milieu. We found that resident peritoneal cells from TLR 7.1 animals were more sensitive to LZ induced necroptosis and had elevated ISG signatures relative to littermate controls (Figure 2.6F,G). Additionally, we observed that MLKL expression is significantly higher in resting TLR 7.1 resident peritoneal cells.

To corroborate these findings, BMDMs from TLR 7.1 littermate controls can be sensitized to undergo maximal cell death with as little as 20 IU IFNβ, for 8 hours prior to LZ stimulation (Figure 2.6M). Together, these results show that elevated constitutive IFN-signaling, such as in the case of autoimmunity, can sensitize cells to necroptosis.

2.3 Discussion

Our findings prompt a new model of the necroptosis pathway (Figure 2.7). During homeostatic cellular turnover, DNA, possibly from DNA damage-repair[263] or mitochondrial stress[264], activates the cGAS / STING pathway leading to constitutive IFN production that feeds back onto cells to sustain expression of many ISGs. MLKL ("ISG-2" in Figure 2.7) is one of these ISGs, which must be expressed at levels sufficient to facilitate oligomerization (Figure 2.5E) and cell death (Figure 2.5F). Interestingly, MLKL overexpression was not sufficient to restore necroptosis in *Ifnar*$^{-/-}$ macrophages (Figure 2.5J), suggesting that at least one additional ISG ("ISG-1" in Figure 2.7) is

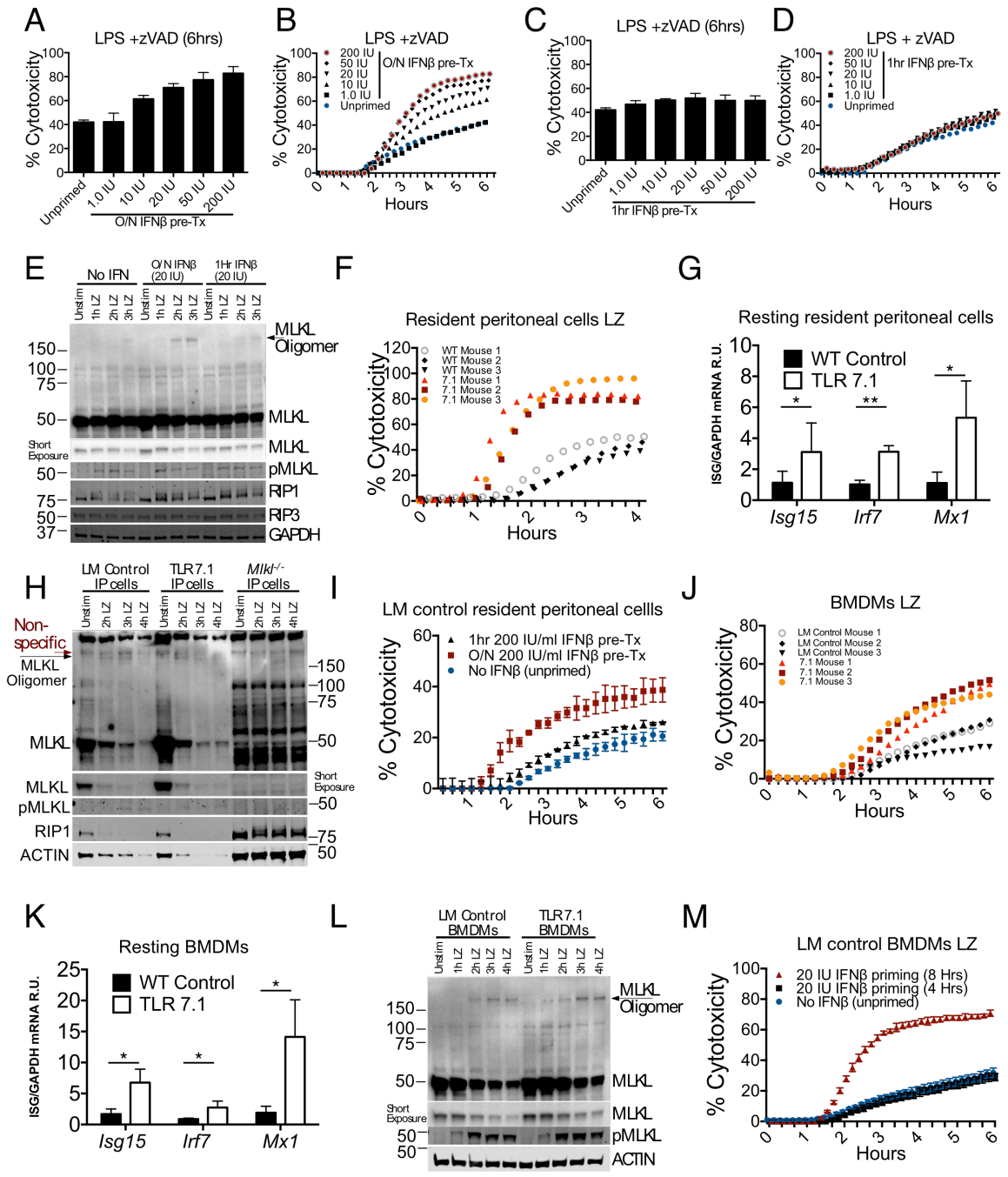

Figure 2.6: High levels of type-I interferon (IFN-I) predispose cells to necroptosis
(A, B) Propidium iodide incorporation of B6 BMDMs at six hours (A) or kinetically over 6 hours (B) of LPS/zVAD treatment with overnight pre-treatment of recombinant IFNβ. (C, D) Propidium iodide incorporation of B6 BMDMs at six hours (C) or kinetically over 6 hours (D) of LPS/zVAD treatment with one hour pre-treatment of recombinant IFNβ. (E) Western blots of multiple proteins with LPS/zVAD treatment of B6 BMDMs with indicated IFNβ pre-treatment (F) Propidium iodide incorporation over 4 hours of TLR7.1 and littermate control resident peritoneal cells treated with LPS/zVAD. (G) Quantitative PCR of ISG mRNA relative to *Gapdh* from resting TLR7.1 and littermate control

resident peritoneal cells. (H) Western blots of multiple proteins with LPS/zVAD treatment of resident peritoneal cells from TLR 7.1, littermate control and *Mlkl*$^{-/-}$ animals. (I) Propidium iodide incorporation over 6 hours of TLR7.1 littermate control resident peritoneal cells either non-primed or 200 IU/ml IFNβ treated for 1 hours or overnight and treated with LPS/zVAD. (J) Propidium iodide incorporation over 6 hours of TLR7.1 and littermate control BMDMs treated with LPS/zVAD. (K) Quantitative PCR ISG mRNA relative to GAPDH from resting TLR7.1 and littermate control BMDMs. (L) Western blots of multiple proteins with LPS/zVAD treatment of BMDMs from TLR 7.1 or littermate control animals. (M) Propidium iodide incorporation over 6 hours of TLR7.1 littermate control BMDMs either non interferon primed or 20 IU/ml IFNβ treated for 4 or 8 hours and treated with LPS/zVAD. All LPS/zVAD treatments were: LPS [10ng/ml] and zVAD [50uM/ml]. In all cases of IFNβ pre-treatment (overnight or one hour), the IFNβ is washed away before addition of experimental conditions. MLKL oligomers were visualized using non reducing western blots. Cytotoxicity data are representative of three or more experiments. qPCR represent SD from three independent experiments and statistical significance was determined using Student two tailed t test: *$p < 0.05$; **$p<0.01$; ***$p < 0.001$.

needed for RIPK-dependent phosphorylation of MLKL to execute necroptosis. Since RIP3 can phosphorylate MLKL, it is possible that the ISG(s) in question serve a scaffolding function to bring together RIP3 and MLKL for proper necrosome formation[55]. Alternatively, constitutive IFN may be upregulating an inhibitor of necroptosis. So far, expression of Ppm1b[271], TRAF2[272], CHIP[273] and components of the ESCRT-I and III machinery[274] are un-altered by constitutive IFN status (Figure 2.12A,B). Further investigation of differentially expressed ISGs by focusing on the intersections of B6, *Ifnar*$^{-/-}$ and *Sting*$^{-/-}$ will prove to be a powerful approach in identifying new regulators of necroptosis. Previous work has shown that caspase inhibition in the context of viral infection increases constitutive IFN production via mitochondrial DNA damage and the STING/ cGAS pathway[264,280,281]. Elevated constitutive IFN can then function to increase the necroptosis potential to limit viral replication. Additionally, the role of constitutive IFN may permeate more than one type of necrotic cell death. Parallel study in the lab (Liu et al., submitted) found that constitutive IFN governs the rate of Caspase-11

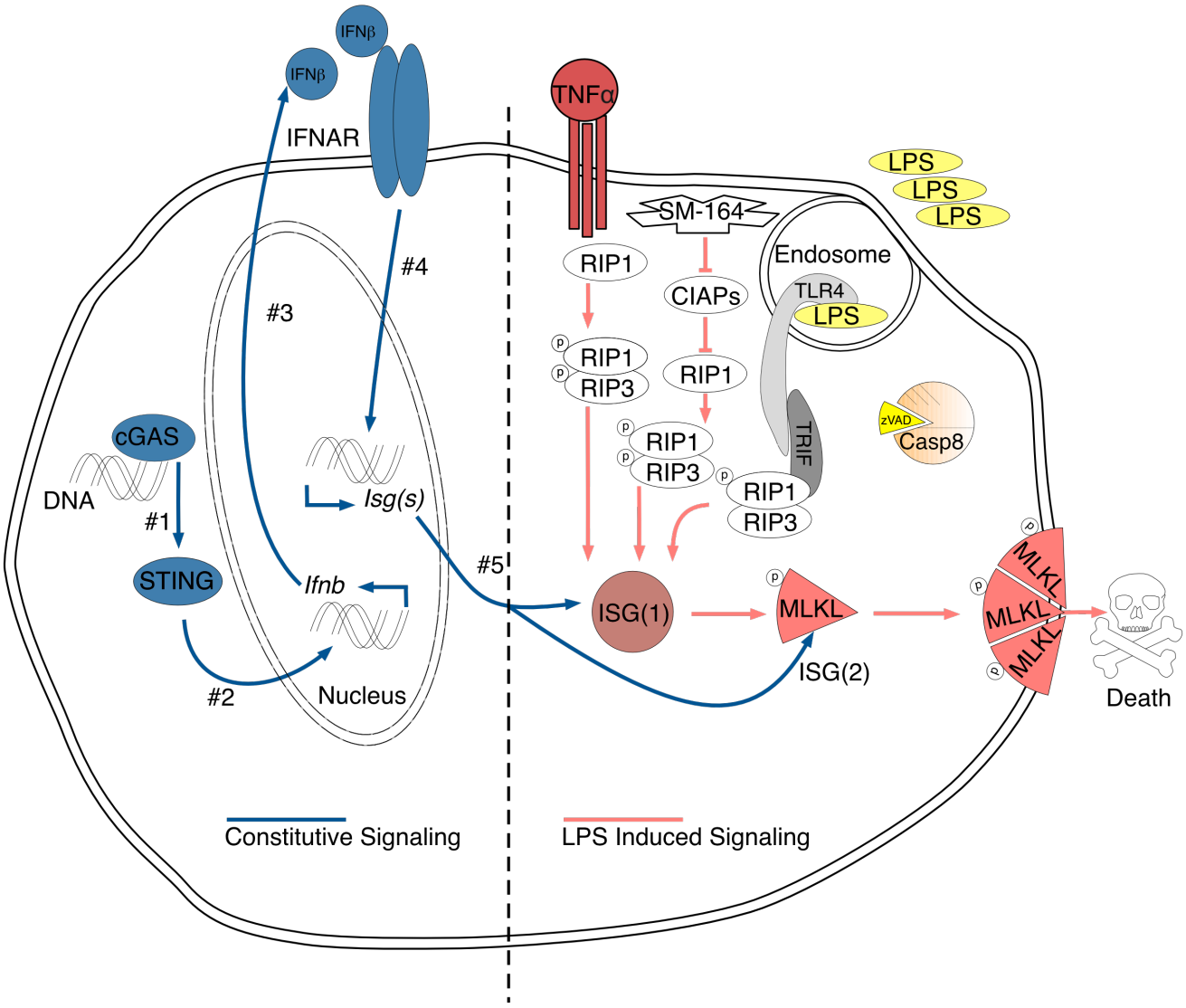

Figure 2.7: Model for the role of interferon in necroptosis
Constitutive IFN signaling (left side, chronologically numbered) is driven by homeostatic cGAS/STING activation from cytosolic DNA sensing. This IFN signaling loop sustains the baseline expression of two or more ISGs. ISG(1) is an unknown effector which acts downstream of TLR4 endocytosis but upstream of MLKL phosphorylation. ISG(2) is MLKL, which must be expressed at adequate levels to allow for oligomerization and subsequent cell death. The requirement for constitutive IFN signaling for cell death is common to LPS, smac mimetic and TNF induced necroptosis all of which also require caspase 8 inhibition.

activation in response to Gram negative bacterial infection, by maintaining steady-state

expression of key upstream mediators known as the Guanylate Binding Proteins (GBPs).

A common theme thus emerges, in which the role of IFN in both cell death pathways is in maintaining expression of critical effectors for cell death. In the case of necroptosis, we will refer to these Constitutive-IFN-Regulated Effectors of Necroptosis as CIREN(s) for short. CIREN protein abundance is central in determining the rapidity by which cell death occurs upon stimulation with a necroptotic signal. In macrophages with adequate constitutive IFN signaling, and thus sufficient for CIREN abundance, we found that necroptosis onset occurs as early as 2 hours post stimulation with LPS/zVAD. In MOLF macrophages and C57BL/6J macrophages deficient for cGAS or STING, we found that although these macrophages can produce IFNβ upon stimulation, they are defective in baseline expression of ISGs. In these macrophages, necroptosis onset suffers significant delay, but eventually does occur. This temporal defect in necroptosis can be explained by time that is required for *de novo* synthesis of CIREN proteins downstream of LPS-induced IFN feedback. Therefore, not only did we elucidate a role for constitutive IFN signaling in licensing necroptosis by maintenance of yet unknown but crucial players of the pathway, we also discovered that *de novo* IFN induction only becomes relevant in cases where constitutive IFN is lacking, to replenish the abundance of said CIREN(s). Presently, we investigated the role of ZBP1/DAI as a plausible CIREN that is mediating LPS-induced necroptosis. Although ZBP1/DAI fit the expression profile in its dependency on constitutive IFN, its loss did not result in a defect in necroptosis or MLKL phosphorylation (Figure 2.5C,D; Figure 2.12D). PKR, an ISG necessary for Interferon induced necroptosis in FADD deficient cells, also fit the expression profile of being maintained by constitutive IFN signaling. However, loss of PKR was not protective for LPS-induced necroptosis[257]. We identified MLKL as a CIREN, but we and others have

shown that MLKL over expression in IFNAR deficient BMDMs is not sensitizing to necroptosis[262] suggesting that there are other unknown CIREN(s).

While loss of constitutive IFN protected cells from necroptosis, elevated IFN signaling, such as in macrophages from the TLR7-overexpression SLE model, sensitized cells to necroptosis. These results are especially relevant given the prevalence of elevated IFN levels in autoimmunity. Necrotic cell death has been proposed as a mechanism by which release of nuclear antigens and damage associated molecular patterns (DAMPs) feed the cycle of SLE pathogenesis[282]. Although the source of necrotic cell death in lupus pathogenesis is unclear, we show here that high IFN levels can pre-dispose macrophages to lytic cell death by which nuclear and cytosolic content could be released. Our results build on the previously reported association between lupus and activation induced B cell necroptosis, suggesting that IFN priming sensitizes cell death in multiple cell types. In further support of this association, recent report by the Kelliher group has shown that hyper-activation of necroptosis leads autoimmunity[261]. Here we show the inverse, in which cells from mice with autoimmunity are more sensitive to necroptosis, suggestive of a IFN-necroptosis feedforward loop (Figure 2.6). Further work will be needed to establish the causality between necroptosis and autoimmunity in human disease.

Our results provide a plausible mechanism behind the association of autoimmunity with high prevalence for transplant rejection. Recent reports defined a role of necroptosis in kidney ischemic reperfusion injury[283], which in itself presents one of the biggest challenges to successful kidney transplantation[284]. Our findings suggest that elevated IFN in lupus patients may exacerbate necroptotic cell death in the transplanted kidney, and that inhibiting necroptosis using necrostatins in combination with anti-IFN therapy prior

to transplantation - or after other ischemic injury - may improve the classically poor outcomes in patients with autoimmune disease[285].

2.4 Materials and methods

2.4.1 Reagents

Lipopolysaccharide (LPS) (Escherichia coli 0111:B4) was purchased from Sigma and used at 10ng/ml. zVAD.fmk was purchased from ApexBio and used at 50uM. Necrostatin-1 was purchased from Sigma and used at 10uM. SM-164 was purchased from ApexBio and used at 1uM. Poly(I:C) was from InvivoGen and used at 25ug/ml. Recombinant mouse IFNβ (12400-1) and recombinant human IFNβ (11415-1) were purchased from PBL Assay Science and used at various concentrations as indicated. In all cases of IFNβ pre-treatment (overnight or one hour), the IFNβ is washed away before addition of experimental conditions. Recombinant moue TNF was purchased from PeproTech and used at a concentration of 50ng/ml. Ruxolitinib was purchased from cayman chemical and used at a concentration of 10uM. Blocking antibody to mouse IFNAR (MAR1-5A3) and control IgG were purchased from BD Pharmingen and used at 20ug/ml. Blocking antibody to human IFNAR (# 21385-1) and control IgG were purchased from PBL and used at a concentration of 20ug/ml. Recombinant proteins were re-constituted in 0.1% endotoxin free BSA from Akron Biotech (AK8917).

2.4.2 Cell viability assays

BMDMs were plated in 96-well plates at $1x10^5$ cells per well in RPMI, 10% FBS, 1%PS. Cells were plated on tissue culture treated clear bottom plates (Costar 3603) in media containing 10 μg/mL propidium iodide (Life Technologies, P3566). TECAN Infinite 200 Pro plate reader was used to maintain temperature at 37°C and 5% CO_2

during infection. Propidium iodide uptake was measured every 15 minutes using bottom read using 535nm excitation and 617nm emission. Wells containing 0.1% TritonX-100 lysed cells were used as 100% cytotoxicity controls. Treatment +zVAD PI incorporation was relative to treatment alone (LPS +zVAD relative to LPS alone). A similar protocol was used previously[286]. For polyI:C induced necroptosis, kinetic microscopy was performed using the Cytation3 Imager (BioTek) and nuclei positive of propidium iodide signal were enumerated. Plate reading function was not used in this case, since PI intercalates with polyI:C, generating high background signal.

2.4.3 Animals

C57BL/6, MOLF/Ei, Ifnar$^{-/-}$(B6.129S2-Ifnar1tm1Agt/Mmjax), Trif-/-(C57BL/6J-Ticam1Lps2/J), MyD88-/-(B6.129P2(SJL)-Myd88tm1.1Defr/J), strains were obtained from The Jackson Laboratory. Tlr7.1 Tg mice[279] (C57BL/6-Tg(Tlr7)1Boll) were obtained from Dr. B. Huber (Tufts). Ifnb$^{-/-}$ were a gift from Dr. S. Vogel (UMaryland). Trif$^{-/-}$/MyD88$^{-/-}$, cGAS$^{-/-}$ and RIP3$^{-/-}$/Caspase8$^{-/-}$ animals were a gift from Dr. K. Fitzgerald (UMass). RIP3$^{-/-}$/Caspase8$^{-/-}$ animal[287] were generated by Dr. D. Green (St. Jude). RIP1 kinase inactive (Rip1D138N/D138N) and Mlkl$^{-/-}$ animals were a gift from Dr. M. Kelliher (UMass). Mlkl$^{-/-}$[288] animals were generated by Dr. W. Alexander (Walter and Eliza Hall Institute). Zbp1$^{-/-}$ mice[289] were a gift from Dr. S. Balachandran. Sting$^{-/-}$ animals were a gift from Dr. G. Barber (UMiami). RIP3 RHIM domain mutant (*Ripk3*$^{\Delta R/\Delta R}$) mice[290] were a gift from Dr. Francis Chan. All genetically modified mice were fully backcrossed to the C57BL/6 background. B6. MOLF-Tmem173molf (*Sting*$^{MOLF/MOLF}$) congenic mice were established by backcrossing to C57BL/6 for 10 generations[268]. All mice were housed in a pathogen-free facility at the Tufts University

School of Medicine and experiments were performed in accordance with regulations and approval of the Tufts University Institutional Animal Care and Use Committee.

2.4.4 RNA preparation and analysis

$5x10^5$ cells were plated on 24 well TC treated plates and cells were lysed with Trizol (Invitrogen) followed by RNA extraction according to the manufacturer's instructions. cDNA was synthesized using M-MuLV reverse transcriptase, RNase inhibitor, random primers 9, and dNTPs (New England BioLabs). cDNA was analyzed for mRNA expression levels using SYBR Green (Applied Biosystems) and intron spanning primers. Gapdh was used to normalize mRNA expression and post amplification melting curve analysis was used for all transcripts to verify specificity.

2.4.5 Mouse Bone Marrow Derived Macrophages (BMDMs)

Bone marrow was isolated by flushing femurs with cold RPMI. Cell pellets were re-suspended in BMDM differentiating media (RPMI with L-glutamine, 20% FBS, 28% L-cell conditioned media, 1% Pen-Strep) and cultured for 7 days at 37°C in 5% CO2 to mature to macrophages. Matured BMDMs were rested overnight in RPMI containing 10% FBS, 2% Penn/Strep, in the absence of L-cell conditioned media prior to experiments.

2.4.6 Human Monocyte Derived Macrophages (MDMs)

De-identified human peripheral blood was purchased from New York Biologics as approved by the Institutional Review Board and Institutional Biosafety Committee at Tufts University. Monocytes were obtained from peripheral blood using the EasySep Direct Monocyte Isolation Kit from STEMCELL technologies (#19669). Monocytes were extracted and differentiated into macrophages over the course of 7 days in RPMI

containing 20% FBS, 2% Penn/Strep, and 100ug/ml of human M-CSF (PeproTech). Matured MDMs were rested for 36 hours in RPMI containing 10% FBS, 2% Penn/Strep, in the absence of M-CSF prior to experiments. Similar protocols were used previously[291].

2.4.7 Western blotting

To prepare whole-cell lysates, cells were lysed directly in 1X Laemmli Buffer with 5% β–mercaptoethanol, boiled for 10 minutes, and incubated on ice for 10 min. Protein lysates were resolved on a 10% Bis-Tris SDS gel and transferred to a nitrocellulose membrane. Blocking conditions were TBS-T with 5% BSA. Primary antibodies were diluted to 1:1000 in TBS-T with 1% BSA, and infrared (700 or 800 nm) secondary antibodies were diluted 1:30,000. Membranes were incubated with protein-specific primary antibodies overnight at 4°C followed by 40-minute room temperature incubation with secondary infrared antibodies and imaged using an Odyssey ® CLx Imaging System. Image analysis was done using Image Studio software. STAT1(#9172), STAT2 (#72604) pSTAT1-Tyr701(#9167), RIP1 (#D94C12), phospho-RIP1-S166 (#65746), phospho-p38 MAPK-Thr180/Tyr182 (#9211), IRF-3 (#4302), phospho-IRF-3- Ser396 (#4947) GAPDH (#2118) and ACTIN (#3700) antibodies were purchased from Cell Signaling. RIP3 antibody (#2283) was purchased from ProSci. Total MLKL antibody was purchased from Millipore (#MABC604). Phospho-MLKL- S345 (#ab196436), and phospho-RIP3- S227 (#ab209384) antibodies were purchased from Abcam. CYLD antibody (clone 733) was purchased from Invitrogen. ZBP1 antibody (clone Zippy-1) was purchased from Adipogen. For visualizing MLKL oligomers, samples were processed in the same way as for a standard western blot but Laemmli Buffer was free from β–mercaptoethanol. MLKL was detected using the same antibody from Millipore

(#MABC604), and anti-rat HRP (CST #7077) 1:2000 dilution. HRP was developed using SuperSignal™ West Femto (34095) from Thermo and visualized using a BioRAD ChemiDoc digital chemiluminescence imager.

2.4.8 High Content Imaging

Cells were seeded at a density of 0.5x 10^6 cells/cm^2 on MatriPlate 0.17mm glass bottom plates (DOT Scientific) in RPMI containing 10% FBS. At indicated time points post treatment, cells were fixed for ten minutes with 4% paraformaldehyde, then washed with blocking buffer (10% goat serum, 2% FBS in PBS) 3X followed by one hour room temperature incubation with blocking buffer. Overnight 4°C incubation with anti MLKL antibody from Millipore (#MABC604) (1:250 dilution) followed by 3X blocking buffer wash and one hour incubation with goat anti-rat AF488 Thermo (# A-11006) (1:250 dilution). Nuclei were counter-stained with Hoechst [2 μM final] Thermo (#62249) for ten minutes at room temperature flowed by 3X BPS wash. For washing procedure, imaging plate was first centrifuged at 200 x g for five minutes, then plate was dumped to remove liquid instead of aspiration to avoid removing loosely adhered cells. 25 fields at 20x magnification were captured and stitched by the Cytation3 automated microscope, generating fields of view with approximately 3000 cells each for image quantification. Signal intensity for MLKL was analyzed with the Gen5 software using $MLKL^{-/-}$ macrophages as negative controls to determine the nonspecific background signal intensity.

2.4.9 MLKL Over Expression

The open reading frame of murine MLKL was cloned into pLEX lentiviral plasmid using BamHI and NotI sites. To reduce the extent of cell death caused by MLKL over-

expression toxicity, the full length CMV promoter of pLEX was reduced resulting in minimal CMV promoter driving expression of MLKL. 293T cells were transfected with lipofectamine 2000 reagent according to manufacturer suggestions. Briefly, each transfection required a 90% confluent 10cm plate of 293T cells in 14ml DMEM media (10% FBS, 2% PS). Cells were transfected with 2ug plasmid (MLKL or empty vector), 1.5ug pSPAX1, 0.5ug MD2.G with 12 ul transfection reagent in 200ul Opti-Mem. Virus was collected after 48 hours 37°C incubation and sterile filtered with 0.22 um syringe filter to remove cell debris. Each 10cm plate of 293T cells produced enough virus to transduce 3-4 plates of BMDMs. Mouse bone marrow was plated at 2-3 million undifferentiated cells per 10 cm non-tissue culture treated petri dish with 14ml BMDM media and virus was added during initial plating of bone marrow. Cells would normally be selected with puromycin at 5ug/ml for 48 hours starting on day 5, however, we found that puromycin selection affected cell death sensitivity and thus cells were not puromycin selected for MLKL over expression experiments. Cells were counted, re-plated in complete RPMI on day seven of differentiation and rested overnight before experiments.

2.4.10 Next Generation Sequencing

Total RNA was isolated from resting BMDMs using TRIzol and used to make a directional cDNA library using TrueSeq kit. Seventy-five bp pair-end reads from cDNA libraries were generated on MiSeq (Illumina) and aligned using TopHat2 and Cufflinks software. Log-transformed values were displayed by heat map. The data are available at the National Center for Biotechnology Information Gene Expression Omnibus:

https://www.ncbi.nlm.nih.gov/geo/query/acc.cgi?acc=GSE83885

2.4.11 Primers

Primers for mouse Irf7: (F) 5’-CTTCAGCACTTTCTTCCGAGA-3’, (R) 5’-TGTAGTGTGGTGACCCTTGC-3’; Isg15: (F) 5’-GAGCTAGAGCCTGCAGCAAT-3’, (R) 5’-TTCTGGGCAATCTGCTTCTT-3’, Mx1: (F) 5’-TCTGAGGAGAGCCAGACGAT-3’, (R) 5’-ACTCTGGTCCCCAATGACAG-3’. Gapdh: (F) 5’-GGAGAGTGTTTCCTCGTCCC-3’, (R) 5’-TTCCCATTCTCGGCCTTGAC- 3’. Ticam1 (F) 5’-TACCAGCTAAGACCCCTACA-3’, (R) 5’-GTCCCTTTCCAAGGCACCTA- 3’. Primers for human IRF7: (F) 5'-CTTGGCTCCTGAGAGGGCAG-3', (R) 5'-CGAAGTGCTTCCAGGGCA-3'; human ISG15: (F) 5'-TCCTGCTGGTGGTGGACAA-3', (R) 5'-TTGTTATTCCTCACCAGGATGCT-3'; human Mx1: (F) 5’-GTGCATTGCAGAAGGTCAGA-3’, (R) 5’-TCAGGAGCCAGCTTAGGTGT-3’; human GAPDH: (F) 5'-GCTCCTCCTGTTCGACAGTCA-3', (R) 5'-ACCTTCCCCATGGTGTCTGA-3'.

2.4.12 ELISA

Cell free supernatants were analyzed for IFNβ as published in[292] and TNFα using the DuoSet elisa kit from R&D (DY410).

2.4.13 Statistical analysis

Values presented as mean ± standard deviation (SD). Error bars in kinetic viability experiments represent the SD from the mean of triplicate samples. Error bars in qPCR experiments represent the SD from duplicate samples. Data for kinetic viability experiments and qPCR are representative of three or more independent experiments. Time point quantifications of cytotoxicity represent SD from three independent

experiments and statistical significance was determined using Student two tailed t test: ns is non-significant ($p > 0.05$); *$p < 0.05$; **$p<0.01$; ***$p < 0.001$. Comparisons are between two conditions indicated by the ends of the solid lines.

2.4.14 Acknowledgements

We thank Dr. Katherine Fitzgerald for sharing resources and for helpful suggestions. We thank Dr. Stefanie Vogel, Dr. Michelle Kelliher, Dr. Francis Chan, Dr. Douglas Green, Dr. Warren Alexander, Dr. Shizuo Akira and Dr. Siddharth Balachandran and Dr. Glen Barber for sharing various mouse strains used in this study. This work was supported by NIH grants 4R01AI056234-13 and 1R21AI126050-01 (A.P.).

2.4.15 Author Contributions

J.S., B.C.L, and A.P. conceived the study, designed experiments, interpreted data and wrote the paper. J.S., H.M. and I.S. performed experiments and processed samples. V.I., A.B, and A.P. performed RNA-sequence and data analysis. C.G.W. provided TLR7.1 animals and experimental insights.

2.4.16 Conflicts of Interest

The authors declare no conflict of interest.

2.5 Supplemental Figures and Legends

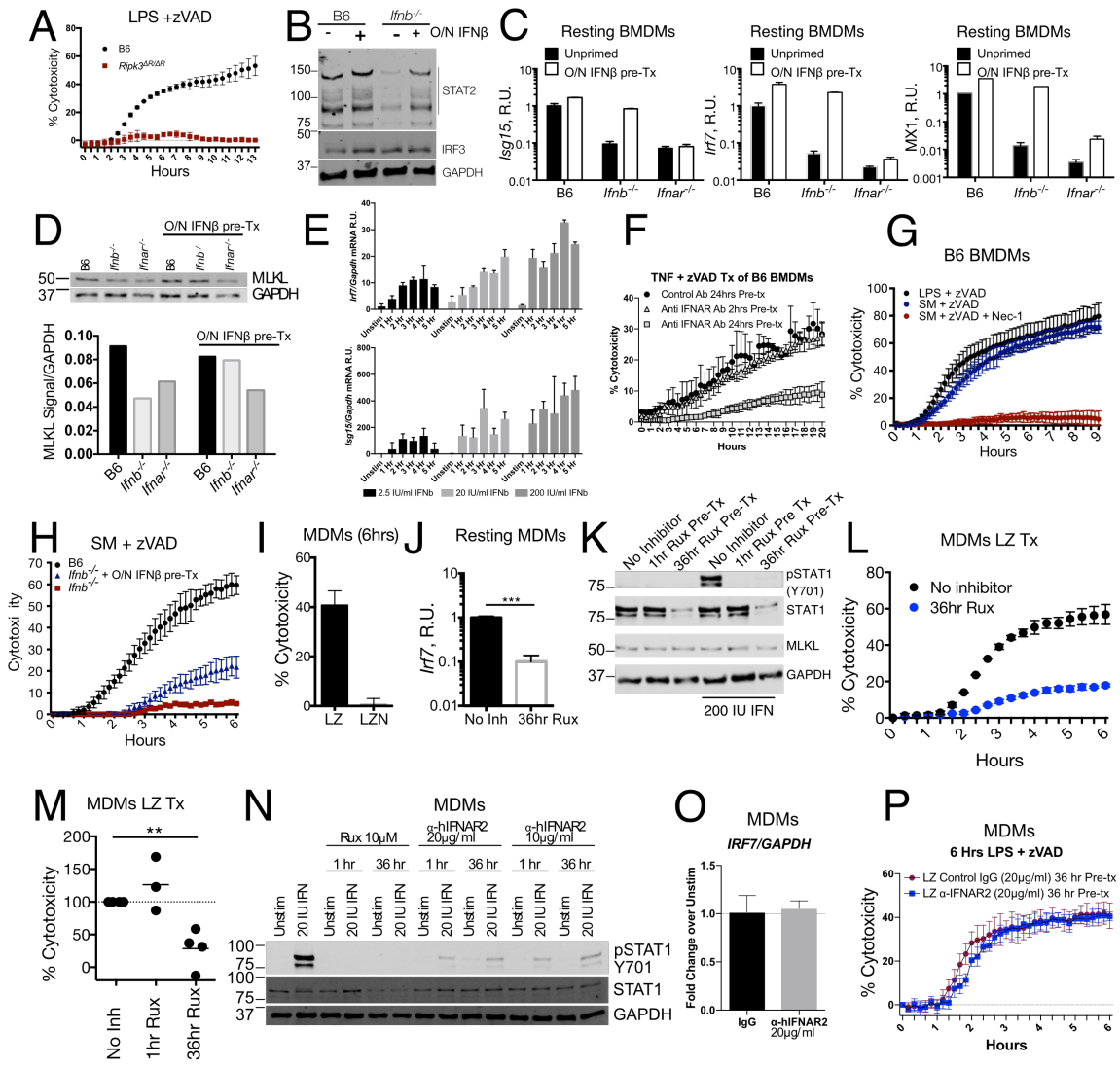

Figure 2.8: Related to Figure 2.1

(A) Propidium iodide incorporation as a readout of cytotoxicity, measured every 30 minutes following LPS/zVAD treatment of B6 and *Ripk3*$^{\Delta R/\Delta R}$ BMDMs . (B) Western blot of STAT2, IRF3 and GAPDH from resting B6 and *Ifnb*$^{-/-}$ BMDMs with or without overnight interferon treatment (2.5 IU IFNβ/ml). (C) Quantitative PCR *Isg15*, *Irf7* and *Mx1* mRNA relative to *Gapdh* from resting B6, *Ifnb*$^{-/-}$ and *Ifnar*$^{-/-}$ BMDMs with or without overnight interferon treatment of 2.5 IU/ml IFNβ. (D) Western blot and quantification of MLKL and GAPDH from resting BMDMs of indicated genotype with or without overnight 2.5 IU/ml IFNβ treatment. (E) Quantitative PCR *Isg15*and *Irf7* relative to *Gapdh* from B6 BMDMs treated with indicated doses of recombinant IFNβ for 1-5 hours. (F) Propidium iodide incorporation of B6 BMDMs treated with TNF (50 ng/ml) /zVAD (50 μM) with indicated pre-treatments of IFNAR blocking antibody. (G) Propidium iodide incorporation of B6 BMDMs with LPS/zVAD, SMAC mimetic (SM-164, 1uM) /zVAD or SMAC mimetic (SM-164, 1uM) /zVAD and Nec-1. (H) Propidium iodide incorporation over the first 6 hours of SMAC mimetic (SM-164, 1uM) /zVAD

treatment of B6 and *Ifnb*$^{-/-}$ BMDMs that were either untreated or IFN primed (2.5 IU IFNβ/ml) overnight. (I) Propidium iodide incorporation as a measure of cytotoxicity 6 hours following LPS /zVAD (Nec-1 addition indicated) treatment of Human monocyte derived macrophages (MDMs). (J) Quantitative PCR of *Irf7* mRNA relative to *Gapdh* from resting human monocyte derived macrophages (MDMs) that were either untreated or pre-treated for 36 hours with Jak1/2 inhibitor, Ruxolitinib (10uM). (K) Western blot for indicated proteins from MDMs either untreated or pre-treated for one hour or 36 hours with Ruxolitinib (10uM) and then stimulated with 200 IU/ml recombinant human IFNβ for 30 minutes. (L) MDMs were either untreated or pre-treated for 36 hours with Jak1/2 inhibitor, Ruxolitinib (10uM) and then stimulated with LPS/zVAD (LZ) and monitored for viability over six hours. (M) Percent cytotoxicity relative to no inhibitor for MDMs that were either untreated (no inh) or pre-treated for one hour or 36 hours with Ruxolitinib from 3-4 independent experiments. (N) MDMs were pre-treated with either Ruxolitinib (10uM) or human IFNAR blocking antibody (10 or 20 ug/ml) for 1 or 36 hours and stimulated with 20 IU/ml recombinant human IFNβ for 1 hour. (O,P) MDMs were treated with human IFNAR blocking antibody (20 ug/ml) or control IgG (20 ug/ml) for 36 hours and analyzed for resting IRF7 mRNA relative to GAPDH (O) or LPS/zVAD induced cytotoxicity (P). Time point quantifications of cytotoxicity represent SD from three independent experiments and statistical significance was determined using Student two tailed t test: ns is non-significant ($p > 0.05$); *$p < 0.05$; **$p<0.01$; ***$p < 0.001$. Comparisons are between two conditions indicated by the ends of the solid lines. qPCR and all kinetic cytotoxicity assay data are representative of three or more independent experiments. All LPS/zVAD treatments were: LPS [10ng/ml] and zVAD [50uM/ml].

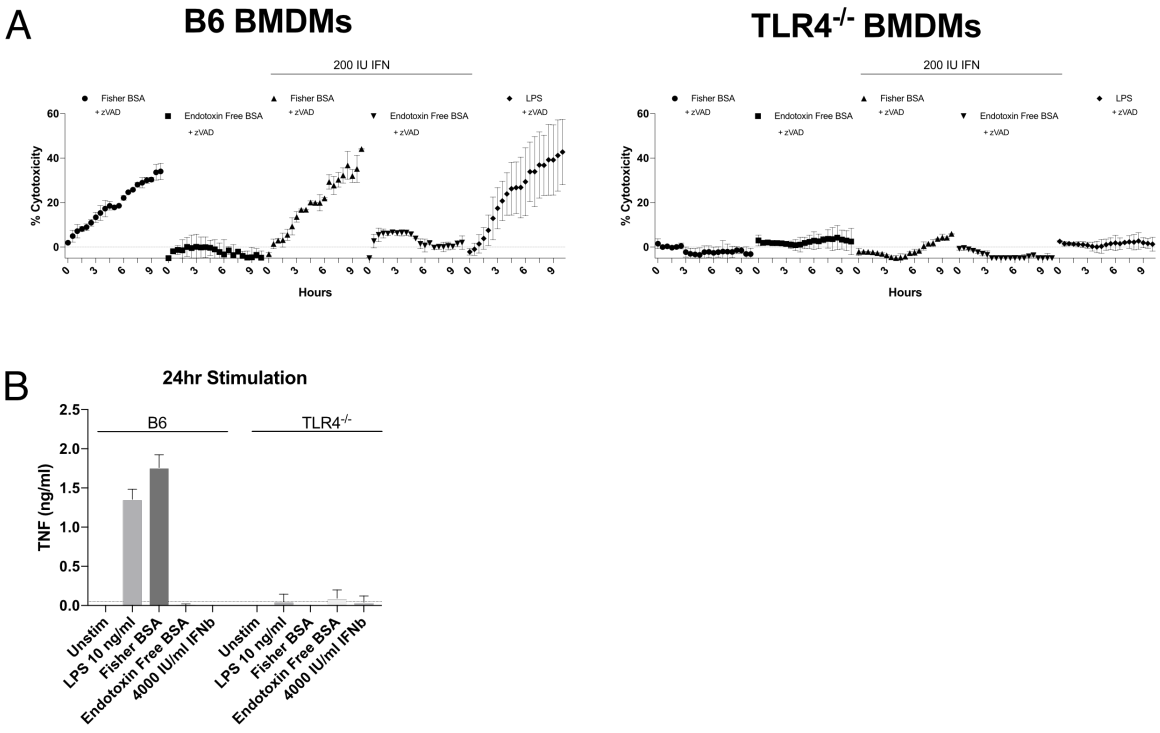

Figure 2.9: Related to Figure 2.2

Propidium iodide incorporation as a readout of cytotoxicity, measured every 30 minutes for 10 hours of B6 and *TLR4*$^{-/-}$ BMDMs with indicated treatment conditions. (B) TNF ELISA from supernatant of B6 and *TLR4*$^{-/-}$ BMDMs stimulated 24 hours with indicated conditions (A,B) Concentrations of reagents used in these experiments: LPS (10 ng/ml), Fisher BSA (BP 1600-100) (0.2 ug/ml), endotoxin free BSA from Akron Biotech (AK 8917) (0.2 ug/ml), IFNβ (4000 IU/ml) and zVAD (50uM).

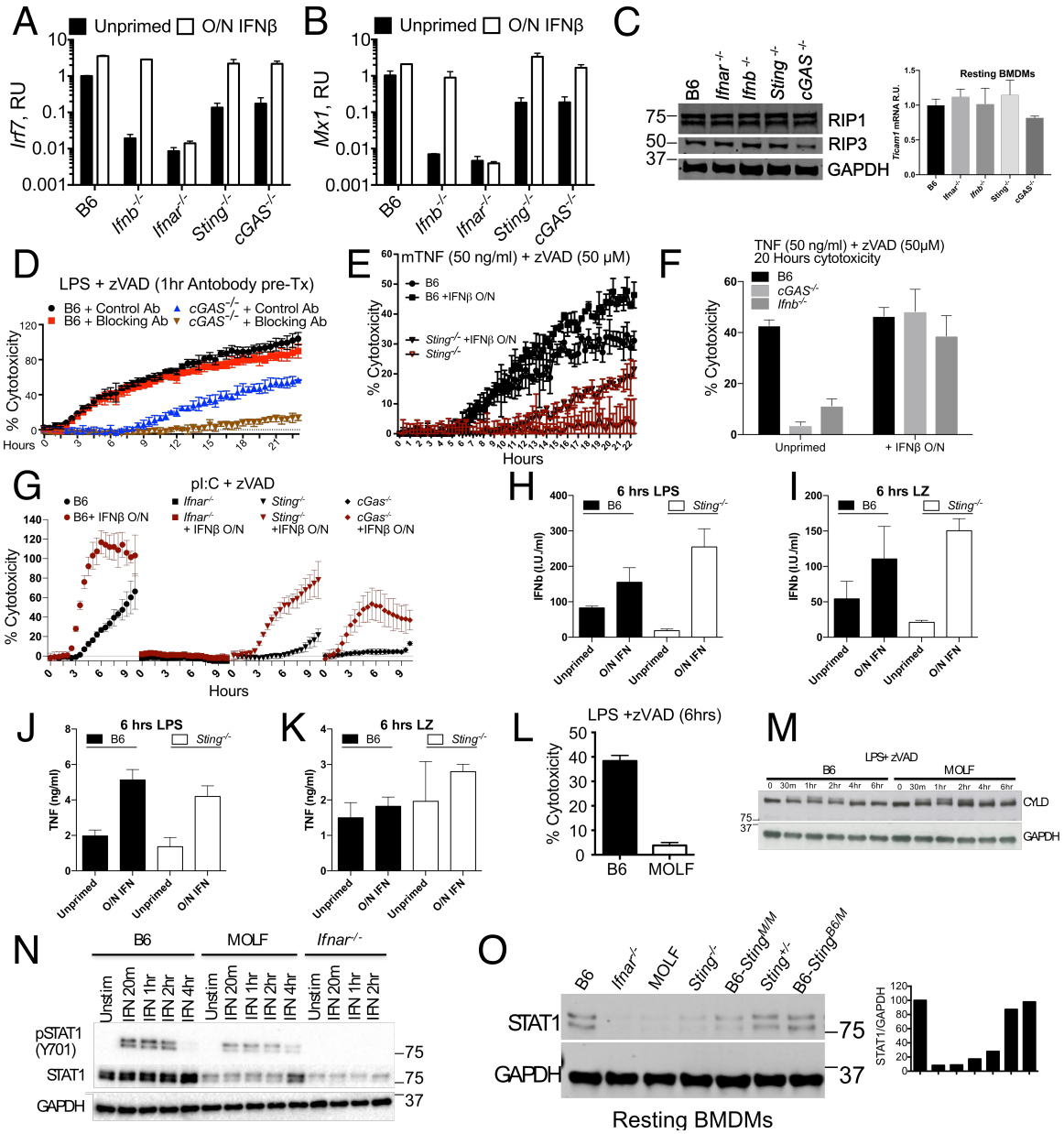

Figure 2.10: Related to Figure 2.3

(A,B) Quantitative PCR of *Irf7* (A) and *Mx1* (B) mRNA relative to *Gapdh* from resting B6, *Ifnb*$^{-/-}$, *Ifnar*$^{-/-}$, *Sting*$^{-/-}$, and *cGAS*$^{-/-}$ BMDMs that were untreated or pre-treated with IFNβ overnight (2.5 IU IFNβ/ml). (C)Western blot of resting B6, *Ifnar*$^{-/-}$, *Ifnb*$^{-/-}$, *Sting*$^{-/-}$, and *cGAS*$^{-/-}$ BMDMs for indicated proteins and Quantitative PCR of *Ticam1*

relative to *Gapdh* from resting BMDMs. (D) B6 and cGAS$^{-/-}$ BMDMs were pretreated one hour with MAR1 IFNAR blocking or isotype control antibody and monitored for LPS/zVAD induced cytotoxicity. (E) B6 and *Sting*$^{-/-}$ with or without overnight IFNβ treatment (2.5IU/ml) were stimulated with mouse TNF (50 ng/ml) and zVAD (50 uM) and monitored for viability over time. (F) B6, *cGAS*$^{-/-}$ and *Ifnb*$^{-/-}$ BMDMs with or without overnight IFNβ treatment (2.5IU/ml) were stimulated with TNF (50 ng/ml) and zVAD (50 uM) and measured for percentage PI positive cells 20 hours after stimulation. (G) BMDMs of indicated genotype with or without overnight IFN® treatment (2.5IU/ml) were stimulated with pI:C (25ug/ml) and zVAD (50 uM) and measured. for cytotoxicity over time by quantifying the number of PI positive nuclei using an imaging cytometer. (H-K) B6, and Sting$^{-/-}$ BMDMs with or without overnigh2.5 IU IFNβ/ml treatment were stimulated with LPS (H,J) or LPS/zVAD (I, K) for six hours and supernatant IFNβ or TNFα was measured by ELISA. (L)Propidium iodide incorporation as a measure of cytotoxicity 6 hours following LPS /zVAD treatment of B6 and MOLF BMDMs. (M) B6 and MOLF BMDMswere treated with LPS /zVAD for indicated durations and analyzed for CYLD and GAPDH by western blotting. (N) B6, MOLF and *Ifnar*$^{-/-}$ BMDMs werestimulated with 100 IU recombinant IFNβ for indicated time points and analyzed by wester blotting for pSTAT1, STAT1 and GAPDH. (O) Western blot andquantification of STAT1 and GAPDH from unstimulated BMDMs of indicated genotype. All data are representative of three or more independent experiments. All LPS/zVAD treatments were: LPS [10ng/ml] and zVAD [50uM/ml].

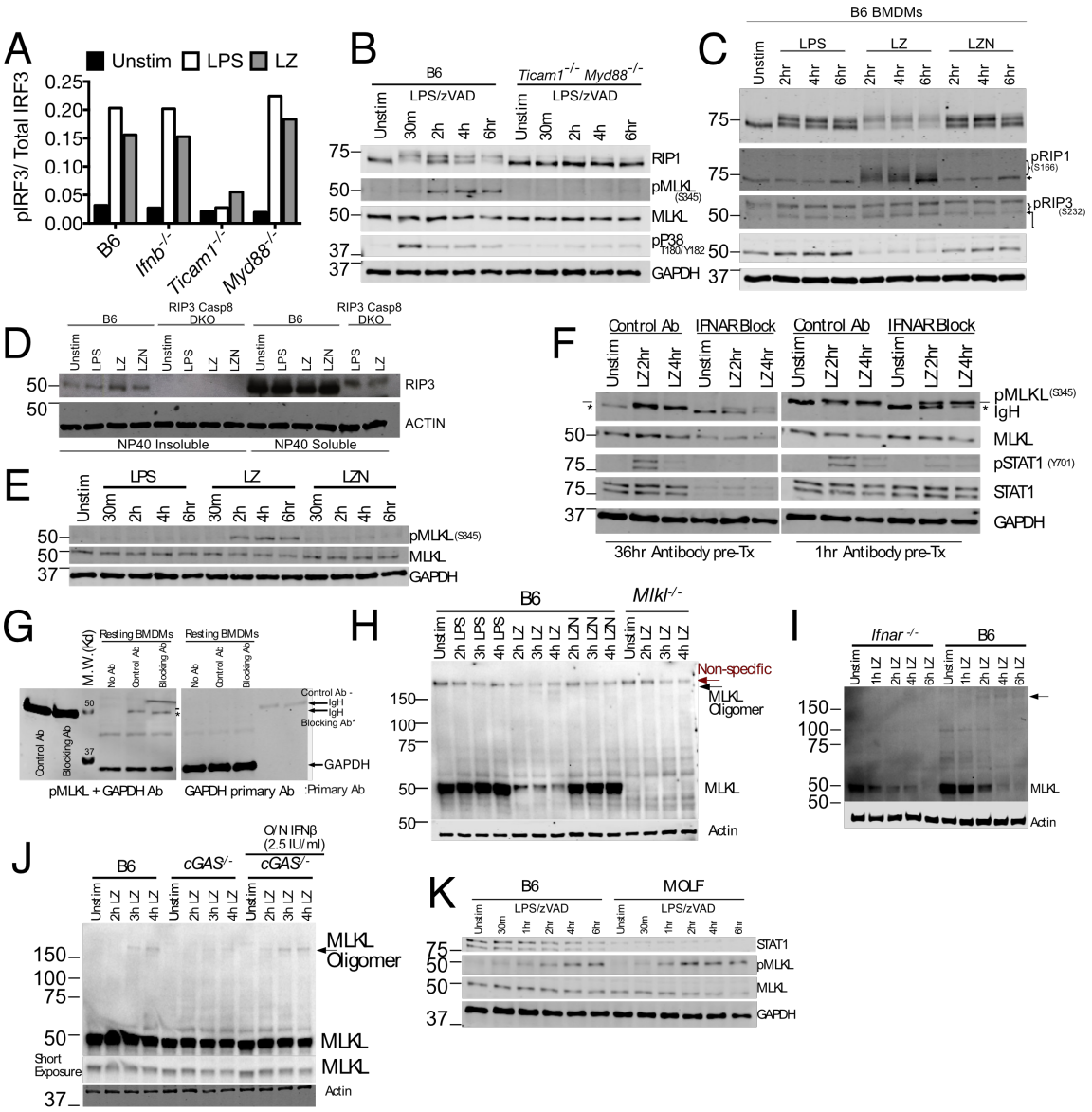

Figure 2.11: Related to Figure 2.4

(A) Quantification of pIRF3 signal relative to total IRF3 from Figure 2.4A (B) Western blots of indicated proteins from B6 and *Ticam1*$^{-/-}$ */Myd88*$^{-/-}$ BMDMs stimulated with LPS/zVAD for various time points. (C) Western blots of indicated proteins from B6 BMDMs that were stimulated with LPS, LPS/zVAD or LPS/zVAD/Nec-1 for various time points. (D) Western blot of RIP3 and Actin from B6 and *RIP3*$^{-/-}$ */ Casp8*$^{-/-}$ BMDMs treated with indicated conditions for 2 hours. This blot is meant to show signal specificity of the RIP3 antibody. Both NP-40 insoluble "necrosome" and NP-40 soluble lysates run on the same gel (E) Western blots of pMLKL, MLKL and GAPDH from B6 BMDMs treated with indicated conditions. (F) Western blots for indicated proteins from B6 BMDMs that were treated with antibody (MAR1 IFNAR blocking or isotype control antibody) 36 hours or only one hour prior to LPS /zVAD treatment. Heavy chain from blocking or control antibody is labeled by IgH and appears below the pMLKL specific

band. (G) Western blot of resting B6 BMDMs untreated or treated with either control or IFNAR blocking antibody for one hour. The same quantity of recombinant antibody (blocking or control) added to the cells was loaded directly into the gel on the left and right hand sides of the gel. The membrane was incubated with either pMLKL antibody or GAPDH as indicated and then developed with the same anti rabbit 800nm antibody. The signal shows that the pMLKL antibody strongly reacts with the heavy chain of the IFNAR blocking and control antibody, explaining the nonspecific band appearing below the pMLKL signal in (F). (H) Non reducing western blot for MLKL and ACTIN in B6 and *Mlkl*$^{-/-}$ BMDMs treated with indicated conditions. (I) Non reducing western blot for MLKL and ACTIN in *Ifnar*$^{-/-}$ and B6 BMDMs treated with LPS/zVAD for indicated time-points. (J) Non-reducing western blot featuring MLKL oligomers from B6 and *cGAS*$^{-/-}$ BMDMs (with or without overnight 2.5 IU/ml IFNβ) treated with LPS /zVAD for indicated times. (K) Western blots of indicated proteins from B6 and MOLF BMDMs stimulated with LPS/zVAD for indicated time points. All data are representative of three or more independent experiments. All LPS/zVAD treatments were: LPS [10ng/ml] and zVAD [50uM/ml].

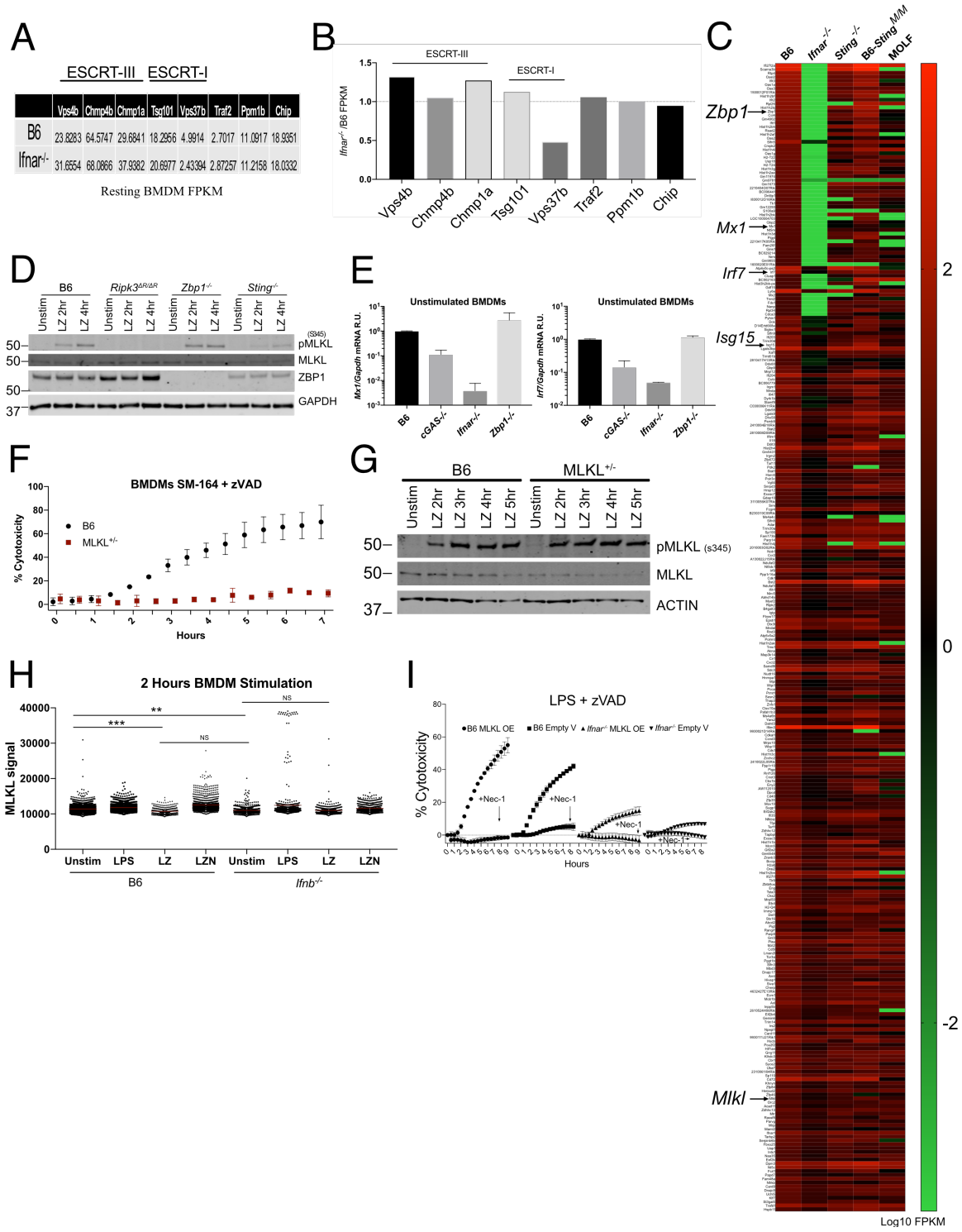

Figure 2.12: Related to Figure 2.5

(A,B) Resting state expression of various known inhibitors of necroptosis in B6 and *Ifnar*$^{-/-}$ BMDMs. (A) FPKM values from RNA sequencing of *Ifnar*$^{-/-}$ and B6 BMDMs and (B) ratio of FPKM values from RNA sequencing of *Ifnar*$^{-/-}$ BMDMs / B6 BMDMs

where values greater than one indicate higher expression in *Ifnar*$^{-/-}$ compared to B6. (C) RNA sequencing of resting BMDMs showing top 300 genes (>4 FPKM in B6) down-regulated in *Ifnar*$^{-/-}$ BMDMs compared to B6. Resting gene expression is also included for *Sting*$^{-/-}$, and $_{Sting}$*MOLF/MOLF* and MOLF BMDMs. Certain genes of interest (*Zbp1*, *Mx1*, *Irf7*, *Isg15* and *Mlkl*) are pointed outwith arrows. (D) Western blots of pMLKL, MLKL, ZBP1 and GAPDH of BMDMs from indicated genotypes stimulated with LPS/zVAD. (E) Resting BMDM qPCR from B6, *cGAS*$^{-/-}$, *Ifnar*$^{-/-}$ and *Zbp1*$^{-/-}$ BMDMs. (F) 7 hrs time-course of viability of SM-164 (1uM) /zVAD (50uM) treated B6 and Mlkl$^{+/-}$ BMDMs. (G) Western blot of indicated pMLKL, MLKL and ACTIN of B6 and *Mlkl*$^{+/-}$ BMDMs stimulated with LPS/zVAD for various time- points. (H) High content imaging of endogenous MLKL in PFA fixed B6 and *Ifnb*$^{-/-}$ BMDMs treated two hours with LPS, LPS/zVAD, LPS/zVAD/Nec-1. (I) B6 and Ifnar$^{-/-}$ BMDMs transduced with either empty virus of MLKL over expressing virus and analyzed for LPS/zVAD and LPS/zVAD/Nec-1 induced cytotoxicity. AllLPS/zVAD treatments were: LPS [10ng/ml] and zVAD [50uM/ml]. MLKL signal compared using student two tailed t test: ns is non-significant ($p > 0.05$); *$p < 0.05$; **$p<0.01$; ***$p < 0.001$. All western blot and kinetic cytotoxicity data are representative of three or more experiments.

Chapter 3: Caspase-8 induces cleavage of multiple Gasdermins to elicit pyroptosis during *Yersinia* infection[293]

[293]Sarhan, J., Liu, B. C., Muendlein, H. I., Li, P., Nilson, R., Tang, A. Y., Rongvaux, A., Bunnell, S. C., Shao, F., Green, D. R., & Poltorak, A. (2018). Caspase-8 induces cleavage of gasdermin D to elicit pyroptosis during Yersinia infection. Proceedings of the National Academy of Sciences of the United States of America, 115(46), E10888–E10897.

3.1 Background

Cell death and inflammation are critical regulators of immune responses which must be carefully balanced to ensure host survival during infection. Upon initial pathogen contact with innate immune cells, the host cell signaling through Toll-like Receptors (TLRs) simultaneously engage a cell intrinsic pro-survival program while producing inflammatory cytokines to propagate the alarm of infection [156,293]. These cytokines are critical for the activation and recruitment of further waves of innate and adaptive immunity, as well as reinforcing the inflammation loop via autocrine signaling in the current population. Successful pathogens have therefore evolved ways to evade host cytokine-induction to survive and replicate silently amongst host immune cells. This is done either by modifying surface pathogen associated molecular patterns that cannot be recognized by macrophage TLRs, or via active blockade of macrophage signaling pathways downstream of TLR activation [294,295].

To counteract the latter, these same pro-survival, pro-cytokine signaling pathways also have in-built switches to engage cell death when the cell perceives a block to its ability to produce cytokines [213,296]. One of the best examples of such a switch lies downstream of Tumor Necrosis Factor (TNF) receptor. TNF receptor signaling engages the TNF receptor associated adaptor TRADD [48] to recruit RIP1 via death domain (DD) interactions [49], forming complex I. Complex I formation results in the activation of the MAP kinases and NFκB, which drive the production of inflammatory cytokines and pro-survival factors [50]. In cases in which MAP kinases and/or NFκB signaling is blocked, RIP1 dissociates from TNF receptor to facilitate the formation of complex IIa by interacting with FADD and pro-Caspase-8. Complex IIa leads to caspase 8 activation and

cell death [51]. If caspase activity is blocked, the signaling complex transitions to complex IIb, in which RIP1 engages RIP3 to activate an MLKL dependent necrotic cell death mechanism known as necroptosis [55, 63, 250,298]. Necroptosis has similarly been shown to occur downstream of TLR signaling in recent years [253,255].

The success of MAP kinase and NFκB signaling thus are critical determinants of life and death of a cell. MAP kinase and NFκB pathways diverge from a single protein complex consisted of TGFβ-associated kinase (TAK1), TAB1, and TAB2, where TAK1 experiences constitutive phosphorylation and baseline activity [213,298]. Whole body TAK1 deficiency results in lethality between embryonic days 9.5-10.5 [214]. Follow up studies elucidated that TNF stimulation in the context of TAK1 deficiency leads to cell death via caspases - complex IIa, or death by necroptosis in the case of caspase inhibition - complex IIb [219,220]. Similarly, whole body RIP1 deficiency results in perinatal lethality, where *Rip1*$^{-/-}$ and conditionally null animals show exquisite sensitivity to tonic TNF induced death [50,299].

Given such intertwining relationship between cytokine production and cell death during infection, the central question thus becomes, what is achieved upon cell death if cytokines, the universal alarms, cannot be adequately made in the first place? The well-studied bacteria of the *Yersinia* species may lend an answer. *Yersinia* species express a number of *Yersinia outer proteins (YOPs)* that manipulate various macrophage cytosolic processes [241]. One such protein YopJ, inhibits TAK1via acetylation [242] with consequent induction of macrophage cell death [243]. Yersinia induced cell death was recently shown to be caspase 8 dependent but RIP3 independent. Paradoxically, while *Rip3*$^{-/-}$*Casp8*$^{-/-}$ macrophage are protected from cell death, the animals succumb to the infection, with

higher bacterial burden in various solid organs [244,245]. Similarly, *Yersinia* induced macrophage cell death is strongly RIP1 kinase activity dependent, where RIP1 kinase inactive animals also show increased sensitivity to infection [246]. These studies suggest that macrophage death in the context of *Yersinia* infection is protective for the animal host.

Interestingly, despite the ability of YopJ to dampen cytokine production, *Yersinia* infections in mice elicit a robust IL-1 response, with IL-1 receptor signaling playing a crucial role in the survival of the animal [300]. IL-1 maturation requires the formation of a caspase nucleation event termed the inflammasome. The inflammasome is triggered via the sensing of a cytosolic "danger" signal that nucleates multiple units of pro-caspase-1 for proximity-induced autocleavage and activation. One of the best studied inflammasomes is the NLRP3 inflammasome, which nucleates in response to bacterial components, crystals, or potassium efflux. NLRP3 recruits ASC, upon which ASC recruits pro-caspase-1 via homotypic CARD-domain binding [301,302]. Caspase-1 is activated via autocleavage, by which active caspase-1 cleaves pro-IL-1β and pro-IL-18. The release of mature IL-1β in conjunction with inflammasome-driven cell death was termed pyroptosis [69,303]. With the discovery that Caspase-11 drives pyroptosis via activation of pore forming protein Gasdermin D (GsdmD) [98,305], NLRP3 inflammasome was found to activate as a consequence of plasma membrane rupture and the concurrent efflux of potassium ions [101]. More recently, activation of the NLRP3 inflammasome has also been observed during necroptosis [102], suggesting that inflammasome formation may be a commonality shared amongst many necrotic forms of cell death.

In this work, we set out to investigate the morphological features of the caspase-8 driven cell death during TAK1 inhibition, using *Yersinia pseudotuberculosis* as our infection model. To simplify a complex infection system to minimal manipulate-able units, we additionally use LPS and 5Z-7-Oxozeaenol (5z7), a potent small molecule inhibitor of TAK1 [224], to mimic the basic cell death phenotype induced by *Yersinia.* We found that *Yersinia* induced cell death bears a striking resemblance to pyroptosis in morphology, the involvement of multiple Gasdermins, and the potency of IL-1 production. This led us to conclude that caspase 8 can drive pyroptosis in cases of TAK1 inhibition during inflammatory signaling.

3.2 Results

3.2.1 During TAK inhibition, TLR stimulation drives caspase-8 dependent cell death, with necroptosis as a backup mechanism.

Yersinia species, including *Yersinia pestis* and *pseudotuberculosis*, induce macrophage cell death via effector YopJ inhibition of level three MAP kinase TAK1 [242,243]. We use nuclear incorporation of propidium iodide to monitor the kinetics of cell membrane integrity loss in real time. We see that in B6 macrophages, YopJ-specific macrophage death occurs is complete by 4-6 hours post bacterial challenge, and that macrophages lacking both RIP3 and Caspase-8 are protected (Figure 3.8A), consistent with published reports [244,245]. To investigate the individual contribution of caspase-8 and RIP3, we used small molecule inhibitors zVAD for pan-caspase activation or Nec1 for inhibition of necroptotic machinery. We find that *Y. pseudotuberculosis* driven cell death can be partially rescued by inhibition of caspases or RIP kinases, however, complete ablation of *Yersinia* driven cell death requires the addition of both zVAD and Nec1

(Figure 3.1A, left column). We can effectively mimic this response by co-stimulation of macrophages with the small molecule inhibitor of TAK1 - 5z7 in combination with a TLR agonist, in this case LPS (Figure 3.1A, right column, Figure 3.8B).

Necrostatin-1 (Nec1), the small molecule inhibitor of RIP1 kinase activity, is used to block necroptosis as driven by RIP1/RIP3 and the effector of necroptotic cell death MLKL [306,307]. Given the partial protection with Nec1, we investigated the contribution of necroptotic players during *Yersinia*-driven, as well as LPS/5z7 driven cell death. Using genetic knock-outs of RIP3 and MLKL, we found that *Mlkl*$^{-/-}$ and *Rip3*$^{-/-}$ macrophages are fully susceptible to *Yersinia* and LPS/5z7 driven cell death (Figure 3.1B; Figure 3.8C). With the addition of zVAD, *Rip3*$^{-/-}$ and *Mlkl*$^{-/-}$ macrophages become protected from death, indicating that in the context of TAK inhibition, necroptosis is engaged only when caspase activity is blocked. However, the full susceptibility of RIP3 and MLKL deficient cells to *Yersinia*-driven death argues that necroptosis is not the primary pathway of cell death during *Yersinia* infection. Addition of Nec1 during *Yersinia* challenge or LPS/5z7 stimulation show partial protection regardless of the presence of RIP3 or MLKL.

Working upstream in the pathway, RIP1 kinase activity plays critical roles for the initiation of necroptosis during caspase inhibition [307,308]. However, RIP1 also has a role in TNF driven apoptosis via the formation of complex II [49,309]. We found that RIP1 kinase inactive (RIP1$^{K45A/\ K45A}$) macrophages are partially protected from *Yersinia* and LPS/5z7 driven cell death, recapitulating the effect of Necrostatin-1 addition (Figure 3.1C) [246]. RIP3 kinase inactive (RIP3$^{K51A/\ K51A}$) macrophages behave as *Rip3*$^{-/-}$ macrophages (Figure 3.8D), and RIP1/3 double kinase inactive macrophages show similar

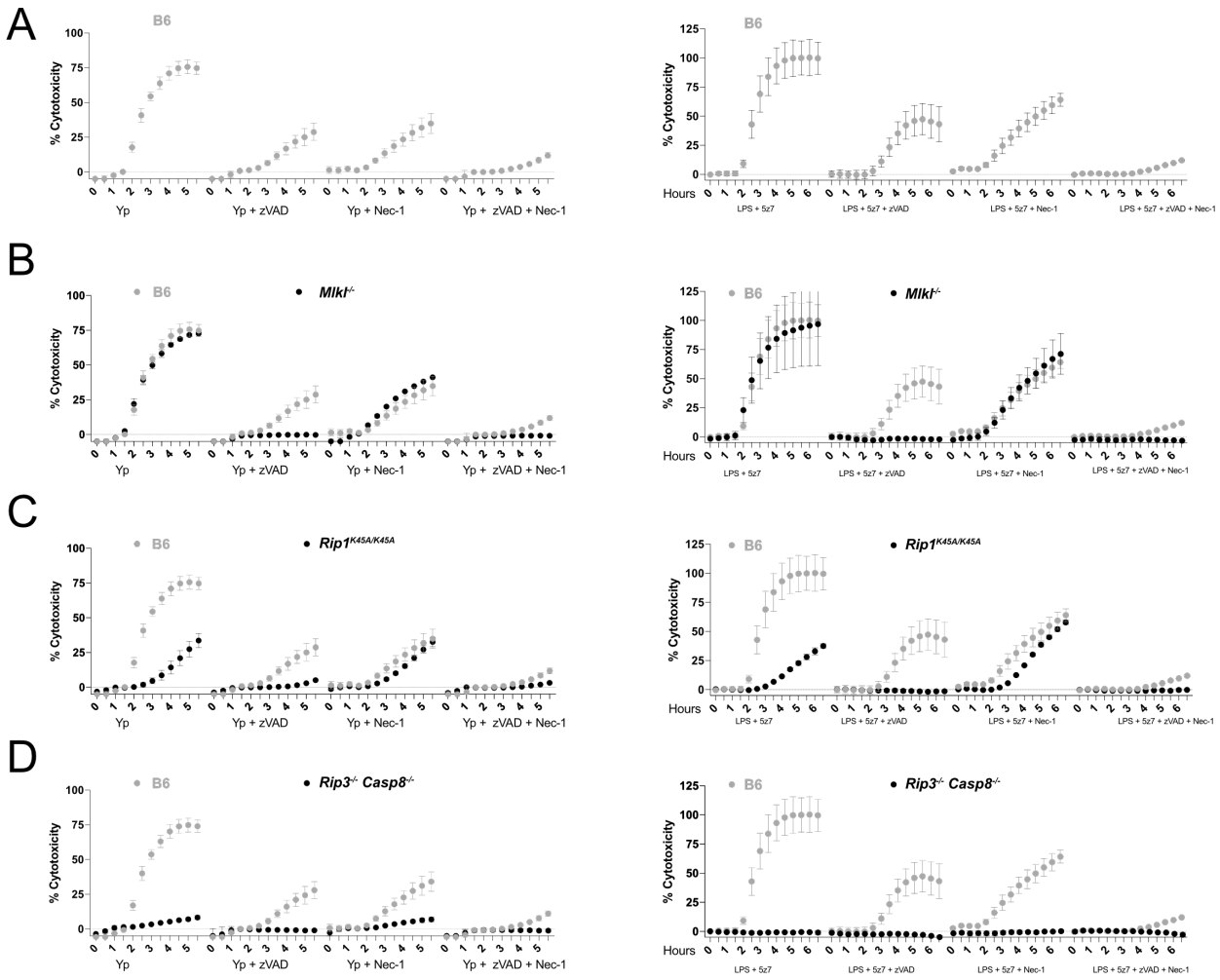

Figure 3.1: During TAK inhibition, TLR stimulation drives caspase-8 dependent cell death, with necroptosis as a backup mechanism.
(A - D) Bone marrow derived macrophages from C57BL/6 (B6) and various genetically modified animals were stimulated with *Yersinia pseudotuberculosis* IP2666 on the left and LPS [10ng/ml] /5z7 [125nM] on the right. *Y. pseudotuberculosis* was infected at an MOI of 30. Percentage cytotoxicity was calculated by 4x microscopy via counts of propidium iodide positive nuclei per field of view, normalized to 100% lysis by 0.1% Triton-X. Caspases were inhibited with zVAD treatment [50 uM], and RIP kinase activity was inhibited with Necrostatin-1 (Nec1) [10uM]. All inhibitors were added simultaneously at time zero. All kinetic cytotoxicity data are representative of three or more experiments. Cytotoxicity curve of each genotype is superimposed over B6 cytotoxicity curves for clarity of comparison.

susceptibility as RIP1 single kinase activity (Figure 3.1C). RIP1 thus plays an

enhancement role in driving cell death during *Yersinia* infection, but is not the critical

factor. Confirming previous findings [244,245], cells deficient for both RIP3 and Caspase 8 are fully protected from *Yersinia* and LPS/5z7 driven cell death (Figure 3.1D). Given that *Rip3*$^{-/-}$ macrophages are fully sensitive to cell death, the additional loss of Caspase 8 lending full protection indicates that caspase-8 is the primary driver of cell death. *Yersinia*-induced, as well as TLR stimulation under TAK1 inhibition thus drives a mode of rapid cell death that is caspase-8 driven, with partial contribution from RIP kinase 1.

3.2.2 TAK-inhibition results in necrotic cell death, exhibiting pan-caspase activation and the externalization of cytosolic content

Traditionally, caspase-8 activation has been associated with apoptosis, characterized morphologically by the shedding of apoptotic bodies and retainment of membrane integrity during death to promote efferocytosis over secondary necrosis and the release of cytosolic contents [310]. However, the rapidity of propidium iodide uptake during *Yersinia* and LPS/5z7 driven cell death is suggestive of necrotic cell death. Indeed, LPS/5z7 induces rapid and indiscriminate release of cytosolic contents into the surrounding culture media as compared to the canonical apoptosis stimulant etoposide, and the recently synthesized small molecule raptinal, which drives cell death via caspase-9 activation of caspases 3 and 7 (Figure 3.2A) [311,312].

Probing for caspase activation and their appearance in the culture media (precipitated supernatant). We found that the majority of fragments corresponding to active caspase 8, caspase 9, caspase 3, and caspase 7 have accumulated extracellularly by 5 hours of LPS/5z7 stimulation (Figure 3.2B). In contrast, these cleaved caspase fragments can be seen by 5 hours in cell lysates of etoposide treated cells, but the appearance of cleaved

caspase 3 and caspase 7 are not seen in the supernatant until over 16 hours after stimulation.

Additional cytosolic contents released upon LPS/5z7 stimulation include cleaved PARP, cyclophilinA, and Gapdh. Congruent with the cell death kinetics, the apoptosis machinery is blocked with addition of zVAD, which switches the cell fate to necroptosis, as indicated by the appearance of phosphorylated-MLKL in conditions with zVAD addition (Figure 3.2C). We confirmed with macrophages deficient for both RIP3 and Caspase 8 that the release of cytosolic content during LPS/5z7 stimulation is as a consequence of cell death. With *Rip3*$^{-/-}$ *Casp8*$^{-/-}$ macrophages, the cleavage of Caspase 3 and PARP are no longer present beyond baseline levels, and cytosolic proteins such as cyclophilinA, Gapdh, and Actin remains intracellular during LPS/5z7 stimulation (Figure 3.2D).

3.2.3 Yersinia and LPS/5z7 driven cell death resembles pyroptosis by morphology

Apoptosis, necroptosis, and pyroptosis are morphologically distinct from each other. Using time lapse microscopy, we followed the progression of macrophages undergoing each of these three well defined modes of cell death to determine the morphology taken by cells dying by LPS/5z7 or *Yersinia* (Figure 3.3A-E).

For a rapid form of apoptosis, we use the small molecule raptinal, which engages caspase 9 activation [311]. Raptinal treated cells progress to membrane rupture by 2-3 hours post stimulation, therefore placing it on a similar timescale to LPS/5z7 induced cell death (Figure 3.3A). Cells undergoing raptinal treatment display classic signs of cell shrinkage and extensive blebbing as early as 30 minutes post stimulation. AnnexinV positivity as an

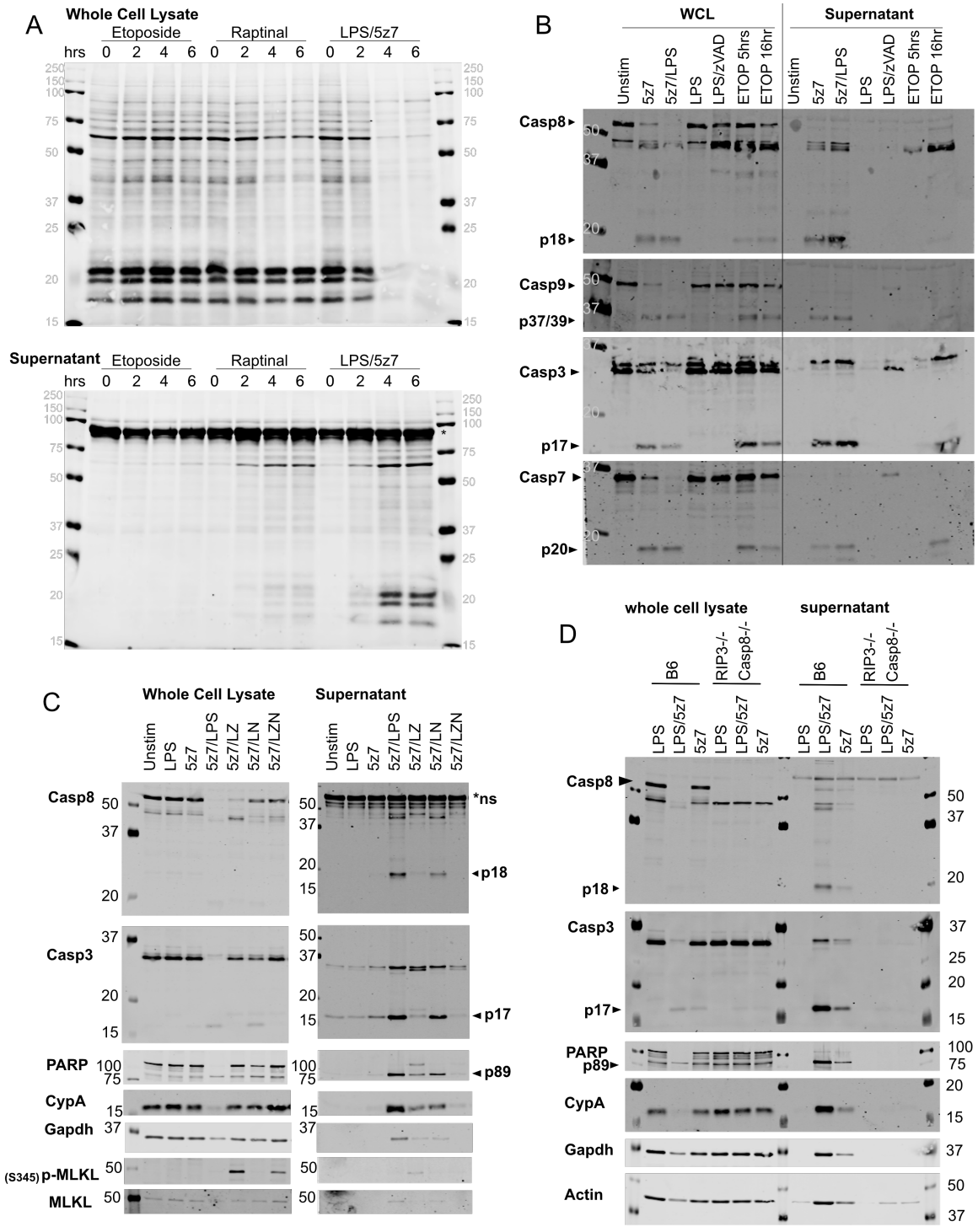

Figure 3.2: TAK-inhibition results in necrotic cell death, exhibiting pan-caspase activation and the externalization of cytosolic content

(A) Bone marrow derived macrophages were stimulated with etoposide, raptinal, or LPS/5z7 for 0-6 hours. Cellular lysate and precipitated supernatant were run on SDS-PAGE gels and total protein was stained by LiCOR total protein stain. * indicates serum proteins from residual FBS in the culture media. (B) Bone marrow derived macrophages

were stimulated as indicated for 5 hours, expect for etoposide, which had an additional 16hr stimulation timepoint. Cellular lysate and precipitated supernatant were run on SDS-PAGE gels and probed for pro- and cleaved forms of various apoptotic caspases. (C) Bone marrow derived macrophages were stimulated with LPS/5z7 for 5 hours, in the presence of zVAD or Nec1 to block caspase or RIP kinase activity, respectively. Cellular lysate and precipitated supernatant were run on SDS-PAGE gels and probed for caspases, caspase substrate PARP, cytosolic proteins CyclophilinA (CypA) and Gapdh, and phosphorylated/total MLKL. (D) Bone marrow derived macrophages from B6 and Rip3-/- Casp8-/- animals were stimulated with LPS, LPS/5z7, or 5z7 for 5 hours. Cellular lysate and precipitated supernatant were run on SDS-PAGE gels and probed for caspases, caspase substrate PARP, cytosolic proteins CyclophilinA (CypA), Gapdh, and actin.

indication of phosphatidylserine externalization is rampant by 40 minutes, and this phase is extended for at least one hour. 2 hours post stimulation, cell membrane ruptures as indicated by nuclear propidium iodide signal, with morphology of the dying cell marked by multiple necrotic bubbles resembling that of secondary necrosis [105].

Recently, Gong *et. al.* showed that necroptosis, although a necrotic form of cell death, can display phosphatidylserine externalization prior to membrane rupture [274]. We confirm that with LPS/zVAD induced necroptosis, AnnexinV binding is evident by 50-60 minutes post stimulation in the absence of cell shrinkage as seen in apoptosis. Membrane ruffling is seen during the AnnexinV positive phase, and plasma membrane rupture takes the form of 1-2 large necrotic bubbles per cell that coincides with nuclear propidium iodide positivity. Necroptotic cells takes 50 minutes to 1 hour from the onset of phosphatidylserine externalization to plasma membrane rupture (Figure 3.3B).

To trigger pyroptosis, LPS was transfected into the cytosol to activate caspase-11 [93,94]. Unlike necroptosis and apoptosis, cells undergoing pyroptosis do not show overt signs of impending membrane rupture in the hours leading up to cell death, although weak propidium iodide signal from the nuclei can be observed. Propidium iodide nuclear

signal is simultaneous with AnnexinV positivity as the cell balloons out into a spherical morphology (Figure 3.3C).

With LPS/5z7 co-stimulation, dying cells retain extensive lammelipodia up to 10-20 minutes before membrane rupture. At 10 minutes prior to loss of membrane integrity, the cell rapidly shrinks, followed by simultaneous onset of weak AnnexinV positivity, blebbing, and a weak propidium iodide signal seeping into the nucleus. Within 10 minutes of AnnexinV binding, the cell then bursts with one large, spherical balloon along with full nuclear propidium iodide signal (Figure 3.3D). The identical progression of cell death is seen during *Yersinia*-induced cell death (Figure 3.3E).

To quantify this phenotype on a population level, images were taken at 4x magnification with 3000-4000 cells captured per frame. AnnexinV and propidium iodide signal intensity per cell were plotted on the Y and X axis, respectively. Representative frames at 1.5hr and 3hr are shown for LPS/zVAD and LPS/5z7 (Figure 3.3F, G, Supplemental video 1, 2). On a population level, necroptotic cells show a distinct population of AnnexinV+PI- cells that transition into PI positivity (Figure 3.3F). In contrast, LPS/5z7 stimulated cells progress from dual negative to PI+AnnexinV^{weak} state, and gains AnnexinV positivity over time (Figure 3.3G). Our data show that with TAK1 inhibition-induced cell death, rapidity of membrane rupture curtails the process of phosphatidylserine externalization, leading to a pyroptotic-like cell death morphology.

3.2.4 Caspase-8 induces GsdmD cleavage to drive pyroptosis, curtailing apoptosis

GasderminD and GasderminE are two effectors of pyroptosis downstream of caspase activation (Shi et al. 2015; Kayagaki et al. 2015; Wang et al. 2017; Rogers et al. 2017).

To determine whether GsdmD and GsdmE are involved for LPS/5z7 and *Yersinia* induced cell death, macrophages were stimulated with various cell death stimulants, and

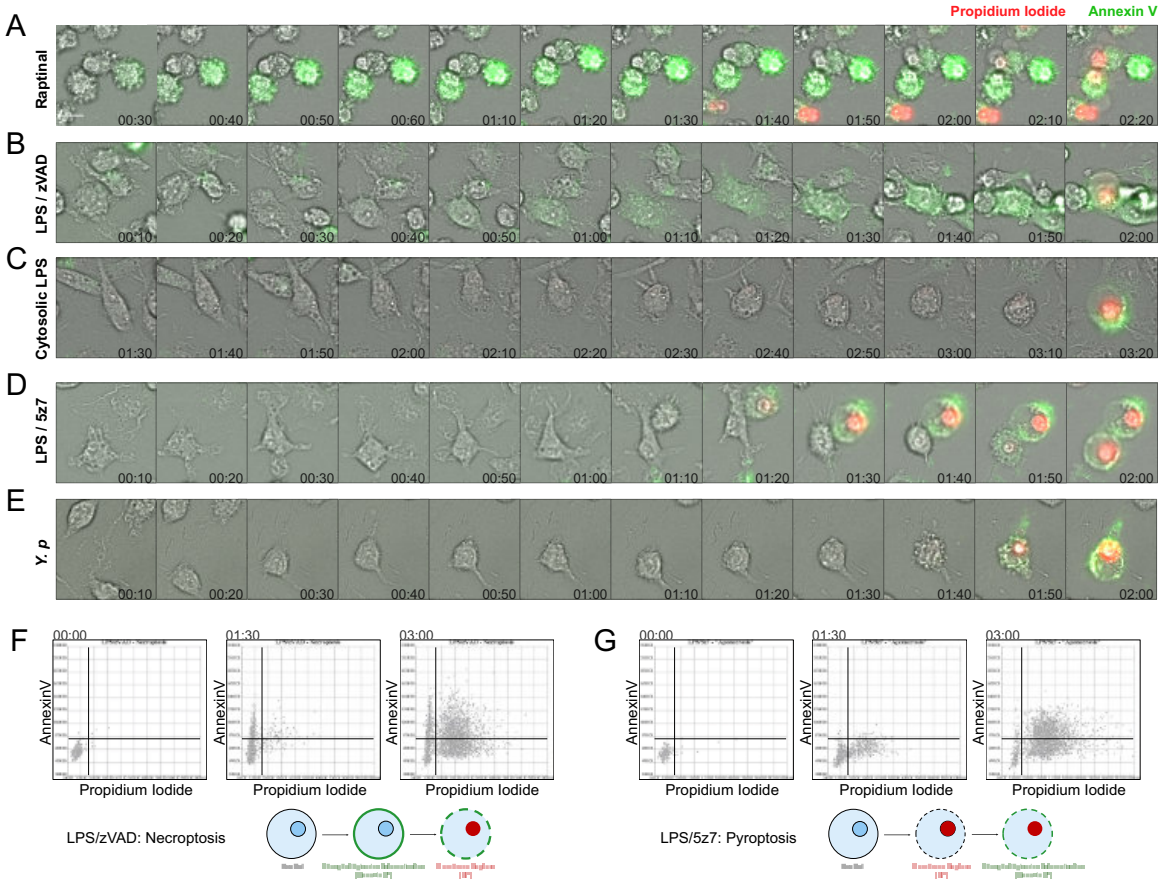

Figure 3.3: Yersinia and LPS/5z7 driven cell death resembles pyroptosis by morphology

(A - E) B6 bone marrow derived macrophages were stimulated as indicated. Y.p. stands for Y. pseudotuberculosis. Shown are 10 minute frames from time lapse microscopy performed at 40x magnification of AnnexinV and propidium iodide dual staining during the progression of cell death. 12 frames preceding membrane rupture are shown to depict the two hours of cell death progression leading to loss of membrane integrity. Scale bar = 10um (F, G) Cells are stained with wheat germ agglutinin, AnnexinV, and PI are imaged at 4x magnification, 2 minute intervals, with 4000 cells per field of view. AnnexinV and PI signals were extracted from wheat germ agglutinin labeled cells, converted into numerical values, and plotted on the Y axis for AnnexinV, and X axis for PI. Representative time points of 0, 1.5hr, and 3hr are shown. Bottom cartoons depict our simplified model of the progression of phosphatidylserine externalization and membrane rupture during necroptosis or LPS/5z7 driven cell death.

cell lysates were probed for active cleavage products of GsdmD and GsdmE. We observed that GsdmD and GsdmE are both cleaved to generate the active p30 fragment within 3 hours of LPS/5z7 stimulation as well as *Yersinia* challenge (Figure 3.4A). In addition to the active p30 fragment generated by caspase-1 and caspase-11 as previously described [97,98, 305,314], we also observe a higher GsdmD fragment near 40kDa, likely the inactive p43 recently reported downstream of caspase-3 activity [314]. Macrophages lacking GsdmD show a significant delay in propidium iodide incorporation during challenge with either LPS/5z7 or *Yersinia* (Figure 3.4B, C). Morphologically, the curtailed AnnexinV staining in GsdmD sufficient cells became robust and prolonged with the loss of GsdmD, recapitulating an apoptotic morphology (Figure 3.4D, E). This can be seen on a population view with LPS/5z7 that drives a synchronized cell death response (Figure 3.4D), as well as on individual cellular basis during *Yersinia* infection (Figure 3.4E).

To determine which caspases are responsible for the cleavage of GsdmD and GsdmE, we stimulated macrophages from various combinations of caspase knock-out animals with LPS/5z7 to observe for gasdermin cleavage as well as cell death. We found that all three cleavage products of GsdmD were abolished in *Rip3*$^{-/-}$ *Casp8*$^{-/-}$ macrophages (Figure 3.4F). The p43 subunit is no longer present in *Casp3*$^{-/-}$ and *Casp3*$^{-/-}$*7*$^{-/-}$ macrophages, with heightened presence of the p30 fragment. All three fragments are present in the *Casp9*$^{-/-}$ macrophages. *Casp1*$^{-/-}$*11*$^{-/-}$ and *Asc*$^{-/-}$ macrophages show minor to no decrease in the appearance of p30 (Figure 3.4F). The complete loss of all three fragments in the *Rip3*$^{-/-}$ *Casp8*$^{-/-}$ macrophages in conjunction with the minor loss of the p30 fragment in *Casp1*$^{-/-}$*11*$^{-/-}$ and *Asc*$^{-/-}$ macrophages shows that Caspase 8 is necessary for the generation of active GsdmD during TAK1 inhibition.

For GsdmE cleavage, just as with GsdmD, the p30 fragment is absent in *Rip3*$^{-/-}$ *Casp8*$^{-/-}$ macrophages. The p30 fragment is mostly abolished in *Casp3*$^{-/-}$ macrophages and completely abolished in *Casp3*$^{-/-}$*7*$^{-/-}$ macrophages (Figure 3.4F). Caspase-8 hence drive GsdmE cleavage primarily via Caspase 3 with minor contribution from Caspase 7, consistent with previous report [314].

Testing the Caspase knockout macrophages for cell death, we observed mild kinetic delays in *Casp3*$^{-/-}$*7*$^{-/-}$, *Casp9*$^{-/-}$, *Casp1*$^{-/-}$*11*$^{-/-}$ and *Asc*$^{-/-}$ macrophages (Figure 3.4G). These mild delays in cell death are consistent with the model of overlapping functions of multiple effector proteins in driving cell death. Caspase 8 is the critical initiator that drives both arms of Gasdermin activation, generating p30 fragments of GsdmD and GsdmE. *Casp9*$^{-/-}$ show no defect in the cleavage of either Gasdermins, but do display a mild delay in cell death kinetics. Caspase 9 may drive mitochondrial dysfunction and ROS accumulation, which has been previously reported during TAK inhibition [298,315 316].

3.2.5 IL-1 maturation requires two distinct cell populations to generate signal 1 and signal 2

NLRP3 activation via potassium efflux as a consequence of membrane pores have recently been shown to occur during both pyroptosis and necroptosis [97,101,102]. Potassium efflux induced inflammasome activation thus may be a commonality shared amongst various necrotic modes of cell death [317]. We therefore wanted to know if TAK inhibition-induced death, with its semblance to pyroptosis in morphology, has the ability to induce inflammasome activation and IL-1 release.

BMDMs stimulated simultaneously with LPS/5z7 or LPS alone did not lead to release of IL-1β in the supernatant (Figure 3.5A), perhaps unsurprising due to the requirement of

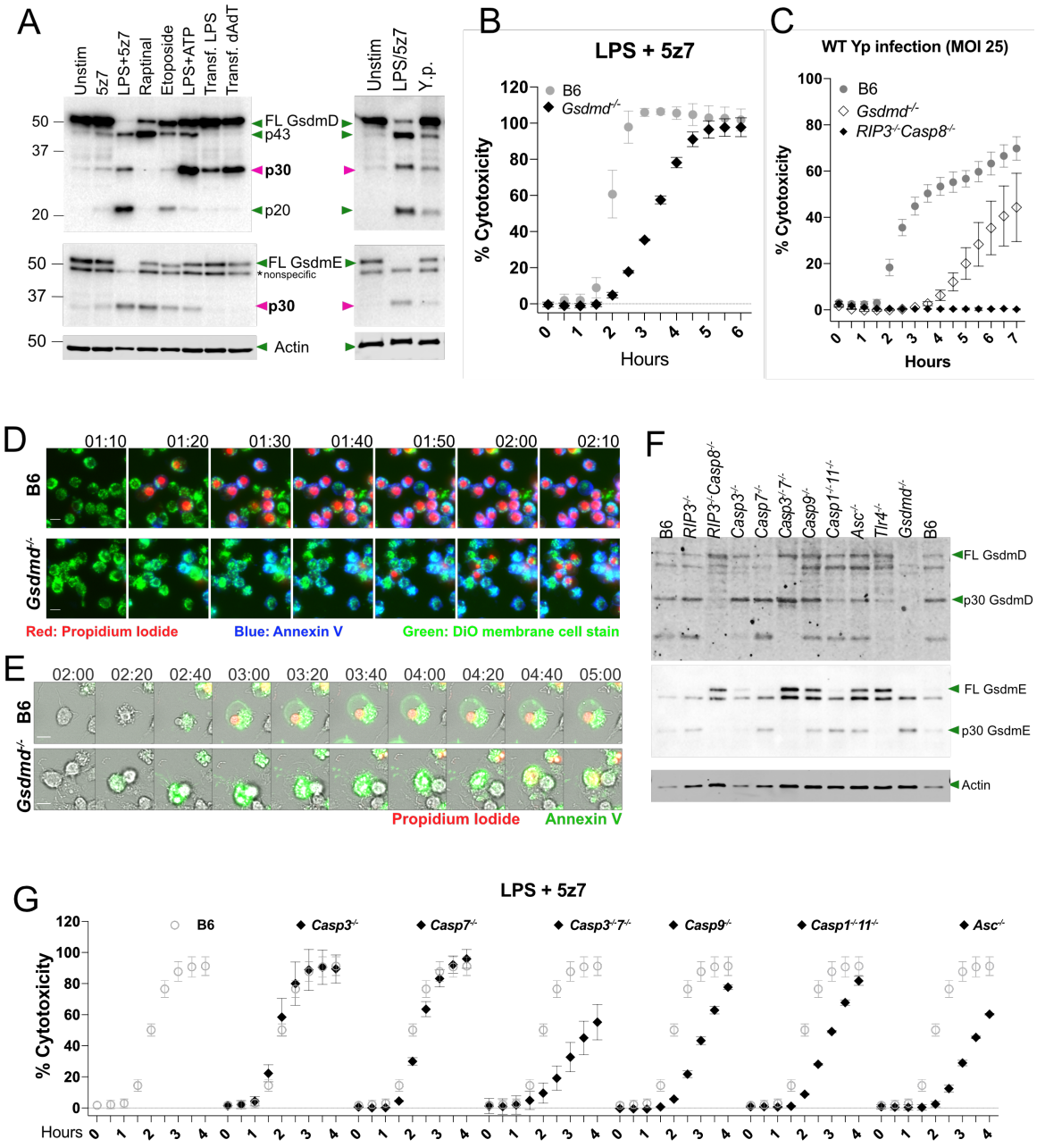

Figure 3.4: Caspase-8 induces GsdmD cleavage to drive pyroptosis, curtailing apoptosis

(A) Cleavage products of GsdmD and GsdmE in cell lysate when BMDMs are stimulated with various cell death triggers and Yersinia infection. Time point shown is 3 hours post stimulation or infection. (B) Cell death kinetics by PI incorporation in B6 and Gsdmd-/- BMDMs stimulated with LPS/5z7. (C) Cell death kinetics by PI incorporation in B6, Gsdmd-/-, Rip3-/-Casp8-/- BMDMs infected with Yersinia. (D) Time lapse microscopy of B6 and GsdmD-/- BMDMs triple stained with Neuro-DiO, AnnexinV, and PI imaged at 20x magnification. Cells were stimulated with LPS/5z7. Image series depict the hour leading up to membrane rupture in GsdmD-/- BMDMs. Scale bar = 10um. (E) Time lapse

microscopy of B6 and GsdmD-/- BMDMs triple stained with AnnexinV and PI imaged at 40x magnification. Cells were infected with Yersinia and imaged series depict the 3 hours leading to membrane rupture in GsdmD-/- BMDMs. Scale bar = 10um. (F) Cleavage products of GsdmD and GsdmE in cell lysate of BMDMs deficient for various caspases when stimulated with LPS/5z7 for 2 hours. (G) LPS/5z7 driven cell death kinetics by PI incorporation in BMDMs deficient for various caspases.

MAPK and NFκB signaling for pro-IL-1 synthesis, which would be inhibited with 5z7. Much like IL-1β, TNF is undetectable when TAK1 is inhibited by 5z7 (Figure 3.5B). Using *Rip3*$^{-/-}$ *Casp8*$^{-/-}$ macrophages to bypass cell death, we found that 5z7 is still effective in blocking all pro-IL-1β induced by LPS stimulation (Figure 3.5C). Similarly, at a *Y. pseudotuberculosis* MOI that is effective in inducing RIP3/Casp8 dependent cell death (MOI 15) we find that pro- IL-1β synthesis is sufficiently blocked in the presence of YopJ (Figure 3.5D).

Interestingly and unlike agonist-driven cell death, during low MOI *Yersinia* infection, IL-1α and IL-1β are found in the supernatant in a RIP3/Casp8 dependent manner (Figure 3.5E). We observed an inverse correlation between IL-1β abundance and infection MOI, with lower *Yersinia* MOI correlating with higher cytokine levels in the supernatant (Figure 3.5E). Of note, at doses where abundant IL-1β secretion is observed, cell death as measured by PI+ nuclei approaches the lower limit of detection (Figure 3.5F). Peterson *et. al.* has recently shown with TNF that during *Yersinia* infection, since the bacterial population do not uniformly translocate adequate levels of YopJ to fully block TAK1 activity, insufficiently-intoxicated cells retain the ability to synthesize cytokines[318]. Similarly, we observe that cellular pro-IL-1β is synthesized when the macrophage population is challenged with diminishing doses of YopJ-sufficient *Yersinia* (Figure 3.5G).

IL-1β maturation requires an additional inflammasome signal to activate caspase-1. With IL-1β release being inverse to cell death, yet still requiring cell death, we hypothesized that two cellular populations are needed to generate the two signals required for IL-1β production during *Yersinia* infection. We propose that pro-IL-1β is synthesized in cells that still retain TAK1 function. This population could be experiencing TLR activity via contact with lesser virulent bacteria in the inoculum or bacterial-shed outer membrane vesicles [319–321]. The inflammasome signal is provided by the TAK-inhibited cells that are unable to synthesize cytokines but are driven to necrotic cell death via Caspase 8 induced GsdmD activation. Upon the death of TAK-inhibited cells, the release of active inflammasome results in the cleavage and maturation of IL-1β in pro-IL-1β sufficient cells. Our line of thinking is supported by findings that oligomerized ASC and functional NLRP3 inflammasome can be transferred from cell to cell [322,323]. Alternatively, the dying population of macrophages may be exposing endogenous oxidized phospholipids from 1-palmitoyl-2-arachidonyl-sn-glycero-3-phosphorylcholine (PAPC), also known as oxPAPC, which has recently been shown to be a potent inducer of IL-1 production in both macrophages and dendritic cells [324,325].

We tested this model by artificially generating two populations during LPS/5z7 treatment (Figure 3.5H-J). LPS serves as Signal 1, to generate pro-IL-1 synthesis. 6 hours later, 5z7 is added to the cells alone or in combination with a second population of naïve cells (Figure 3.5H). We found that unlike cells treated simultaneously with LPS and 5z7, cultures where cells experienced sequential LPS treatment followed by TAK inhibition released IL-1β into the supernatant. This effect is even more pronounced when the second cell population was added simultaneously with 5z7 (Figure 3.5I).

Taking this one step further, we used *Rip3*$^{-/-}$ *Casp8*$^{-/-}$ macrophages as the LPS-primed population. 6 hours after LPS stimulation, B6 BMDMs were added in the presence or absence of 5z7. Significantly elevated supernatant IL-1β was detected in mixed cultures that contained LPS-activated *Rip3*$^{-/-}$*Casp8*$^{-/-}$ cells and B6 cells in the presence of 5z7. Mixed cultures containing LPS-activated *Rip3*$^{-/-}$*Casp8*$^{-/-}$ cells and B6 cells in the absence of 5z7 did not produce significantly more IL-1β than homogeneous *Rip3*$^{-/-}$ *Casp8*$^{-/-}$ cell cultures stimulated with LPS alone (Figure 3.5J). Our findings indicate that a population of actively pyroptotic cells as well as a population of non-TAK inhibited cells are both needed for IL-1 release.

3.2.6 Human macrophages are resistant to TAK-inhibition induced cell death with no consequent secretion of IL-1

In mouse macrophage cultures, YopJ-dependent cell death is observable across a range of bacteria MOIs. At high infection MOI, YopJ-independent cell death predominates, likely due to bacterial overload. YopJ specific cell death is apparent at MOI lower than 60, optimal around 30, and lower doses approaching background levels (Figure 3.6A). Human cells, in contrast, do not display a YopJ dependent cell death process at any MOI tested. We challenged human peripheral blood mononuclear cell (PBMC) derived macrophages (Figure 3.6B), the monocyte-like cell line U937 (Figure 3.9A) and monocyte-derived macrophages (Figure 3.9B). In all cases, bacterial outgrowth-induced cytotoxicity is readily observed at MOI of 120. However, we were unable to detect YopJ dependent cytotoxicity when cells were challenged with WT *Y. pstb* or the *ΔyopJ* mutant, ranging from MOI 120 down to MOI 15 (Figure 3.6B; Figure

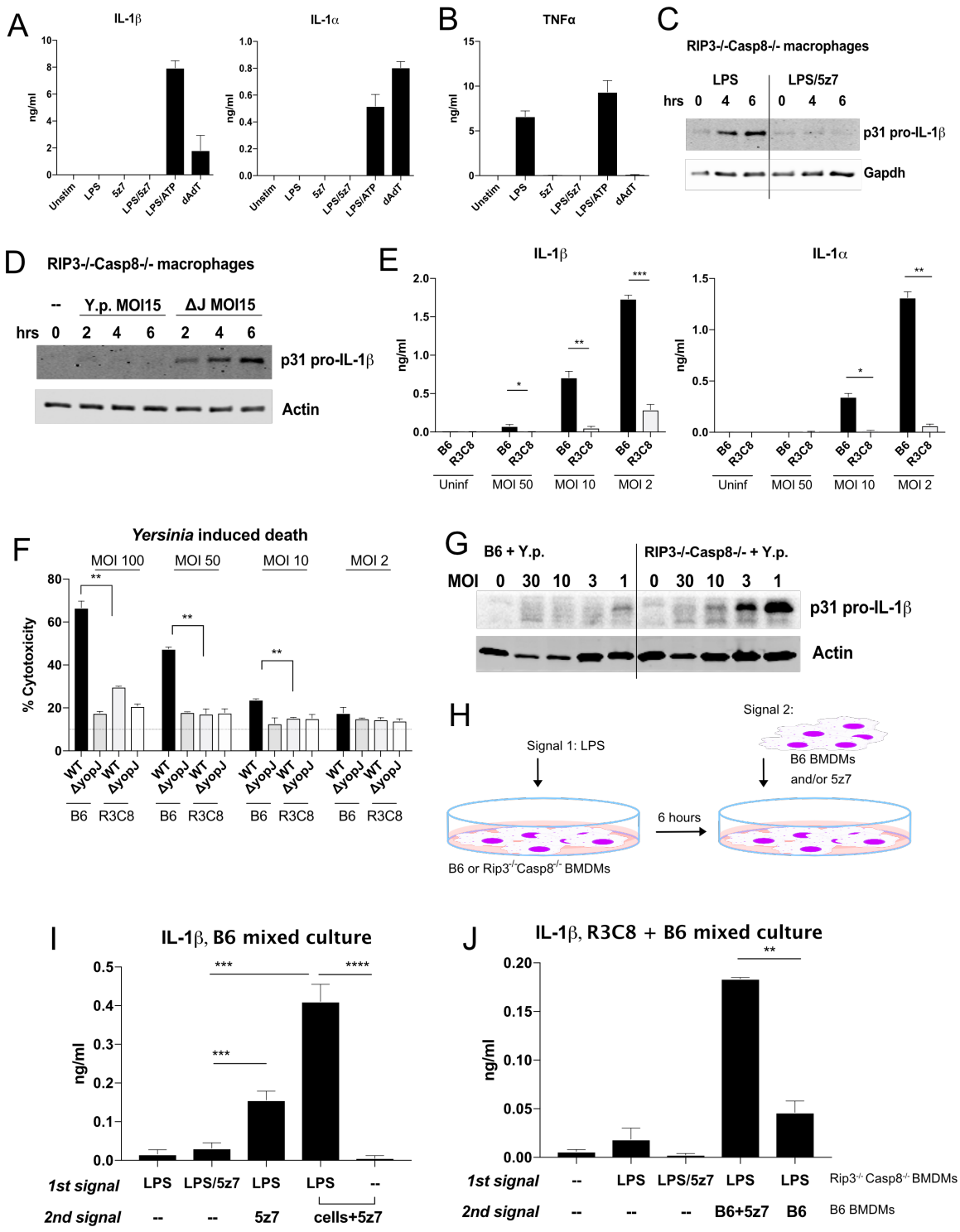

Figure 3.5: IL-1 maturation requires two distinct cell populations to generate signal 1 and signal 2

(A) Supernatant IL-1β, IL-1α measured by ELISA 6 hours post stimulation by LPS/5z7 as compared to canonical inflammasome stimuli. (B) TNF secretion measured by ELISA 6 hours post stimulation by LPS/5z7 as compared to canonical inflammasome stimuli.

(C, D) Pro- IL-1β from cell lysates of *Rip3*$^{-/-}$*Casp8*$^{-/-}$ BMDMs, stimulated with agonists (C) or infected with *Yersinia* (MOI 15) at the indicated time points (D). (E) Supernatant IL-1β, IL-1α measured by ELISA 16 hours post *Yersinia* infection of B6 and *Rip3*$^{-/-}$ *Casp8*$^{-/-}$ BMDMs as a function of decreasing bacterial MOI. (F) *Yersinia* YopJ induced cytotoxicity in B6 and *Rip3*$^{-/-}$*Casp8*$^{-/-}$ BMDMs 6 hours post infection as a function of decreasing bacterial MOI. (G) YopJ-sufficient *Yersinia* infected at decreasing MOI, Pro-IL-1β synthesis measured from cell lysate of B6 and *Rip3*$^{-/-}$*Casp8*$^{-/-}$ BMDMs (16hrs). (H) Experimental schematics for (I, J): (I) IL-1β ELISA from B6 BMDMs where cells are asynchronously stimulated with indicated signals with one hour between first and second stimulus. The last two conditions represent addition of B6 BMDMs and 5z7 for the second signal. (J) IL-1β ELISA from mixed cultures of B6 and *Rip3*$^{-/-}$*Casp8*$^{-/-}$ BMDMs where cells are asynchronously stimulated with indicated signals with one hour between first and second stimulus. The first population of cells are *Rip3*$^{-/-}$*Casp8*$^{-/-}$ BMDMs plated overnight and experience 1st signal for one hour before addition of second signal. The second signal is either absent, or B6 BMDMs with or without 5z7. Time point cytotoxicity quantification and ELISA are +/- SD from three independent experiments compared using student two tailed t test: ns is non-significant ($p > 0.05$); *$p < 0.05$; **$p<0.01$; ***$p < 0.001$. All western blot data are representative of three or more experiments.

3.9A,B). Similarly, human cells were resistant to killing by LPS/5z7 (Figure 3.6C,D), which is consistent with previously published work [315]. With the additional treatment of zVAD, human cells undergo rapid necroptosis with dual AnnexinV and PI positivity (Figure 3.6C,D). In terms of cytokine production, the presence of YopJ reduces pro-IL-1β synthesis from human PBMC-derived macrophages (Figure 3.6E, left). Similarly, 5z7 effectively block LPS-induced pro-IL-1β synthesis (Figure 3.6E, right), and TNF production from PBMC-derived macrophages and monocyte-derived macrophages (Figure 3.6G, Figure 3.9D). IL-1β in the supernatant of human PBMC-derived macrophages and monocyte derived macrophages toward *Yersinia* infection are at the level of LPS-induced IL-1 secretion (Figure 3.6G; Figure 3.9C). Lower infection MOIs did not increase IL-1β release into the supernatant, consistent with the lack of cell death-related inflammasome activation. In contrast, TNFα production from challenge with YopJ-sufficient *Y. pstb* did increase with diminishing MOI (Figure 3.6G; Figure 3.9D),

consistent with Peterson *et al.* 2016, that reduced YopJ efficacy allows for break-through of NFκB activity[318].

We considered the possibility that human macrophages may be able to up-regulate pro survival factors more quickly with LPS stimulation which would allow the cells to survive simultaneous LPS + 5z7 treatment. Indeed, when human PBMC derived macrophages are pre-treated for 2 hours with 5z7 and then stimulated with LPS, we are able to detect cell death (Figure 3.6H; Figure 3.9E) as well as caspase activation and GsdmE cleavage (Figure 3.6I). Of note, we are unable to detect the p30 fragment of GsdmD. However, even with 5z7 pre-treatment, the percentage of cell death was only modest, suggesting that pro-survival factors may be able to bypass TAK1 inhibition in human cells.

3.3 Discussion

In the present study, we demonstrate that *Yersinia* YopJ-induced murine macrophage death involved caspase-8 induced cleavage of both GsdmD and GsdmE. The ensuing cell death is rapid, morphologically pyroptosis, and induces IL-1 maturation (Figure 3.7). At the time of writing this manuscript, work from the Kanneganti lab described the genetic ablation of TAK1 from myeloid cells resulted in spontaneous cell death during macrophage maturation [218]. Their work shows that loss of TAK1 leads to spontaneous cell death, NLRP3 activation and IL-1 production in macrophages due to tonic TNF signaling. The genetic ablation of TAK1 by the Kanneganti lab beautifully complements our work with *Yersinia* infection and acute TAK1 inhibition with 5z7 to provide further evidence for the central role of TAK1 in cell death and inflammation. The cleavage of Gasdermins may have farther reaching implications than cellular obliteration. Work by

both the Shao and Lieberman labs elegantly demonstrated that cleaved GsdmD can attack bacteria and reduce their viability [99,100]. Other work by the Miao lab has also shown that

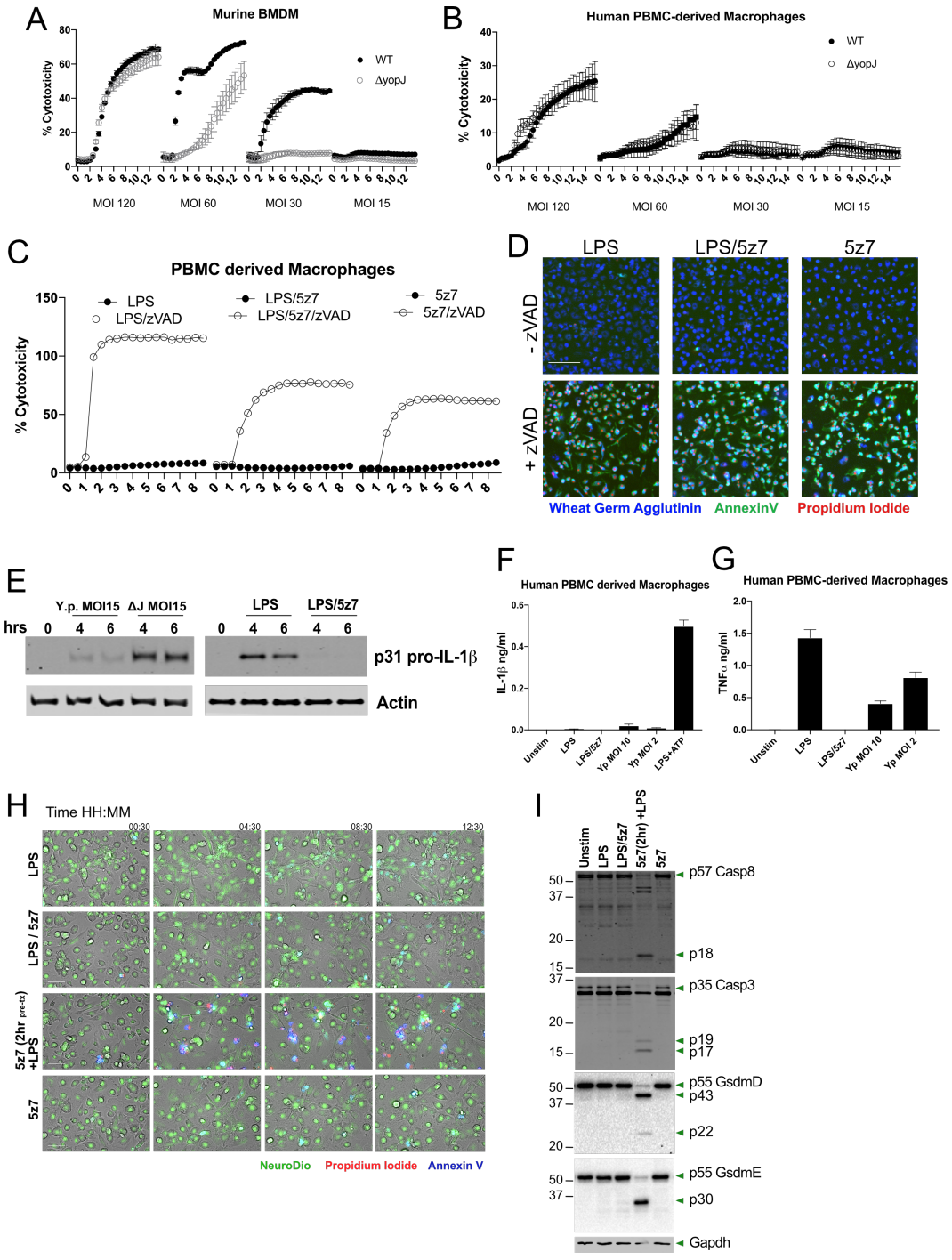

Figure 3.6: human macrophages are resistant to TAK-inhibition induced cell death with no consequent secretion of IL-1
(A) *Yersinia* induced murine macrophage cell death at various bacterial MOI, where MOI of 60-30 show YopJ specific cell death. (B) *Yersinia* induced death of human monocyte-derived macrophages. Bacteria were infected at multiple MOI, with no YopJ dependent killing observed. (C) Human PBMC-derived macrophages were treated with LPS, LPS/5z7, or 5z7, in the presence of absence of zVAD [50uM]. Kinetics of cell death was measured by PI+ nuclei. (D) Representative images of triple stained human PBMC-derived macrophages taken at 4x magnification. PBMC-derived macrophages were stimulated as in (C), image shown is at 7.5 hours post stimulation. Scale bar = 100um. (E) Pro- IL-1β from cell lysates of human PBMC-derived macrophages challenged with *Yersinia* at the indicated MOI and time points (left) or stimulated with LPS +/- 5z7 (right). (F) Supernatant IL-1β and TNF (G) from human PBMC derived macrophages stimulated with LPS/5z7 or Yersinia at MOI that elicit robust IL-1α/β secretion from murine macrophages. (H) Human PBMC derived macrophages were stimulated with indicated conditions and kinetically imaged with triple staining (NeuroDio, Propidium Iodide and AnnexinV). Second from the bottom row involved a 2 hour 5z7 pre-treatment before LPS stimulation. (I) Human PBMC derived macrophages were stimulated with indicated conditions for 4 hours and analyzed by western blotting for Caspase 8 and 3 cleavage as well as Gasdermin D and E. Second to last condition involved 2 hour 5z7 pre-treatment before LPS stimulation. All kinetic cytotoxicity data, western blots, ELISA and imaging experiments are representative of three or more experiments.

pyroptosis can result in pore induced intracellular traps (PITs), leading to retainment of intracellular bacteria within the carcass of dying cells to facilitate phagocytic clearance [326]. Jorgensen's work places the importance of macrophage pyroptosis into an *in vivo* context, in which IL-1 production during pyroptosis recruits secondary phagocytic cells to the site of infection to engulf dead cell carcasses along with its damaged bacterial load. During traditionally pyroptotic infections such as *Legionella, Salmonella, Francisella*, and *Burkholdia,* IL-1 maturation is intrinsic to the infected, dying cell [327–331]. The case of *Yersinia* infection is particularly interesting since MAPK signaling is inhibited by YopJ, effectively blocking pro-IL-1 synthesis in doomed, infected macrophages. Since bacterial populations are not homogenous in their virulence, some percentage of macrophages at the site of infection will not be sufficiently intoxicated by YopJ, thus retaining the ability to synthesize MAPK dependent cytokines (Peterson et al. 2016). We postulate that these

MAPK competent cells are also the producers of pro-IL-1, with neighboring pyroptosing

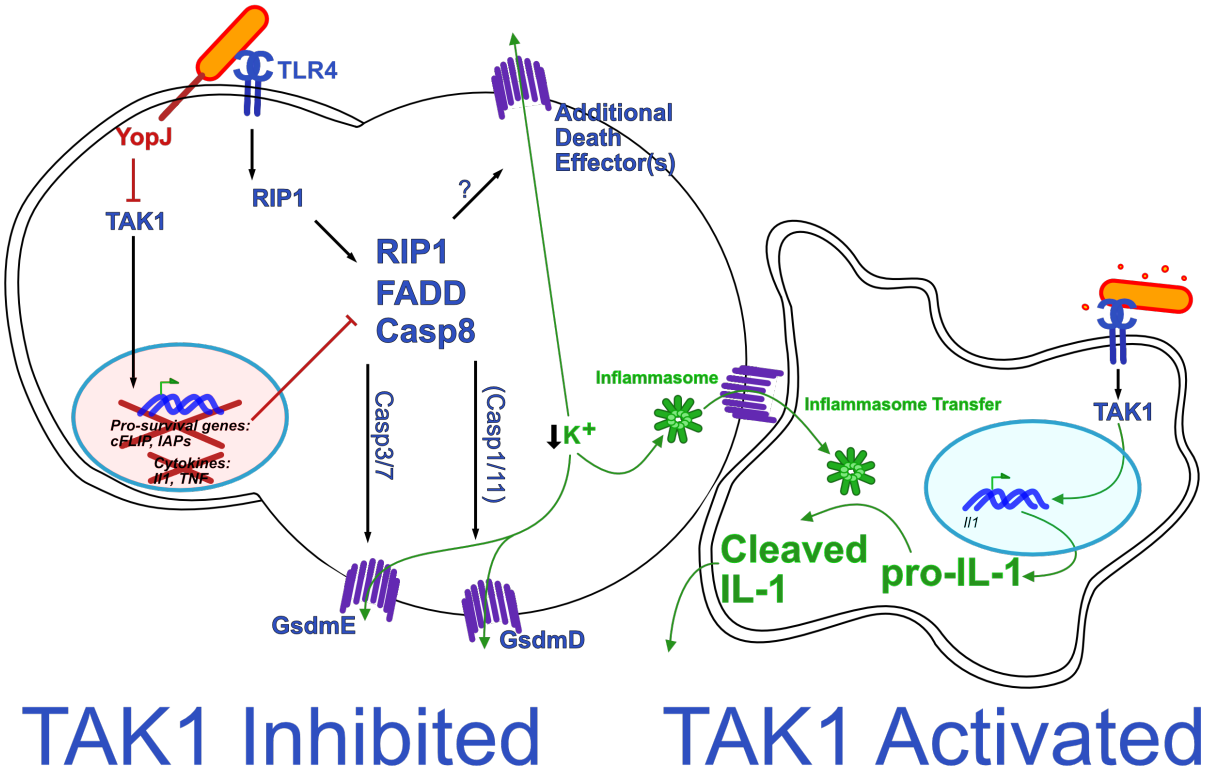

Figure 3.7: Model of Yersinia induced cell death and Il-1 production
Two mouse macrophages are illustrated, the macrophage to the left (dying cell- TAK1 inhibited) is sufficiently intoxicated with *Yersinia* YopJ to inhibit TAK1. The bacterium is also recognized by TLR4, which signals via RIP1 to form a cell death complex composed of RIP1, Caspase8 and likely FADD. This death complex drives GsdmD cleavage and activation partially via caspase 1/11, and GsdmE cleavage via caspase 3/7, both of which result in cell membrane permeabilization and subsequent death. There are likely additional effectors of cell death driven to activation, which in conjunction with GsdmD and GsdmE leads to potassium flux out of the cell and subsequent inflammasome activation. This activated inflammasome is then transferred to a second macrophage either through efferocytosis of the dying cell or uptake of externalized inflammasome. IL-1 maturation occurs via the TAK1 activated macrophage, which is insufficiently intoxicated by YopJ and hence has sufficient TAK1 activation-induced pro-IL-1β. Pro-IL-1β is then cleaved by the transferred inflammasome to produce active IL-1β, which is then released to alert neighboring cells. Alternatively, the TAK1 activated cell may be sensing endogenous oxidized phospholipids from dying cells such as 1-palmitoyl-2-arachidonyl-sn-glycero-3-phosphorylcholine (PAPC), oxPAPC to cleave/ release IL-1β.

cells serving as platforms for potassium efflux induced inflammasome formation (Figure

3.7). We predict that the MAPK competent cells then complete the processing of IL-1

maturation by efferocytosing dead cells [333,334] or by acquiring extracellular ASC/NLRP3 inflammasomes released by dying cells [322,323]. Alternatively the live macrophages may be sensing endogenous oxidized lipids such as oxPAPC, from dying cells which are known to induce IL-1 production in macrophages and dendritic cells via activation of caspase-11 [324,325].

Taken together, macrophages that are defective for the death response, such as *Rip3*$^{-/-}$ *Casp8*$^{-/-}$ and RIP1 kinase dead (RIP1K45A), would therefore be defective for IL-1 maturation as well, lending the animals more susceptible to uncontrolled *Yersinia* replication [244–246]. Extending this line of thought, we found that human macrophages do not undergo YopJ dependent cell death with minimal production of IL-1β during Yersinia infection, an observation that may provide some insight to the devastation of the Plague. In the present study, we used IP2666 *Y. pseudotuberculosis*, which expresses hexa-acylated LPS capable of triggering TLR4. The more dangerous *Yersinia pestis* evolved from *Yersinia pseudotberculosis* and in the process acquired a hypoacylated TLR4-evasive LPS [238,239]. Additionally, hypoacylated Lipid IVa acts as an antagonist for TLR4 activation in human macrophages, although weakly stimulatory against TLR4 of murine macrophages [335]. With YopJ-inhibition of TAK1 tolerated by human macrophages, in combination with a TLR-4 evasive LPS structure, *Y. pestis* effectively creates a silent infection. This point is neatly demonstrated by the forced expression of E.coli LPS on the Kim4 strain of *Y. pestis* as an attenuation strategy [240].

Other examples of necrotic forms of cell death lending protection to the infected host can be found with necroptosis studies. RIP3 has been shown to be protective in the case of vaccinia virus infection [307], CMV infection [336] as well as during HSV replication by

induction of cell death in infected mouse cells [129,130]. In the case of HSV, necroptosis in mouse cells serves to limit viral replication, while the absence of necroptosis in human cells leads to uncontrolled viral replication. These findings with HSV bear striking similarity to the differential species-based cell death responses and pathogen replication highlighted in our study.

Human macrophages therefore may have an inborn tolerance to highly pathogenic bacterial neighbors, to the detriment of the organism. On the macrophage level, the resistance to death may lie in higher expression or longer half-life of key pro-survival proteins. In mouse macrophages, complex IIa forms when there is inadequate pro-survival factors including Cellular FLICE-inhibitory protein (c-FLIP) [51,337] and inhibitors of apoptosis (IAPs) [308]. More recent work has also implicated the loss of IAP and cFLIP during TAK1 inhibition as a reason for cell death [221]. The regulation of IAPs and FLIP are top candidates to investigate the defect in cell death in human macrophages.

Very recent investigations in the field of cell death also show that MAPK-activated protein kinase 2 (MK2), a downstream target of P38 and TAK1, is required for RIP1 phosphorylation at Ser321 [209–212]. This MAPK driven RIP1 phosphorylation inhibits complex II formation and thus limits cell death. The state of RIP1 regulation in human macrophages may also be an area of interest.

The differential response of human and murine macrophages demonstrated by our study and others [129,130,316] thus call to attention the need to study both mouse and human cells to understand course of illness in humans, especially when rodents are reservoirs for the human disease of interest. Beyond *Yersinia*, the anthrax toxin and lethal factor effectors of *Bacillus anthracis* inhibit MAPK activation and has been observed to elicit

cell death and IL-1 production [247,248]. Investigating the role of gasdermins and the presence of pyroptotic features in this and other infectious systems known to inhibit MAPK or NFκB signaling may provide deeper understanding of the mechanism and scope of necrotic cell death in host defense.

3.4 Author Contribution

J.S., B.C.L, R.N., and A.T. conducted experiments. J.S. and B.C.L initiated the study, designed experiments, interpreted results, and wrote the paper. A.R. generated and provided various caspase single and double deletion animals. S.C.B. aided in image analysis and critical discussion. A.P. sponsored the research.

3.5 Materials and Methods

3.5.1 Macrophages and Mice

C57BL/6, *Casp1*$^{-/-}$*Casp11*$^{-/-}$ mice were obtained from Jackson Laboratory. *Casp11*$^{-/-}$ mice were kind gifts from Dr. Vishva Dixit (Genentech) [89]. Animals were housed under protocol approved by the Tufts University Medical School Animal Care and Use Committees. Bones from *Casp3*$^{-/-}$, *Casp3*$^{-/-}$*Casp7*$^{-/-}$, *Casp9*$^{-/-}$ were generated and provided by Dr. Anthony Rongvaux [264]. Bones from *Gsdmd*$^{-/-}$ mice and *Rip3*$^{-/-}$ mice were gifts from Dr. Kate Fitzgerald, generated by Dr. Vishva Dixit [97,339]. Bones from *Rip3*$^{-/-}$*Casp8*$^{-/-}$ mice were given by Dr. Kate Fitzgerald, generated by Dr. Doug Green [58]. Bones from *Ripk1*$^{K45A/K45A}$, *Ripk3*$^{K51A/K51A}$ mice were gifts from Dr. Alexi Degterev and generated by Dr. John Bertin and Dr. Peter J Gough from GlaxoSmithKline (PA, USA) [339,340]. Bone marrow-derived macrophages were isolated from mice and propagated for 7 days in RPMI containing 20% FBS, 30% L cell supernatant, 2% Penn/Strep on non-tissue culture treated Petri dishes. Unless otherwise noted, cells were plated at a density of 1x 10^6 cells

per cm^2 for experiments in RPMI containing 10% FBS, no antibiotics were used during infection.

3.5.2 Inhibitors and TLR agonists

Lipopolysaccharide (LPS) *S. minnesota* R5 [10ng/ml] and 5z7 [125nM] were purchased from Sigma. For LPS transfections, we used *E. coli LPS* 0111:B4 [2ug/ml] and Lipofectamine 2000 from Thermo according to manufacturer suggestions. zVAD.fmk was purchased from Millipore and used at 50uM. Necrostatin-1 [10uM], Etoposide [150 uM] and Raptinal [10uM] were purchased from Sigma.

3.5.3 Yersinia pseudotuberculosis Infection

Y. pseudotuberculosis strains of IP2666 wild type and *ΔyopJ* were gifts from Dr. Ralph Isberg and Dr. Joan Mecsas, used as previously described [341]. *Yersinia* bacteria were grown on LB plates containing Irgasan. Single colonies were picked for 16hr overnight cultures grown in 2xYT media at 26°C, followed by back-dilution to an OD_{600} of 0.2 with supplemented 20mM $MgCl_2$ and 20mM NaC_2O_4. Back-diluted cultures were grown at 26°C for 2 hours followed by 37°C for 2 hours. Macrophage cultures were infected at MOI ranges indicated in figures and figure legends.

3.5.4 Human macrophages

De-identified human peripheral blood was obtained from New York Biologics. The use of de-identified human samples followed a protocol approved by the Tufts University School of Medicine Institutional Review Board. Peripheral blood mononuclear cells were isolated via Ficoll gradient. Monocytes were obtained from peripheral blood using the EasySep Direct Monocyte Isolation Kit (STEMCELL technologies). $CD14^+CD16^-CD68^-$ monocytes were extracted and differentiated into $CD14^+CD16^-CD68^+$ macrophages over

the course of 7 days in RPMI containing 20% FBS, 200U/ml Penicillin and 200µg/ml Streptomycin. and 100 µg/ml of human monocyte colony stimulating factor (M-CSF; PeproTech) [342,343]. Differentiated macrophages were cultured for 40 hours further in RPMI containing 10% FBS, 200U/ml Penicillin and 200µg/ml Streptomycin, in the absence of M-CSF prior to infection or agonist stimulation.

3.5.5 Time lapse microscopy and kinetic cytotoxicity assay

The Cytation3 automated microscope was used to maintain temperature at 37°C and 5% CO_2 for kinetic imaging of live cell cultures. Cells were seeded in 0.17mm thickness glass bottom imaging plates, in RPMI (Hyclone) media. For kinetic cytotoxicity assays, cells were imaged at 30 minute interviews with 4x magnification to capture 3000-4000 cells per field of view. Propidium iodide (10µg/mL, Life Technologies, P3566) was detected via 535 nm excitation and 617 nm emission, with individual puncta of 4um-10um in size counted as nuclei. For 100% cytotoxicity control, cells were treated with 0.1% Triton X-100, similar to protocols for measuring Lactate Dehydrogenase (Promega). AnnexinV binding requires media controlled at pH 7.2-7.5 (1mM HEPES) and supplemented up to 2mM $CaCl_2$ [344,345]. For kinetic image cytometry in detection of dual AnnexinV and PI positivity, cells were labeled with a total cell stain via Neuro-DiO (ex. 488) or Wheat Germ Agglutinin (ex. 350). AnnexinV was imaged on ex.350 or ex.488, depending on the total cell stain used. Images were taken at 4x magnification, every 2 minutes, and image stacks were analyzed on iVision, where cellular masks were generated via the total cell stain. Signal intensities of AnnexinV and PI were extracted from masked area, and signal intensity was plotted as numerical values to generate

kinetic cytometry plots. 20x and 40x magnification images were taken under similar conditions.

3.5.6 Western blotting

At the desired time points post stimulation or infection, media supernatant was collected, and cells were lysed directly in 1X Laemmli Buffer with 5% β-mercaptoethanol, boiled for 10 minutes, and incubated on ice for 10 min prior to loading on SDS PAGE gels. Supernatant proteins were precipitated via methanol/chloroform extraction, and precipitated proteins were resuspended and denatured in 1X Laemmli Buffer with 5% β-mercaptoethanol. Primary antibodies against caspase-3, caspase-7, caspase-8, caspase-9, CypA, Gapdh, and PARP were purchased from Cell Signaling Technologies. Antibodies to Gasdermins were purchased through abcam: anti-mouse GsdmD (ab209845), anti-human (ab210070) and anti-human/mouse GsdmE (ab215191). Total MLKL antibody was purchased from Millipore (#MABC604). Phospho-MLKL-S345 (#ab196436) antibody purchased from Abcam.

3.5.7 ELISA for cytokine secretion

Murine IL-1α, IL-β, TNFα ELISAs, and human IL-1α, IL-1β, TNFα ELISAs were DuoSet ELISA kits purchased from R&D, used according to manufacturer's instructions.

3.5.8 Statistical Analysis

Statistical analyses were performed using the Student's t test (two-tailed) using GraphPad Prism. Where *$p < 0.05$; **$p<0.01$; ***$p < 0.001$.

3.6 Supplemental Figures and Legends

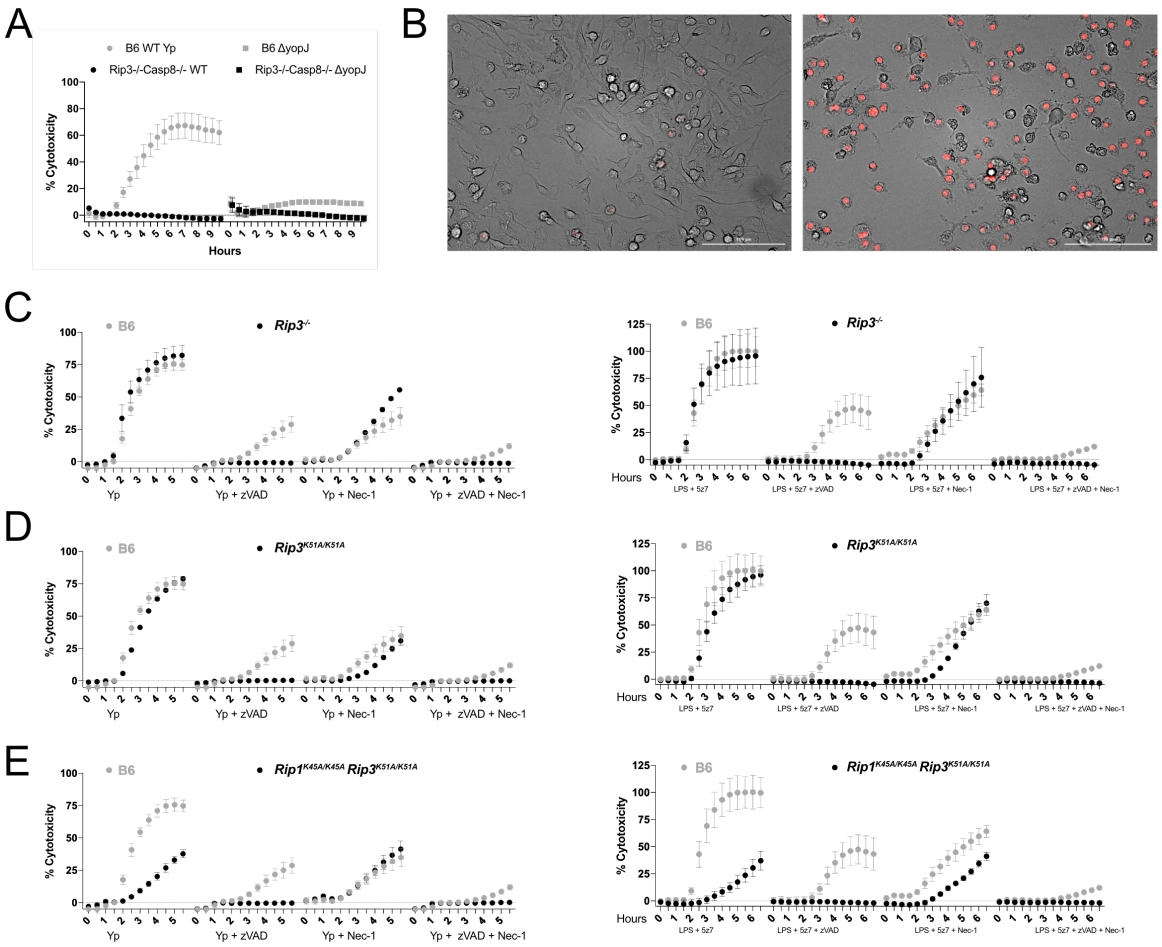

Figure 3.8: Related to Figure 3.1

(A) Bone marrow derived macrophages from C57BL/6 (B6) and Rip3-/-Casp8-/- animals were infected with *Yersinia pseudotuberculosis* IP2666 at MOI of 30. Kinetic cytotoxicity monitored via nuclear incorporation of propidium iodide, images of cell culture taken every 30 minutes. (B) B6 BMDMs are stimulated with [10ng/ml] /5z7 [125nM], representative image of propidium iodide positive cells from unstimulated and 4 hour stimulated cells are shown. Current image at 20x magnification to show cellular morphology and nuclear propidium iodide, scale bar measures 100um. (C - E) BMDMs from C57BL/6 (B6) and various genetically modified animals were stimulated with *Yersinia pseudotuberculosis* on the left, or LPS [10ng/ml] /5z7 [125nM] on the right. Percentage cytotoxicity was calculated by microscopy via counts of propidium iodide positive nuclei per field of view, normalized to 100% lysis by 0.1% Triton-X. Caspases were inhibited with zVAD treatment [50 uM], and RIP kinase activity was inhibited with Necrostatin-1 (Nec1) [10uM]. All inhibitors were added simultaneously at time zero. All kinetic cytotoxicity data are representative of three or more experiments.

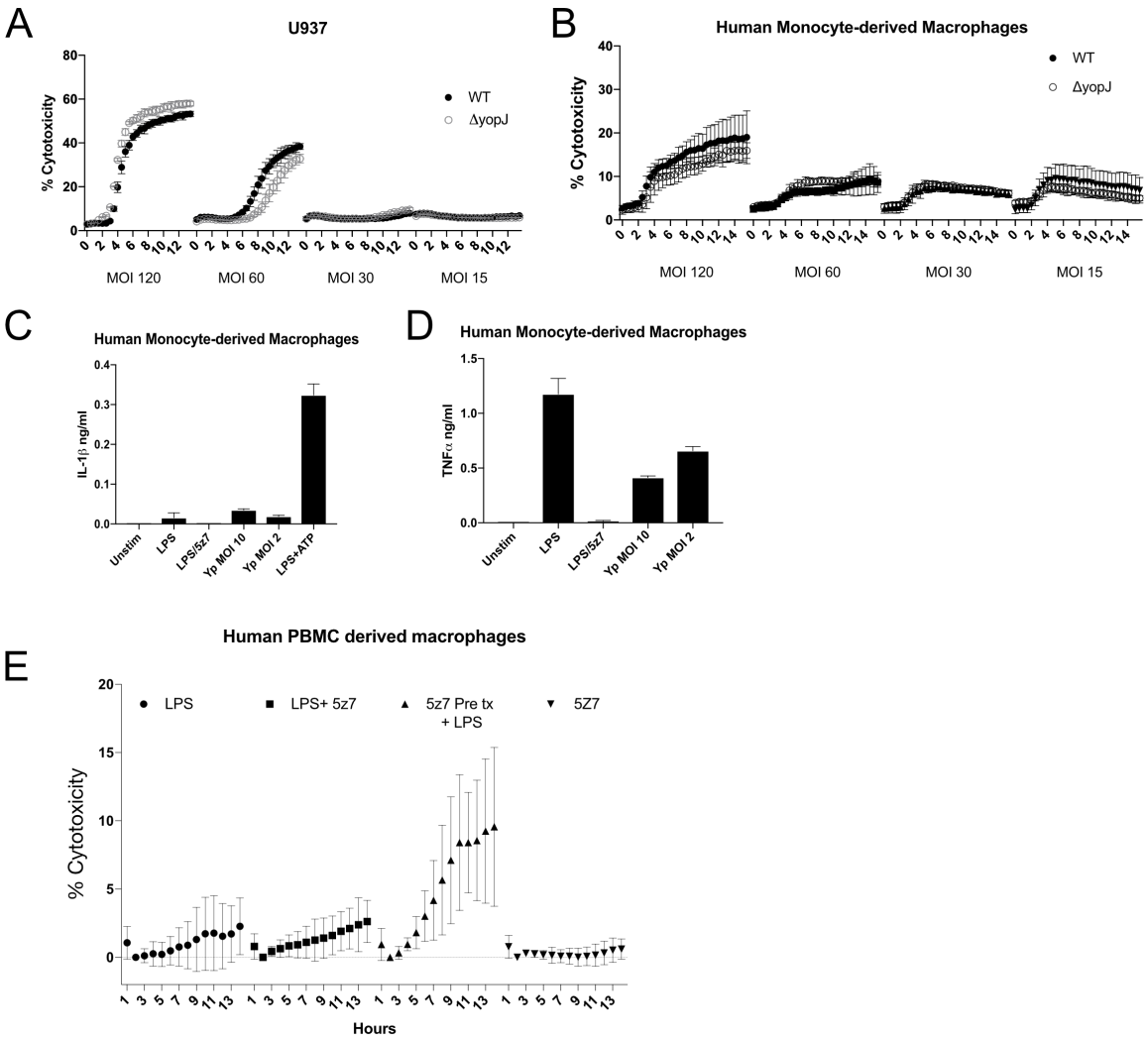

Figure 3.9: Related to Figure 3.6
(A - B) Yersinia induced death of PMA activated U937 cells (A) or human peripheral blood mononuclear cell (PBMC) derived macrophages (B). Bacteria were infected at multiple MOI, with no YopJ dependent killing observed. (C) Supernatant IL-1β and TNF (D) from human monocyte derived macrophages stimulated with LPS/5z7 or Yersinia at MOI that elicit robust IL-1 secretion from murine macrophages. (E) Human PBMC derived macrophages weer stimulated with indicated conditions and monitored for cytotoxicity over time. The 5z7 pre treatment condition is for 2 hours prior to LPS stimulation. All kinetic cytotoxicity data, and ELISA are representative of three or more experiments.

Chapter 4: Discussion

Cell death and inflammation are key components of the innate and adaptive immune response. In our first manuscript on necroptosis we are proposing a model where IFNb does not directly kill macrophages but rather regulates the expression of at least two ISGs necessary for necroptosis (Figure 2.7). This model is in agreement with the well accepted anti-viral function of IFNs being based on the function of ISGs[176,346]. An alternative model of IFN function in necroptosis proposes association of IFNAR and RIP1 as shown in Figure 6 of the 2012 Nature Immunology paper on IFNAR and *Salmonella* induced necroptosis by Nirmal Robinson and Subash Sad[258]. In this paper, the authors predicted association between RIP1 and IFNAR based on well-established association between RIP1 and TNFR that has been well characterized by Hailing Hsu and David Goeddel's 1996 paper showing the death domain dependent interaction of TNFR with RIP1 via TRADD[49]. This model however, does not support Robinson and Sad hypothesis regarding domain interactions between RIP1 and IFNAR, because IFNAR does not have a death domain. Therefore, a non-transcriptional mechanism for how type I IFN promotes necroptosis remains to be elucidated.

Our findings show that total levels of MLKL can regulate necroptosis. If we assume that protein dimerization is the first step to higher level multimerization, we can use some basic principles of thermodynamics to predict the effect of protein monomer concentration on dimerization potential. Indeed, this application of thermodynamics to study protein dimerization has been well documented[347]. We know that the chemical reaction proceeds to equilibrium from monomer association to form a dimer.

$$[Monomer] + [Monomer] \rightleftarrows [Dimer]$$

Based on the rate of dimer association at varying temperatures, one can determine the association constant *Ka*, which will be a fixed value[347].

$$Ka = \frac{[Dimer]}{[Monomer]^2}$$

From the fixed value of Ka for a given dimerizing protein, one can see that there is an exponential relationship between total protein levels and dimerization. In the case of MLKL that would mean that higher cellular total MLKL levels would predispose to dimerization (**Figure 4.1**)

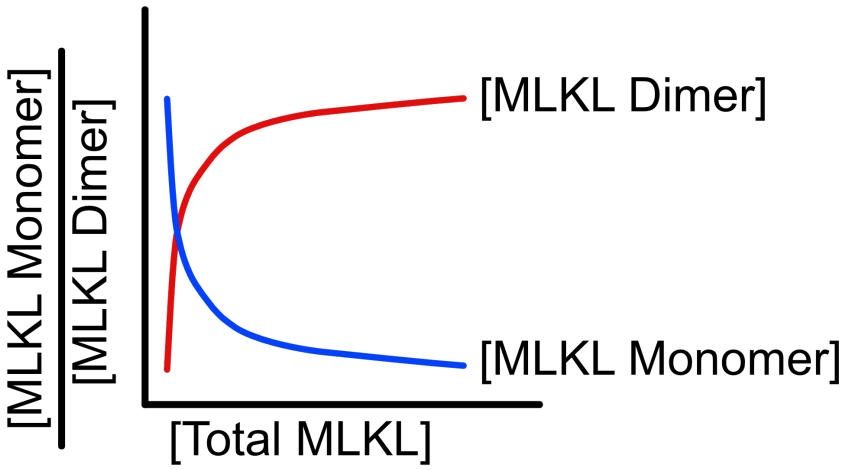

Figure 4.1: Diagram showing the relationship between total MLKL concentration and presence of monomer and dimer concentration.
As MLKL concentration increases, the concentration of dimerization goes up.

Since MLKL is the effector of necroptosis, there has luckily been extensive biochemical characterization. Indeed, MLKL dimerization alone (with synthetic dimerization domains) is enough to cause cell death via oligomerization[252,349–352], lending legitimacy to the importance of protein dimerization as the first step in the polymerization cascade[65,66]. Other work has also nicely shown that over-expression of MLKL without any additional stimulus can cause cell death[352,353]. Several phospho mimetic mutants including S345D as well as C-terminal truncations leaving intact the

deadly N-terminus can more potently induce protein oligomerization cell death upon over-expression without additional stimulus[354]. These experimental observations further highlight the importance of balanced MLKL as well as other death effector oligomerizing proteins notably including the gasdermin family of pyroptosis effectors.

I first appreciated the importance of balanced expression of MLKL, when it killed all of my cells before I was able to use them for experiments. This lead us to develop an attenuated promoter to reduce MLKL over-expression. However, the inducible over-expression systems are also another more controlled approach to limit cytotoxicity. Our lab has cloned murine MLKL into a doxycycline inducible system also encoding an internal ribosomal entry site (IRES) followed by GFP. This generates a system where we can induce untagged MLKL expression and have a proportional GFP signal, which can be used to monitor the effects of MLKL levels on necroptosis using live cell microscopy. Single cell imaging techniques to study cell death have been wonderfully applied in the field of Apoptosis in work by Bree Aldridge and Peter Sorger[355]. Indeed, I think the field is ready to now study life and death signaling for necrotic forms of cell death at the single level[356].

We showed that constitutive IFN signaling is critical for maintaining adequate expression of MLKL, however we were also unable to re-sensitize IFN deficient cells to necroptosis with MLKL over-expression. This suggests that there are either additional effectors of necroptosis that need to be maintained by constitutive IFN signaling or there exists an inhibitor of necroptosis that is over-expressed in the absence of constitutive IFN signaling. Known inhibitors of necroptosis including Ppm1b[271], TRAF2[272], CHIP[273] and components of the ESCRT-I and III[274] machinery are un-altered by constitutive IFN

status. To help determine the exact level of defect in the necroptosis cascade in the context of IFNAR deficiency we would have to express inducible dimerizable RIP1, RIP3 and MLKL. I would predict that MLKL dimerization should be able to induce cell death in IFNAR deficient animals unless there is high basal expression of a downstream inhibitor of necroptosis such as the thiol oxidoreductase thioredoxin-1 (Trx1)[357]. Similarly, I predict that RIP1 or RIP3 dimerization should not be able to induce death in IFNAR deficient animals because of low MLKL expression. However, the more interesting question is whether RIP1 or RIP3 dimerization can induce death in IFNAR deficient animals that are re-constituted for MLKL expression. These experiments with dimerizable constructs would surely help shed more mechanistic insight into the role of IFNAR signaling in necroptosis.

Additionally, newly developed CRISPR screening techniques should be able to enrich for genes required for necroptosis. This screen would involve transducing a genome wide gRNA library into Cas9 expressing BMDMs[358–360]. After differentiation, the cells would then be primed with IFNβ before treatment to push non transduced cells toward 100% cytotoxicity. The cells would then be treated with zVAD and a combination of various known inducers of necroptosis including LPS, TNF and SM. The surviving cells would be enriched with critical components of the necroptosis machinery. Our RNA sequencing analysis has already identified many genes regulated by constitutive IFN. However, we should be able to significantly reduce our list of candidate genes by overlapping the set of genes regulated by constitutive IFN and those enriched by the CIRSPR screen.

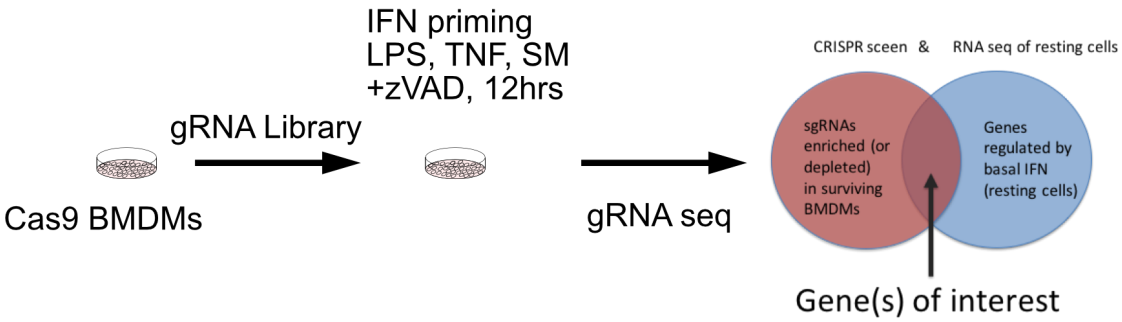

Figure 4.2: Schematic outlining a Crispr screen to identify further effectors of necroptosis regulated by constitutive IFN signaling.

The screening approach discussed above would help uncover new effectors of necroptosis, however, there origin of constitutive IFN is still a wide open question. We see that mice with defective cytosolic DNA sensing are low in constitutive IFN. However, the source of cytosolic DNA is unknown and there are many possibilities including mitochondrial DNA[264], efferocytosis[361], endogenous retorviruses[195], DNA damage[263] and more. To help determine the origin of constitutive IFN, I propose generating a constitutive IFN reporter by crossing an Mx1 Cre mouse to a fluorescent reporter mouse with an upstream loxP site flanked stop codon[362]. In this mouse, cells experiencing constitutive IFN would engage the Mx1 Cre to cut out the stop codon and allow for fluorescent protein (FP) expression. This system would turn on FP expression once the cells have experienced a strong enough stimulus and the cells would stay positive for the remainder of their existence. A more flexible (though more costly) system would involve generating and Mx1-FP transgenic animal, which should produce FP in direct proportion to the magnitude of constitutive IFN status. One could then monitor the differentiating macrophages kinetically to see if the cells with high IFN status have eaten their neighbors (efferocytosis), experienced mitochondrial or lysosomal stress, using mitotracker and lysotracker. One could also sort out the high and low constitutive IFN

macrophages for further study including functional testing as well as sequencing, and mass spec. Additionally, these reporter animals could also be studied In Vivo. The reason behind not directly tagging IFN, is that even induced levels are hard to detect with FP signals[363], though luciferase reporter animals[364] have proven useful for non-kinetic studies.

Yet another area for further expansion of our work on necroptosis would involve crossing MLKL, and RIPK deficient animals to models of autoimmunity, including the TLR7.1 model of autoimmunity we used in our study. While we see that the IFN primed macrophages of the TLR7.1 animals pre-disposes cells to necroptosis, we do not know if deficiency in necroptosis genes would be protective or harmful in disease.

In the second project, we found that TAK1 inhibition leads to initiation of Gasdermin mediated pyroptosis rather than apoptosis. Our first hint that we were dealing with caspase dependent necrotic death came from the observation that cells deficient in MLKL were fully sensitive to LPS + 5z7 (L5Z) induced cytotoxicity and that zVAD could inhibit the death fully. Indeed, we showed that necroptosis is the backup mechanism of cell death. While performing biochemical experiments, L5Z treated cells seemed to evaporate off the plate. This made doing western blotting rather complicated as total cellular protein was drastically lower in L5Z treated cells. Ultimately this turned out to be a symptom of the necrotic nature of the cell death, which we were able to visualize with simultaneous Annexin V binding, propidium iodide incorporation and necrotic bubble formation during kinetic microscopy. We were then able to find that Gasdermin D is cleaved and needed for the necrotic morphology of cell death. Indeed, we see that with Gasdermin D deficiency, the delayed cell death appears to have apoptotic morphology by

extensive single positive Annexin V staining and absence of necrotic bubbles. Investigating the role of other Gasdermins, including Gasdermin E, in this process would be very interesting.

The connection between Caspase 8 and Gasdermin D is another area that deserves more work. Indeed, it would be interesting to see if recombinant Caspase 8 is able to cleave Gasdermn D into the active killer fragment. Additionally, we could explore this question by over-expressing fluorescently tagged Gasdermin D and fluorescently tagged Caspase 8 to see if we can detect any stimulus dependent co-localization. Since cellular cytotoxicity reaches 100% in L5Z treated cells, we should be able to enrich protective gRNAs. Doing the screen using a Gasdermin D knockout would prove useful to determine what is the compensatory pathway the cells take to die. Additional informative screening strategies would include proteome wide mass spectrometry, especially in *RIP3*$^{-/-}$ *Casp8*$^{-/-}$ BMDMs as presumably important cellular changes (including pro-survial factor degredation) are happening upstream of Caspase 8 activation.

The role of TAK1 in mouse development is well highlighted by embryonic lethality in whole body knockout[214]. Therefore, it would be interesting to see if whole body TAK1 deficiency could be rescued by crossing onto Gasdermin D deficient animals. Additionally, since TAK1 deficiency in BMDM development results in TNF dependent death, it would be interesting to do a 'drop out' CRISPR screen in B6 and *TNF*$^{-/-}$ animals to identify genes or pathways similarly dependent on TNF for inducing cell death in developing macrophages. Another interesting way to induce TAK1 deficiency would also involve tamoxifen inducible viral over-expression of YopJ. This would need to be controlled by an inducible promoter, otherwise cells would die due to

tonic TNF signaling[219]. Alternatively, one could over-express YopJ in TNF deficient animals and look for cell death responses upon LPS or TNF stimulation. Using this infection relevant method of TAK1 inhibition may reveal important differences from traditional chemical inhibition with 5z7 or genetic deletion.

Applications for studying the mechanism of TAK1 induced death is clear from the context of extensive small molecule development for cancer treatment and inflammatory diseases[225–229,366]. Additionally, a significant part of our work explores the role of TAK1 inhibition in the context of *Yersina pseudotuberculosis* infection. Yersinia infection had for a long time known to induce cell death, which was recently proposed to be RIP1 kinase dependent non necroptotic apoptosis[246]. Here we present data to suggest that Yersinia induced death is actually Gasdermin D mediated pyroptosis. We also found that human macrophages do not undergo YopJ dependent cell death and IL1 production, resulting in an immunologically silent infection. Human macrophages were also resistant to LPS + 5z7 treatment but could be sensitized to cell death with 5z7 pre-treatment. We suspect that this may be because human macrophages are faster at initiating the pro survival signals in response to LPS, but this would need to be tested.

Recent work from the Lieberman lab has shown that Gasdermin D can kill bacteria[99]. We have preliminary results confirming these findings in our system, where there is a higher bacterial CFU count in *RIP3*$^{-/-}$ *Casp8*$^{-/-}$ BMDMs infected with Yersinia. It would be interesting to see if human macrophages, pretreated with 5z7 to sensitize to cell death, would have lower Yersinia CFU.

Much of the cell death work done with *Yersinia pestis* has been with the KIM5 mutant strain[245,300] which expresses immuno-stimulatory E. coli LPS[240]. Virulent *Yersinia*

pestis expresses immuno-evasive LPS, which I predict would result in an entirely different cell death response. In fact, the cell death would likely resemble treatment with 5z7 alone, resulting in slow TNF dependent cytotoxicity. Indeed, it would be an interesting experiment for anyone with BSL3 facilities and approval to test whether or not fully virulent *Yersinia pestis* can induce YopJ dependent cell death. If virulent Yersinia does not induce cell death, then this may be yet another immuno-evasive strategy.

Other applications for the LPS + 5z7 model of cell death includes other infections which are known to inhibit TAK1, which includes but is not limited to *Bacillus anthracis*, and *Porphyromonas gingivalis*. These two bacterial infections are particularly interesting since they both potently inhibit TAK1, but result in completely different outcomes in terms of cell viability. Indeed, *Porphyromonas gingivalis* infection of cells does not result in cell death in macrophages in experiments I assisted with George Papadopoulos. This means that while *P. gingivalis* can potently inhibit TAK1as shown by work from Caroline Genco's lab[366,367], the bacterium is able to avoid a cell death response in infected cells. This may be due to Gingipain induced inactivating cleavage of other key components of the pathway including possibly Gasdermin family members. *Bacillus anthracis* on the other hand is known to induce cell death in macrophages, which has been previously described as apoptosis[247,248,368,369]. Perhaps it is worth revisiting whether *Bacillus anthracis* may be inducing pyroptosis? There are many other infections which inhibit MAPK signaling[294] and determining whether or not cell death is happening could provide important insights into disease pathogenesis as well as cell death mechanisms.

Caspase 8 mediated pyroptosis may have functions beyond those outlined above in the context of infection. In looking at work from our lab by Bridget Larkin on STING activation mediated cell death in T cells[370], we see that both caspase inhibition and Nec-1 treatment is needed to inhibit DMXAA induced cell death in T cells (Figure 4). If the cell death is being regulated in such a way that it is absent in *RIP3*$^{-/-}$ *Casp8*$^{-/-}$ T cells but unaffected in *RIP3*$^{-/-}$ T cells, then we are dealing with a Caspase 8 mediated form of cell death. Indeed, one would have to further characterize the nature of cell death both kinetically and morphologically to see if it more closely resembles apoptosis or necrosis. Indeed, it is possible that in this context Caspase 8 is driving a necrotic death pathway via Gasdermin D cleavage, but this would have to be tested as extrinsic apoptosis is also likely to play a role. Other examples of Caspase 8 potentially driving necrotic cell death includes work by Kim Newton and Domagoj Vucic[135]. Using a model of TNF induced systemic inflammatory response syndrome (SIRS), they show that *RIP3*$^{-/-}$ *Casp8*$^{-/-}$ animals are significantly more protected than *RIP3*$^{-/-}$ and *Casp8*$^{+/-}$ animals to high dose TNF induced hypothermia (Figure 6). Again, Caspase 8 may be driving Gasdermin activation resulting in cell death. There are surely more examples of Caspase 8 driven cell death which we have assumed are resulting from extrinsic apoptosis, which we can now re-visit knowing that Caspase 8 can initiate pyroptosis.

Chapter 5: Bibliography

1. Christopoulou-Aletra, H. & Papavramidou, N. The Manifestation of ‘Gangrene’ in the Hippocratic Corpus. *Ann. Vasc. Surg.* **23,** 548–551 (2009).
2. Sachs, M., Bojunga, J. & Encke, a. Historical evolution of limb amputation. *World J. Surg.* **23,** 1088–93 (1999).
3. Whitaker, I. S., Twine, C., Whitaker, M. J., Welck, M., Brown, C. S. & Shandall, A. Larval therapy from antiquity to the present day: mechanisms of action, clinical applications and future potential. *Postgrad. Med. J.* **83,** 409–413 (2007).
4. Gambarotto, A. Lorenz Oken (1779-1851): Naturphilosophie and the reform of natural history. *Br. J. Hist. Sci.* **50,** 329–340 (2017).
5. Clarke, P. G. H. & Clarke, S. Nineteenth century research on cell death. *Exp. Oncol.* **34,** 139–145 (2012).
6. Gerschenson, L. E. & Geske, F. J. Virchow and apoptosis. *Am. J. Pathol.* **158,** 1543 (2001).
7. Kerr, J. F., Wyllie, A. H. & Currie, A. R. Apoptosis: a basic biological phenomenon with wide-ranging implications in tissue kinetics. *Br. J. Cancer* **26,** 239–57 (1972).
8. Esposti, M. D. Apoptosis: who was first? *Cell Death Differ.* **5,** 719 (1998).
9. André, N. Hippocrates of Cos and apoptosis. *Lancet (London, England)* **361,** 1306 (2003).
10. Sulston, J. E. & Horvitz, H. R. Post-embryonic cell lineages of the nematode, Caenorhabditis elegans. *Dev. Biol.* **56,** 110–156 (1977).
11. Hedgecock, E. M., Sulston, J. E. & Thomson, J. N. Mutations affecting programmed cell deaths in the nematode Caenorhabditis elegans. *Science* **220,** 1277–9 (1983).
12. Robbins, R. B. Some Applications of Mathematics to Breeding Problems III. *Genetics* **3,** 375–89 (1918).
13. Morton, N. E. A history of association mapping. *Methods Mol. Biol.* **376,** 17–21 (2007).
14. Ellis, H. M. & Horvitz, H. R. Genetic control of programmed cell death in the nematode C. elegans. *Cell* **44,** 817–829 (1986).
15. Yuan, J. & Horvitz, H. R. The Caenorhabditis elegans genes ced-3 and ced-4 act cell autonomously to cause programmed cell death. *Dev. Biol.* **138,** 33–41 (1990).
16. Yuan, J., Shaham, S., Ledoux, S., Ellis, H. M. & Horvitz, H. R. The C. elegans cell death gene ced-3 encodes a protein similar to mammalian interleukin-1β-converting enzyme. *Cell* **75,** 641–652 (1993).
17. Xue, D., Shaham, S. & Horvitz, H. R. The Caenorhabditis elegans cell-death protein CED-3 is a cysteine protease with substrate specificities similar to those of the human CPP32 protease. *Genes Dev.* **10,** 1073–1083 (1996).
18. Hengartner, M. O. & Horvitz, H. R. C. elegans cell survival gene ced-9 encodes a functional homolog of the mammalian proto-oncogene bcl-2. *Cell* **76,** 665–676 (1994).
19. Cotter, T. G., Glynn, J. M., Echeverri, F. & Green, D. R. The induction of apoptosis by chemotherapeutic agents occurs in all phases of the cell cycle. *Anticancer Res.* **12,** 773–9 (1992).
20. Liu, X. Induction of Apoptotic Program in Cell-Free Extracts: Requirement for dATP and Cytochrome c. *Cell* **86,** 147–157 (1996).

21. Zou, H., Henzel, W. J., Liu, X., Lutschg, A. & Wang, X. Apaf-1, a human protein homologous to *C. elegans* CED-4, participates in the cytochrome c-dependent activation of caspase-3. *Cell* **90,** 405–413 (1997).
22. Kluck, R. M., Bossy-wetzel, E., Green, D. R. & Newmeyer, D. D. The Release of Cytochrome c from Mitochondria : A Primary Site for Bcl-2 Regulation of Apoptosis. **275,** (1997).
23. Chinnaiyan, A. M., O'Rourke, K., Lane, B. R. & Dixit, V. M. Interaction of CED-4 with CED-3 and CED-9: A molecular framework for cell death. *Science (80-.).* **275,** 1122–1126 (1997).
24. Wu, D., Wallen, H. D. & Nun, G. Interaction and Regulation of Subcellular Localization of CED-4 by CED-9. **275,** 1126–1130 (1997).
25. Trauth, B., Klas, C., Peters, A., Matzku, S., Moller, P., Falk, W., Debatin, K. & Krammer, P. Monoclonal antibody-mediated tumor regression by induction of apoptosis. *Science (80-.).* **245,** 301–305 (1989).
26. Chinnaiyan, A. M., O'Rourke, K., Tewari, M. & Dixit, V. M. FADD, a novel death domain-containing protein, interacts with the death domain of fas and initiates apoptosis. *Cell* **81,** 505–512 (1995).
27. Kuang, A. A., Diehl, G. E., Zhang, J. & Winoto, A. Accelerated Publication - FADD is required for DR4- and DR5-mediated apoptosis. Lack of trail-induced apoptosis in FADD-deficient mouse embryonic fibroblasts. *J. Biol. Chem.* **275,** 25065–25068 (2000).
28. Irmler, M., Thome, M., Hahne, M., Schneider, P., Hofmann, K., Steiner, V., Bodmer, J. L., Schröter, M., Burns, K., Mattmann, C., *et al.* Inhibition of death receptor signals by cellular FLIP. *Nature* **388,** 190–195 (1997).
29. Alnemri, E. S., Livingston, D. J., Nicholson, D. W., Salvesen, G., Thornberry, N. a, Wong, W. W. & Yuan, J. Human ICE/CED-3 protease nomenclature. *Cell* **87,** 171 (1996).
30. Whitmore, A. V, Lindsten, T., Raff, M. C. & Thompson, C. B. The proapoptotic proteins Bax and Bak are not involved in Wallerian degeneration. *Cell Death Differ.* **10,** 260–261 (2003).
31. Viganò, E., Diamond, C. E., Spreafico, R., Balachander, A., Sobota, R. M. & Mortellaro, A. Human caspase-4 and caspase-5 regulate the one-step non-canonical inflammasome activation in monocytes. *Nat. Commun.* **6,** 1–13 (2015).
32. Casson, C. N., Yu, J., Reyes, V. M., Taschuk, F. O., Yadav, A., Copenhaver, A. M., Nguyen, H. T., Collman, R. G. & Shin, S. Human caspase-4 mediates noncanonical inflammasome activation against gram-negative bacterial pathogens. *Proc. Natl. Acad. Sci.* **112,** 6688–6693 (2015).
33. Koenig, U., Eckhart, L. & Tschachler, E. Evidence that caspase-13 is not a human but a bovine gene. *Biochem. Biophys. Res. Commun.* **285,** 1150–1154 (2001).
34. Saleh, M., Mathison, J. C., Wolinski, M. K., Bensinger, S. J., Fitzgerald, P., Droin, N., Ulevitch, R. J., Green, D. R. & Nicholson, D. W. Enhanced bacterial clearance and sepsis resistance in caspase-12-deficient mice. *Nature* **440,** 1064–1068 (2006).
35. Vande Walle, L., Jiménez Fernández, D., Demon, D., Van Laethem, N., Van Hauwermeiren, F., Van Gorp, H., Van Opdenbosch, N., Kayagaki, N. & Lamkanfi, M. Does caspase-12 suppress inflammasome activation? *Nature* **534,** E1–E4 (2016).

36. Xu, X., Liu, T., Zhang, A., Huo, X., Luo, Q., Chen, Z., Yu, L., Li, Q., Liu, L., Lun, Z. rong, *et al.* Retraction to Reactive oxygen species-triggered trophoblast apoptosis is initiated by endoplasmic reticulum stress via activation of caspase-12, CHOP, and the JNK pathway in Toxoplasma gondii infection in mice [Infection and Immunity, 80, 6 (2012) 2121-21. *Infect. Immun.* **83,** 1735 (2015).
37. Mikolajczyk, J., Scott, F. L., Krajewski, S., Sutherlin, D. P. & Salvesen, G. S. Activation and substrate specificity of caspase-14. *Biochemistry* **43,** 10560–10569 (2004).
38. Guo, H., Pétrin, D., Zhang, Y., Bergeron, C., Goodyer, C. G. & LeBlanc, A. C. Caspase-1 activation of caspase-6 in human apoptotic neurons. *Cell Death Differ.* **13,** 285–292 (2006).
39. Guo, H., Albrecht, S., Bourdeau, M., Petzke, T., Bergeron, C. & LeBlanc, A. C. Active caspase-6 and caspase-6-cleaved tau in neuropil threads, neuritic plaques, and neurofibrillary tangles of Alzheimer's disease. *Am. J. Pathol.* **165,** 523–531 (2004).
40. Giaime, E., Sunyach, C., Druon, C., Scarzello, S., Robert, G., Grosso, S., Auberger, P., Goldberg, M. S., Shen, J., Heutink, P., *et al.* Loss of function of DJ-1 triggered by Parkinson's disease-associated mutation is due to proteolytic resistance to caspase-6. *Cell Death Differ.* **17,** 158–169 (2010).
41. Gringhuis, S. I., Kaptein, T. M., Wevers, B. A., Theelen, B., Van Der Vlist, M., Boekhout, T. & Geijtenbeek, T. B. H. Dectin-1 is an extracellular pathogen sensor for the induction and processing of IL-1β via a noncanonical caspase-8 inflammasome. *Nat. Immunol.* **13,** 246–254 (2012).
42. Gurung, P., Burton, A. & Kanneganti, T.-D. NLRP3 inflammasome plays a redundant role with caspase 8 to promote IL-1β-mediated osteomyelitis. *Proc. Natl. Acad. Sci. U. S. A.* **113,** 4452–7 (2016).
43. Mascarenhas, D. P. A., Cerqueira, D. M., Pereira, M. S. F., Castanheira, F. V. S., Fernandes, T. D., Manin, G. Z., Cunha, L. D. & Zamboni, D. S. Inhibition of caspase-1 or gasdermin-D enable caspase-8 activation in the Naip5/NLRC4/ASC inflammasome. *PLoS Pathog.* **13,** 1–28 (2017).
44. Pore, M., Ba, ¸, Stró, A., Yk, ˙, Salvesen, G. S. & Dra¸g, M. Caspase Substrates and Inhibitors. 1–20 (2013). doi:10.1101/cshperspect.a008680
45. Lüthi, A. U. & Martin, S. J. The CASBAH: A searchable database of caspase substrates. *Cell Death Differ.* **14,** 641–650 (2007).
46. Kumar, S., van Raam, B. J., Salvesen, G. S. & Cieplak, P. Caspase cleavage sites in the human proteome: CaspDB, a database of predicted substrates. *PLoS One* **9,** e110539 (2014).
47. Beaudouin, J., Liesche, C., Aschenbrenner, S., Hörner, M. & Eils, R. Caspase-8 cleaves its substrates from the plasma membrane upon CD95-induced apoptosis. *Cell Death Differ.* **20,** 599–610 (2013).
48. Hsu, H., Xiong, J. & Goeddel, D. V. The TNF receptor 1-associated protein TRADD signals cell death and NF-κB activation. *Cell* **81,** 495–504 (1995).
49. Hsu, H., Huang, J., Shu, H. B., Baichwal, V. & Goeddel, D. V. TNF-dependent recruitment of the protein kinase RIP to the TNF receptor-1 signaling complex. *Immunity* **4,** 387–396 (1996).
50. Kelliher, M. A., Grimm, S., Ishida, Y., Kuo, F., Stanger, B. Z. & Leder, P. The

death domain kinase RIP mediates the TNF-induced NF-κB signal. *Immunity* **8,** 297–303 (1998).
51. Micheau, O. & Tschopp, J. Induction of TNF Receptor I- Mediated Apoptosis via Two Sequential Signaling Complexes. **114,** 181–190 (2002).
52. Holler, N., Zaru, R., Micheau, O., Thome, M., Attinger, a, Valitutti, S., Bodmer, J. L., Schneider, P., Seed, B. & Tschopp, J. Fas triggers an alternative, caspase-8-independent cell death pathway using the kinase RIP as effector molecule. *Nat. Immunol.* **1,** 489–495 (2000).
53. Degterev, A., Huang, Z., Boyce, M., Li, Y., Jagtap, P., Mizushima, N., Cuny, G. D., Mitchison, T. J., Moskowitz, M. A. & Yuan, J. Chemical inhibitor of nonapoptotic cell death with therapeutic potential for ischemic brain injury. **1,** (2013).
54. Cho, Y., Challa, S., Moquin, D., Genga, R., Ray, T. D., Guildford, M. & Chan, F. K. M. Phosphorylation-Driven Assembly of the RIP1-RIP3 Complex Regulates Programmed Necrosis and Virus-Induced Inflammation. *Cell* **137,** 1112–1123 (2009).
55. Li, J., McQuade, T., Siemer, A. B., Napetschnig, J., Moriwaki, K., Hsiao, Y. S., Damko, E., Moquin, D., Walz, T., McDermott, A., *et al.* The RIP1/RIP3 necrosome forms a functional amyloid signaling complex required for programmed necrosis. *Cell* **150,** 339–350 (2012).
56. Varfolomeev, E. E., Schuchmann, M., Luria, V., Chiannilkulchai, N., Beckmann, J. S., Mett, I. L., Rebrikov, D., Brodianski, V. M., Kemper, O. C., Kollet, O., *et al.* Targeted disruption of the mouse Caspase 8 gene ablates cell death induction by the TNF receptors, Fas/Apo1, and DR3 and is lethal prenatally. *Immunity* **9,** 267–276 (1998).
57. Zhang, J., Cado, D., Chen, A., Kabra, N. H. & Winoto, A. Fas-mediated apoptosis and activation-induced T-cell proliferation are defective in mice lacking FADD/Mort1. *Nature* **392,** 296–300 (1998).
58. Oberst, A., Dillon, C. P., Weinlich, R., McCormick, L. L., Fitzgerald, P., Pop, C., Hakem, R., Salvesen, G. S. & Green, D. R. Catalytic activity of the caspase-8–FLIPL complex inhibits RIPK3-dependent necrosis. *Nature* **471,** 363–367 (2011).
59. Kaiser, W. J., Upton, J. W., Long, A. B., Livingston-Rosanoff, D., Daley-Bauer, L. P., Hakem, R., Caspary, T. & Mocarski, E. S. RIP3 mediates the embryonic lethality of caspase-8-deficient mice. *Nature* **471,** 368–372 (2011).
60. Zhang, H., Zhou, X., McQuade, T., Li, J., Chan, F. K.-M. & Zhang, J. Functional complementation between FADD and RIP1 in embryos and lymphocytes. *Nature* **471,** 373–376 (2011).
61. Sun, L., Wang, H., Wang, Z., He, S., Chen, S., Liao, D., Wang, L., Yan, J., Liu, W., Lei, X., *et al.* Mixed lineage kinase domain-like protein mediates necrosis signaling downstream of RIP3 kinase. *Cell* **148,** 213–227 (2012).
62. Zhao, J., Jitkaew, S., Cai, Z., Choksi, S., Li, Q., Luo, J. & Liu, Z.-G. Mixed lineage kinase domain-like is a key receptor interacting protein 3 downstream component of TNF-induced necrosis. *Proc. Natl. Acad. Sci.* **109,** 5322–5327 (2012).
63. Murphy, J. M., Czabotar, P. E., Hildebrand, J. M., Lucet, I. S., Zhang, J., Alvarez-diaz, S., Lewis, R., Lalaoui, N., Metcalf, D., Webb, A. I., *et al.* Article The

Pseudokinase MLKL Mediates Necroptosis via a Molecular Switch Mechanism. *Immunity* **39,** 443–453 (2013).
64. Cai, Z., Jitkaew, S., Zhao, J., Chiang, H.-C., Choksi, S., Liu, J., Ward, Y., Wu, L.-G. & Liu, Z.-G. Plasma membrane translocation of trimerized MLKL protein is required for TNF-induced necroptosis. *Nat. Cell Biol.* **15,** 1–13 (2013).
65. Huang, D., Zheng, X., Wang, Z., Chen, X., He, W., Zhang, Y., Xu, J.-G., Zhao, H., Shi, W., Wang, X., *et al.* The MLKL Channel in Necroptosis Is an Octamer Formed by Tetramers in a Dyadic Process. *Mol. Cell. Biol.* **37,** e00497-16 (2017).
66. Liu, S., Liu, H., Johnston, A., Hanna-Addams, S., Reynoso, E., Xiang, Y. & Wang, Z. MLKL forms disulfide bond-dependent amyloid-like polymers to induce necroptosis. *Proc. Natl. Acad. Sci. U. S. A.* 201707531 (2017). doi:10.1073/pnas.1707531114
67. Kaiser, W. J., Sridharan, H., Huang, C., Mandal, P., Upton, J. W., Gough, P. J., Sehon, C. a., Marquis, R. W., Bertin, J. & Mocarski, E. S. Toll-like receptor 3-mediated necrosis via TRIF, RIP3, and MLKL. *J. Biol. Chem.* **288,** 31268–31279 (2013).
68. Thapa, R. J., Nogusa, S., Chen, P., Maki, J. L., Lerro, A., Andrake, M., Rall, G. F., Degterev, A. & Balachandran, S. Interferon-induced RIP1/RIP3-mediated necrosis requires PKR and is licensed by FADD and caspases. *Proc. Natl. Acad. Sci. U. S. A.* **110,** E3109-18 (2013).
69. Bergsbaken, T., Fink, S. L. & Cookson, B. T. Pyroptosis: host cell death and inflammation. *Nat. Rev. Microbiol.* **7,** 99–109 (2009).
70. Cookson, B. T. & Brennan, M. A. News & Comment New viruses for the new millennium. *TRENDS Microbiol. J. Cereb. Blood Flow Metab. J. Exp. Med* **9,** 1099–1108 (2001).
71. Brennan, M. A. & Cookson, B. T. Salmonella induces macrophage death by caspase-1-dependent necrosis. *Mol. Microbiol.* **38,** 31–40 (2000).
72. Hornung, V., Bauernfeind, F., Halle, A., Samstad, E. O., Kono, H., Rock, K. L., Fitzgerald, K. A. & Latz, E. Silica crystals and aluminum salts activate the NALP3 inflammasome through phagosomal destabilization. *Nat. Immunol.* **9,** 847–856 (2008).
73. Dostert, C., Pétrilli, V., Van Bruggen, R., Steele, C., Mossman, B. T. & Tschopp, J. Innate immune activation through Nalp3 inflammasome sensing of asbestos and silica. *Science* **320,** 674–7 (2008).
74. de Torre-Minguela, C., del Castillo, P. M. & Pelegrín, P. The NLRP3 and pyrin inflammasomes: Implications in the pathophysiology of autoinflammatory diseases. *Front. Immunol.* **8,** (2017).
75. Fernandes-Alnemri, T., Yu, J.-W., Datta, P., Wu, J. & Alnemri, E. S. AIM2 activates the inflammasome and cell death in response to cytoplasmic DNA. *Nature* **458,** 509–513 (2009).
76. Hornung, V., Ablasser, A., Charrel-Dennis, M., Bauernfeind, F., Horvath, G., Caffrey, D. R., Latz, E. & Fitzgerald, K. A. AIM2 recognizes cytosolic dsDNA and forms a caspase-1-activating inflammasome with ASC. *Nature* **458,** 514–518 (2009).
77. Bürckstümmer, T., Baumann, C., Blüml, S., Dixit, E., Dürnberger, G., Jahn, H., Planyavsky, M., Bilban, M., Colinge, J., Bennett, K. L., *et al.* An orthogonal

proteomic-genomic screen identifies AIM2 as a cytoplasmic DNA sensor for the inflammasome. *Nat. Immunol.* **10,** 266–272 (2009).
78. Levy, M., Shapiro, H., Thaiss, C. A. & Elinav, E. NLRP6: A Multifaceted Innate Immune Sensor. *Trends Immunol.* **38,** 248–260 (2017).
79. Xu, H., Yang, J., Gao, W., Li, L., Li, P., Zhang, L., Gong, Y. N., Peng, X., Xi, J. J., Chen, S., *et al.* Innate immune sensing of bacterial modifications of Rho GTPases by the Pyrin inflammasome. *Nature* **513,** 237–241 (2014).
80. Vance, R. E. The NAIP/NLRC4 inflammasomes. *Curr. Opin. Immunol.* **32,** 84–9 (2015).
81. Chavarría-Smith, J. & Vance, R. E. Direct Proteolytic Cleavage of NLRP1B Is Necessary and Sufficient for Inflammasome Activation by Anthrax Lethal Factor. *PLoS Pathog.* **9,** 1–4 (2013).
82. Dinarello, C. A. The history of fever, leukocytic pyrogen and interleukin-1. *Temperature* **2,** 8–16 (2015).
83. BENNETT, I. L. & BEESON, P. B. Studies on the pathogenesis of fever. II. Characterization of fever-producing substances from polymorphonuclear leukocytes and from the fluid of sterile exudates. *J. Exp. Med.* **98,** 493–508 (1953).
84. Auron, P. E., Webb, A. C., Rosenwasser, L. J., Mucci, S. F., Rich, A., Wolff, S. M. & Dinarello, C. A. Nucleotide sequence of human monocyte interleukin 1 precursor cDNA. *Proc. Natl. Acad. Sci.* **81,** 7907–7911 (1984).
85. March, C., Mosley, B., Larsen, A., Cerretti, D., Braedt, G., Price, V., Gillis, S., Henney, C. S., Kronheim, S. K., Grabstein, K., *et al.* Cloning, sequence and expression of two distinct human interleukin-1 complementary DNAs. *Nature* **315,** 641–647 (1984).
86. Dinarello, C. A. Overview of the IL-1 family in innate inflammation and acquired immunity. *Immunol. Rev.* **281,** 8–27 (2018).
87. Dinarello, C. A. An expanding role for interleukin-1 blockade from gout to cancer. *Mol. Med.* **20 Suppl 1,** S43-58 (2014).
88. Guo, B., Fu, S., Zhang, J., Liu, B. & Li, Z. Targeting inflammasome/IL-1 pathways for cancer immunotherapy. *Sci. Rep.* **6,** 1–12 (2016).
89. Kayagaki, N., Warming, S., Lamkanfi, M., Walle, L. Vande, Louie, S., Dong, J., Newton, K., Qu, Y., Liu, J., Heldens, S., *et al.* Non-canonical inflammasome activation targets caspase-11. *Nature* **479,** 117–121 (2011).
90. Wang, S. Y., Miura, M., Jung, Y. K., Zhu, H., Gagliardini, V., Shi, L. F., Greenberg, A. H. & Yuan, J. Y. Identification and Characterization Of Ich-3, a Member Of the Interleukin-1-Beta Converting Enzyme (Ice) Ced-3 Family and an Upstream Regulator Of Ice/. *J. Biol. Chem.* **271,** 20580 (1996).
91. Wang, S., Miura, M., Jung, Y. K., Zhu, H., Li, E. & Yuan, J. Murine caspase-11, an ICE-interacting protease, is essential for the activation of ICE. *Cell* **92,** 501–509 (1998).
92. Vanden Berghe, T., Hulpiau, P., Martens, L., Vandenbroucke, R. E., Van Wonterghem, E., Perry, S. W., Bruggeman, I., Divert, T., Choi, S. M., Vuylsteke, M., *et al.* PasSenger Mutations Confound Interpretation Of All Genetically Modified Congenic Mice. *Immunity* **43,** 200–209 (2015).
93. Hagar, J. A., Powell, D. a, Aachoui, Y., Ernst, R. K. & Miao, E. A. Cytoplasmic LPS activates caspase-11: implications in TLR4-independent endotoxic shock.

Science **341,** 1250–3 (2013).
94. Kayagaki, N., Wong, M. T., Stowe, I. B., Ramani, S. R., Gonzalez, L. C., Akashi-Takamura, S., Miyake, K., Zhang, J., Lee, W. P., Muszyński, A., *et al.* Noncanonical inflammasome activation by intracellular LPS independent of TLR4. *Science* **341,** 1246–9 (2013).
95. Shi, J., Zhao, Y., Wang, Y., Gao, W., Ding, J., Li, P., Hu, L. & Shao, F. Inflammatory caspases are innate immune receptors for intracellular LPS. *Nature* **514,** 187–192 (2014).
96. Ming Man, S., Karki, R., Briard, B., Burton, A., Gingras, S., Pelletier, S. & Kanneganti, T. D. Differential roles of caspase-1 and caspase-11 in infection and inflammation. *Sci. Rep.* **7,** 1–11 (2017).
97. Kayagaki, N., Stowe, I. B., Lee, B. L., O'Rourke, K., Anderson, K., Warming, S., Cuellar, T., Haley, B., Roose-Girma, M., Phung, Q. T., *et al.* Caspase-11 cleaves gasdermin D for non-canonical inflammasome signalling. *Nature* **526,** 666–671 (2015).
98. Shi, J., Zhao, Y., Wang, K., Shi, X., Wang, Y., Huang, H., Zhuang, Y. & Cai, T. Cleavage of GSDMD by inflammatory caspases determines pyroptotic cell death. (2015). doi:10.1038/nature15514
99. Liu, X., Zhang, Z., Ruan, J., Pan, Y., Magupalli, V. G., Wu, H. & Lieberman, J. Inflammasome-activated gasdermin D causes pyroptosis by forming membrane pores. *Nature* **535,** 153–158 (2016).
100. Ding, J., Wang, K., Liu, W., She, Y., Sun, Q., Shi, J., Sun, H., Wang, D. & Shao, F. Pore-forming activity and structural autoinhibition of the gasdermin family. *Nature* **535,** 111–116 (2016).
101. He, W., Wan, H., Hu, L., Chen, P., Wang, X., Huang, Z., Yang, Z.-H., Zhong, C.-Q. & Han, J. Gasdermin D is an executor of pyroptosis and required for interleukin-1β secretion. *Cell Res.* **25,** 1285–1298 (2015).
102. Conos, S. A., Chen, K. W., De Nardo, D., Hara, H., Whitehead, L., Núñez, G., Masters, S. L., Murphy, J. M., Schroder, K., Vaux, D. L., *et al.* Active MLKL triggers the NLRP3 inflammasome in a cell-intrinsic manner. *Proc. Natl. Acad. Sci.* 201613305 (2017). doi:10.1073/pnas.1613305114
103. Gutierrez, K. D., Davis, M. A., Daniels, B. P., Olsen, T. M., Ralli-Jain, P., Tait, S. W. G., Gale, M. & Oberst, A. MLKL Activation Triggers NLRP3-Mediated Processing and Release of IL-1β Independently of Gasdermin-D. *J. Immunol.* **198,** 2156–2164 (2017).
104. Wang, Y., Gao, W., Shi, X., Ding, J., Liu, W., He, H., Wang, K. & Shao, F. Chemotherapy drugs induce pyroptosis through caspase-3 cleavage of a gasdermin. *Nature* **547,** 99–103 (2017).
105. Rogers, C., Fernandes-Alnemri, T., Mayes, L., Alnemri, D., Cingolani, G. & Alnemri, E. S. Cleavage of DFNA5 by caspase-3 during apoptosis mediates progression to secondary necrotic/pyroptotic cell death. *Nat. Commun.* **8,** 14128 (2017).
106. Shi, J., Gao, W. & Shao, F. Pyroptosis: Gasdermin-Mediated Programmed Necrotic Cell Death. *Trends Biochem. Sci.* **42,** 245–254 (2017).
107. Evavold, C. L., Ruan, J., Tan, Y., Xia, S., Wu, H. & Kagan, J. C. The Pore-Forming Protein Gasdermin D Regulates Interleukin-1 Secretion from Living

Macrophages. *Immunity* 1–16 (2017). doi:10.1016/j.immuni.2017.11.013
108. Dixon, S. J., Lemberg, K. M., Lamprecht, M. R., Skouta, R., Zaitsev, E. M., Gleason, C. E., Patel, D. N., Bauer, A. J., Cantley, A. M., Yang, W. S., *et al.* Ferroptosis : An Iron-Dependent Form of Nonapoptotic Cell Death. *Cell* **149,** 1060–1072 (2012).
109. Friedmann Angeli, J. P., Schneider, M., Proneth, B., Tyurina, Y. Y., Tyurin, V. A., Hammond, V. J., Herbach, N., Aichler, M., Walch, A., Eggenhofer, E., *et al.* Inactivation of the ferroptosis regulator Gpx4 triggers acute renal failure in mice. *Nat. Cell Biol.* **16,** 1180–1191 (2014).
110. Baines, C. P., Kaiser, R. A., Purcell, N. H., Blair, N. S., Osinska, H., Hambleton, M. A., Brunskill, E. W., Sayen, M. R., Gottlieb, R. A., Dorn, G. W., *et al.* Loss of cyclophilin D reveals a critical role for mitochondrial permeability transition in cell death. *Nature* **434,** 658–62 (2005).
111. Nakagawa, T., Shimizu, S. & Watanabe, T. Cyclophilin D-dependent mitochondrial permeability transition regulates some necrotic but not apoptotic cell death. **434,** (2005).
112. Schinzel, A. C., Takeuchi, O., Huang, Z., Fisher, J. K., Zhou, Z., Rubens, J., Hetz, C., Danial, N. N., Moskowitz, M. A. & Korsmeyer, S. J. Cyclophilin D is a component of mitochondrial permeability transition and mediates neuronal cell death after focal cerebral ischemia. *Proc. Natl. Acad. Sci.* **102,** 12005–12010 (2005).
113. Linkermann, A., Brasen, J. H., Darding, M., Jin, M. K., Sanz, A. B., Heller, J.-O., De Zen, F., Weinlich, R., Ortiz, A., Walczak, H., *et al.* Two independent pathways of regulated necrosis mediate ischemia-reperfusion injury. *Proc. Natl. Acad. Sci.* **110,** 12024–12029 (2013).
114. Wang, Y., Kim, N. S., Haince, J.-F., Kang, H. C., David, K. K., Andrabi, S. a, Poirier, G. G., Dawson, V. L. & Dawson, T. M. Poly(ADP-Ribose) (PAR) Binding to Apoptosis-Inducing Factor Is Critical for PAR Polymerase-1-Dependent Cell Death (Parthanatos). *Sci. Signal.* **4,** ra20–ra20 (2011).
115. Wang, Y., An, R., Umanah, G. K., Park, H., Nambiar, K., Eacker, S. M., Kim, B., Bao, L., Harraz, M. M., Chang, C., *et al.* A nuclease that mediates cell death induced by DNA damage and poly(ADP-ribose) polymerase-1. *Science (80-.).* **354,** 82–97 (2016).
116. Kroemer, G. & Levine, B. Autophagic cell death: the story of a misnomer. *Nat. Rev. Mol. Cell Biol.* **9,** 1004–1010 (2008).
117. Overholtzer, M., Mailleux, A. A., Mouneimne, G., Normand, G., Schnitt, S. J., King, R. W., Cibas, E. S. & Brugge, J. S. A Nonapoptotic Cell Death Process , Entosis , that Occurs by Cell-in-Cell Invasion. 966–979 (2007). doi:10.1016/j.cell.2007.10.040
118. Brinkmann, V., Reichard, U., Goosmann, C., Fauler, B., Uhlemann, Y., Weiss, D. S., Weinrauch, Y. & Zychlinsky, A. Neutrophil extracellular traps kill bacteria. *Science* **303,** 1532–5 (2004).
119. Medina, E. Neutrophil extracellular traps: a strategic tactic to defeat pathogens with potential consequences for the host. *J. Innate Immun.* **1,** 176–80 (2009).
120. Dotiwala, F., Mulik, S., Polidoro, R. B., Ansara, J. A., Burleigh, B. A., Walch, M., Gazzinelli, R. T. & Lieberman, J. Killer lymphocytes use granulysin, perforin and

granzymes to kill intracellular parasites. *Nat. Med.* **22,** 210–6 (2016).
121. Meier, P., Finch, A. & Evan, G. Apoptosis in development. *Nature* **407,** 796–801 (2000).
122. Beresford, P. J., Xia, Z., Greenberg, A. H. & Lieberman, J. Granzyme a loading induces rapid cytolysis and a novel form of DNA damage independently of caspase activation. *Immunity* **10,** 585–594 (1999).
123. Shi, Y. F., Sahai, B. M. & Green, D. R. Cyclosporin A inhibits activation-induced cell death in T-cell hybridomas and thymocytes. *Nature* **339,** 625–6 (1989).
124. Fogarty, C. E. & Bergmann, A. Killers creating new life: Caspases drive apoptosis-induced proliferation in tissue repair and disease. *Cell Death Differ.* **24,** 1390–1400 (2017).
125. Rudrapatna, V. A., Bangi, E. & Cagan, R. L. Caspase signalling in the absence of apoptosis drives Jnk-dependent invasion. *EMBO Rep.* **14,** 172–177 (2013).
126. Kuida, K., Haydar, T. F., Kuan, C. Y., Gu, Y., Taya, C., Karasuyama, H., Su, M. S. S., Rakic, P. & Flavell, R. A. Reduced apoptosis and cytochrome C-mediated caspase activation in mice lacking Caspase 9. *Cell* **94,** 325–337 (1998).
127. Algeciras-Schimnich, A., Barnhart, B. C. & Peter, M. E. Apoptosis-independent functions of killer caspases. *Curr. Opin. Cell Biol.* **14,** 721–726 (2002).
128. Roberts, A. W., Lee, B. L., Deguine, J., John, S., Shlomchik, M. J. & Barton, G. M. Tissue-Resident Macrophages Are Locally Programmed for Silent Clearance of Apoptotic Cells. *Immunity* 1–15 (2017). doi:10.1016/j.immuni.2017.10.006
129. Huang, Z., Wu, S.-Q., Liang, Y., Zhou, X., Chen, W., Li, L., Wu, J., Zhuang, Q., Chen, C., Li, J., *et al.* RIP1/RIP3 Binding to HSV-1 ICP6 Initiates Necroptosis to Restrict Virus Propagation in Mice. *Cell Host Microbe* **17,** 229–242 (2015).
130. Guo, H., Omoto, S., Harris, P. a., Finger, J. N., Bertin, J., Gough, P. J., Kaiser, W. J. & Mocarski, E. S. Herpes Simplex Virus Suppresses Necroptosis in Human Cells. *Cell Host Microbe* **17,** 243–251 (2015).
131. Upton, J. W., Kaiser, W. J. & Mocarski, E. S. Virus inhibition of RIP3-dependent necrosis. *Cell Host Microbe* **7,** 302–313 (2010).
132. Moriwaki, K. & Chan, F. K. M. Regulation of RIPK3- and RHIM-dependent necroptosis by the proteasome. *J. Biol. Chem.* **291,** 5948–5959 (2016).
133. Kitur, K., Wachtel, S., Brown, A., Wickersham, M., Paulino, F., Pe????aloza, H. F., Soong, G., Bueno, S., Parker, D. & Prince, A. Necroptosis Promotes Staphylococcus aureus Clearance by Inhibiting Excessive Inflammatory Signaling. *Cell Rep.* **16,** 2219–2230 (2016).
134. Kitur, K., Parker, D., Nieto, P., Ahn, D. S., Cohen, T. S., Chung, S., Wachtel, S., Bueno, S. & Prince, A. Toxin-Induced Necroptosis Is a Major Mechanism of Staphylococcus aureus Lung Damage. *PLOS Pathog.* **11,** e1004820 (2015).
135. Newton, K., Dugger, D. L., Maltzman, A., Greve, J. M., Hedehus, M., Martin-McNulty, B., Carano, R. A. D., Cao, T. C., van Bruggen, N., Bernstein, L., *et al.* RIPK3 deficiency or catalytically inactive RIPK1 provides greater benefit than MLKL deficiency in mouse models of inflammation and tissue injury. *Cell Death Differ.* **23,** 1565–1576 (2016).
136. Liu, W. & Xia, Y. Necroptosis in Acute Kidney Injury. **3,** 1–6 (2016).
137. Zhang, T., Zhang, Y., Cui, M., Jin, L., Wang, Y., Lv, F., Liu, Y., Zheng, W., Shang, H., Zhang, J., *et al.* CaMKII is a RIP3 substrate mediating ischemia- and

oxidative stress-induced myocardial necroptosis. *Nat. Med.* **22,** 175–82 (2016).
138. Caccamo, A., Branca, C., Piras, I. S., Ferreira, E., Huentelman, M. J., Liang, W. S., Readhead, B., Dudley, J. T., Spangenberg, E. E., Green, K. N., *et al.* Necroptosis activation in Alzheimer's disease. *Nat. Neurosci.* **20,** 1236–1246 (2017).
139. Boucher, D., Chen, K. W. & Schroder, K. Burn the house, save the day: pyroptosis in pathogen restriction. *Inflammasome* **2,** 1–6 (2016).
140. Doitsh, G., Galloway, N. L. K., Geng, X., Yang, Z., Monroe, K. M., Zepeda, O., Hunt, P. W., Hatano, H., Sowinski, S., Muñoz-Arias, I., *et al.* Cell death by pyroptosis drives CD4 T-cell depletion in HIV-1 infection. *Nature* **505,** 509–514 (2014).
141. Monroe, K. M., Yang, Z., Johnson, J. R., Geng, X., Doitsh, G., Krogan, N. J. & Greene, W. C. IFI16 DNA sensor is required for death of lymphoid CD4 T cells abortively infected with HIV. *Science* **343,** 428–32 (2014).
142. HENLE, W. Interference phenomena between animal viruses; a review. *J. Immunol.* **64,** 203–36 (1950).
143. Hemann, E. A., Gale, M. & Savan, R. Interferon lambda genetics and biology in regulation of viral control. *Front. Immunol.* **8,** (2017).
144. McFarland, A. P., Horner, S. M., Jarret, A., Joslyn, R. C., Bindewald, E., Shapiro, B. a, Delker, D. a, Hagedorn, C. H., Carrington, M., Gale, M., *et al.* The favorable IFNL3 genotype escapes mRNA decay mediated by AU-rich elements and hepatitis C virus-induced microRNAs. *Nat. Immunol.* (2013). doi:10.1038/ni.2758
145. Jarret, A., McFarland, A. P., Horner, S. M., Kell, A., Schwerk, J., Hong, M., Badil, S., Joslyn, R. C., Baker, D. P., Carrington, M., *et al.* Hepatitis-C-virus-induced microRNAs dampen interferon-mediated antiviral signaling. *Nat. Med.* **22,** 1–8 (2016).
146. Broggi, A., Tan, Y., Granucci, F. & Zanoni, I. IFN-λ suppresses intestinal inflammation by non-translational regulation of neutrophil function. *Nat. Immunol.* **18,** 1084–1093 (2017).
147. Lin, F.-C. & Young, H. A. The talented interferon-gamma. *Adv. Biosci. Biotechnol.* **04,** 6–13 (2013).
148. Thomas, C., Moraga, I., Levin, D., Krutzik, P. O., Podoplelova, Y., Trejo, A., Lee, C., Yarden, G., Vleck, S. E., Glenn, J. S., *et al.* Structural linkage between ligand discrimination and receptor activation by Type i interferons. *Cell* **146,** 621–632 (2011).
149. Mostafavi, S., Yoshida, H., Moodley, D., Leboité, H., Rothamel, K., Raj, T., Ye, C. J., Chevrier, N., Zhang, S. Y., Feng, T., *et al.* Parsing the Interferon Transcriptional Network and Its Disease Associations. *Cell* **164,** 564–578 (2016).
150. McNab, F., Mayer-Barber, K., Sher, A., Wack, A. & O'Garra, A. Type I interferons in infectious disease. *Nat Rev Immunol* **15,** 87–103 (2015).
151. Takeda, K. & Akira, S. TLR signaling pathways. *Semin. Immunol.* **16,** 3–9 (2004).
152. Yang, K., Puel, A., Zhang, S., Eidenschenk, C., Ku, C. L., Casrouge, A., Picard, C., Von Bernuth, H., Senechal, B., Plancoulaine, S., *et al.* Human TLR-7-, -8-, and -9-mediated induction of IFN-α/β and -λ Is IRAK-4 dependent and redundant for protective immunity to viruses. *Immunity* **23,** 465–478 (2005).
153. Poltorak, A., He, X., Smirnova, I., Liu, M. Y., Van Huffel, C., Du, X., Birdwell,

D., Alejos, E., Silva, M., Galanos, C., *et al.* Defective LPS signaling in C3H/HeJ and C57BL/10ScCr mice: mutations in Tlr4 gene. *Science* **282,** 2085–8 (1998).
154. Kagan, J. C. & Medzhitov, R. Phosphoinositide-mediated adaptor recruitment controls Toll-like receptor signaling. *Cell* **125,** 943–55 (2006).
155. Kagan, J. C., Su, T., Horng, T., Chow, A., Akira, S. & Medzhitov, R. TRAM couples endocytosis of Toll-like receptor 4 to the induction of interferon-β. *Nat. Immunol.* **9,** 361–368 (2008).
156. O'Neill, L. a J., Golenbock, D. & Bowie, A. G. The history of Toll-like receptors - redefining innate immunity. *Nat. Rev. Immunol.* **13,** 453–60 (2013).
157. Oshiumi, H., Matsumoto, M., Funami, K., Akazawa, T. & Seya, T. TICAM-1, an adaptor molecule that participates in Toll-like receptor 3-mediated interferon-β induction. *Nat. Immunol.* **4,** 161–167 (2003).
158. Toshchakov, V., Jones, B. W., Perera, P. Y., Thomas, K., Cody, M. J., Zhang, S., Williams, B. R. G., Major, J., Hamilton, T. A., Fenton, M. J., *et al.* TLR4, but not TLR2, mediates IFN-β-induced STATIα/β-dependent gene expression in macrophages. *Nat. Immunol.* **3,** 392–398 (2002).
159. Kawai, T., Sato, S., Ishii, K. J., Coban, C., Hemmi, H., Yamamoto, M., Terai, K., Matsuda, M., Inoue, J. I., Uematsu, S., *et al.* Interferon-α induction through Toll-like receptors involves a direct interaction of IRF7 with MyD88 and TRAF6. *Nat. Immunol.* **5,** 1061–1068 (2004).
160. Ishikawa, H. & Barber, G. N. STING is an endoplasmic reticulum adaptor that facilitates innate immune signalling. *Nature* **455,** 674–678 (2008).
161. Zhong, B., Yang, Y., Li, S., Wang, Y. Y., Li, Y., Diao, F., Lei, C., He, X., Zhang, L., Tien, P., *et al.* The Adaptor Protein MITA Links Virus-Sensing Receptors to IRF3 Transcription Factor Activation. *Immunity* **29,** 538–550 (2008).
162. Sun, W., Li, Y., Chen, L., Chen, H., You, F., Zhou, X., Zhou, Y., Zhai, Z., Chen, D. & Jiang, Z. ERIS, an endoplasmic reticulum IFN stimulator, activates innate immune signaling through dimerization. *Proc Natl Acad Sci U S A* **106,** 8653–8658 (2009).
163. Burdette, D. L., Monroe, K. M., Sotelo-Troha, K., Iwig, J. S., Eckert, B., Hyodo, M., Hayakawa, Y. & Vance, R. E. STING is a direct innate immune sensor of cyclic di-GMP. *Nature* **478,** 515–518 (2011).
164. Li, X.-D., Wu, J., Gao, D., Wang, H., Sun, L. & Chen, Z. J. Pivotal roles of cGAS-cGAMP signaling in antiviral defense and immune adjuvant effects. *Science* **341,** 1390–4 (2013).
165. Gao, D., Wu, J., Wu, Y. T., Du, F., Aroh, C., Yan, N., Sun, L. & Chen, Z. J. Cyclic GMP-AMP synthase is an innate immune sensor of HIV and other retroviruses. *Science (80-.).* **341,** 903–906 (2013).
166. Hiscott, J., Ryals, J., Dierks, P., Hofmann, V. & Weissmann, C. The expression of human interferon alpha genes. (1984).
167. Tovey, M. G., Streuli, M., Gresser, I., Gugenheim, J., Blanchard, B., Guymarho, J., Vignaux, F. & Gigou, M. Interferon messenger RNA is produced constitutively in the organs of normal individuals. *Proc. Natl. Acad. Sci. U. S. A.* **84,** 5038–42 (1987).
168. Gresser, B. Y. I. O. N., Belardelli, F., Maury, C., Maunoury, T. & Tovey, M. G. Injection of mice with antibody to Interferon enhances the growth of transplantable

murine tumors. **158,** 2095–2107 (1983).
169. Gresser, I., Vignaux, F., Belardelli, F., Tovey, M. G. & Maunoury, M. T. Injection of mice with antibody to mouse interferon alpha/beta decreases the level of 2'-5' oligoadenylate synthetase in peritoneal macrophages. *J. Virol.* **53,** 221–7 (1985).
170. Lienenklaus, S., Cornitescu, M., Zietara, N., Lyszkiewicz, M., Gekara, N., Jablonska, J., Edenhofer, F., Rajewsky, K., Bruder, D., Hafner, M., *et al.* Novel Reporter Mouse Reveals Constitutive and Inflammatory Expression of IFN- In Vivo. *J. Immunol.* **183,** 3229–3236 (2009).
171. Gough, D. J., Messina, N. L., Hii, L., Gould, J. A., Sabapathy, K., Robertson, A. P. S., Trapani, J. A., Levy, D. E., Hertzog, P. J., Clarke, C. J. P., *et al.* Functional crosstalk between type I and II interferon through the regulated expression of STAT1. *PLoS Biol.* **8,** (2010).
172. Abt, M. C., Osborne, L. C., Monticelli, L. A., Doering, T. A., Alenghat, T., Sonnenberg, G. F., Paley, M. A., Antenus, M., Williams, K. L., Erikson, J., *et al.* Commensal Bacteria Calibrate the Activation Threshold of Innate Antiviral Immunity. *Immunity* **37,** 158–170 (2012).
173. Bautista, E. M., Ferman, G. S., Gregg, D. R., Brum, M. C. S., Grubman, M. J. & Golde, W. T. Constitutive expression of alpha interferon by skin dendritic cells confers resistance to infection by Foot-and-mouth disease virus. *J. Virol.* **79,** 4838–4847 (2005).
174. Vogel, S. N. & Fertsch, D. Macrophages from endotoxin-hyporesponsive (Lpsd) C3H/HeJ mice are permissive for vesicular stomatitis virus because of reduced levels of endogenous interferon: possible mechanism for natural resistance to virus infection. *J. Virol.* **61,** 812–818 (1987).
175. tenOever, B. R. The Evolution of Antiviral Defense Systems. *Cell Host Microbe* **19,** 142–149 (2016).
176. Schoggins, J. W. & Rice, C. M. Interferon-stimulated genes and their antiviral effector functions. *Curr. Opin. Virol.* **1,** 519–525 (2011).
177. Samuel, C. E. Antiviral Actions of Interferons. *Clin. Microbiol. Rev.* **14,** 778–809 (2001).
178. Devasthanam, A. S. Mechanisms underlying the inhibition of interferon signaling by viruses. *Virulence* **5,** 270–277 (2014).
179. Yan, N., Regalado-magdos, A. D., Stiggelbout, B. & Lee-kirsch, M. A. The cytosolic exonuclease TREX1 inhibits the innane immune response to HIV. *Nat. Immunol.* **11,** 1005–1013 (2010).
180. Kovarik, P., Castiglia, V., Ivin, M. & Ebner, F. Type I interferons in bacterial infections: A balancing act. *Front. Immunol.* **7,** 1–8 (2016).
181. Boxx, G. M. & Cheng, G. The Roles of Type i Interferon in Bacterial Infection. *Cell Host Microbe* **19,** 760–769 (2016).
182. Perkins, D. J., Rajaiah, R., Tennant, S. M., Ramachandran, G., Higginson, E. E., Dyson, T. N. & Vogel, S. N. *Salmonella* Typhimurium Co-Opts the Host Type I IFN System To Restrict Macrophage Innate Immune Transcriptional Responses Selectively. *J. Immunol.* **195,** 2461–2471 (2015).
183. Carrero, J. A., Calderon, B. & Unanue, E. R. Lymphocytes are detrimental during the early innate immune response against *Listeria monocytogenes*. *J. Exp. Med.* **203,** 933–940 (2006).

184. Gratz, N., Hartweger, H., Matt, U., Kratochvill, F., Janos, M., Sigel, S., Drobits, B., Li, X. D., Knapp, S. & Kovarik, P. Type I Interferon Production Induced By Streptococcus Pyogenes-Derived Nucleic Acids is Required for Host Protection. *PLoS Pathog.* **7,** 1–16 (2011).
185. Hooks, J. J., Jordan, G. W. & Cupps, T. Multiple interferons with the circulation of patients with systemic lupus erythematosus and vasculitis. *Arthritis Rheum.* **25,** 396–400 (1982).
186. Baechler, E. C., Batliwalla, F. M., Karypis, G., Gaffney, P. M., Ortmann, W. A., Espe, K. J., Shark, K. B., Grande, W. J., Hughes, K. M., Kapur, V., *et al.* Interferon-inducible gene expression signature in peripheral blood cells of patients with severe lupus. *Proc. Natl. Acad. Sci. U. S. A.* **100,** 2610–5 (2003).
187. Bauer, J. W., Baechler, E. C., Petri, M., Batliwalla, F. M., Crawford, D., Ortmann, W. A., Espe, K. J., Li, W., Patel, D. D., Gregersen, P. K., *et al.* Elevated serum levels of interferon-regulated chemokines are biomarkers for active human systemic lupus erythematosus. *PLoS Med.* **3,** 2274–2284 (2006).
188. Nestle, F. O., Conrad, C., Tun-Kyi, A., Homey, B., Gombert, M., Boyman, O., Burg, G., Liu, Y. J. & Gilliet, M. Plasmacytoid predendritic cells initiate psoriasis through interferon-alpha production. *J Exp Med* **202,** 135–143 (2005).
189. Zhang, L., Sen, G. L., Ward, N. L., Johnston, A., Chun, K., Chen, Y., Adase, C., Sanford, J. A., Gao, N., Chensee, M., *et al.* Antimicrobial Peptide LL37 and MAVS Signaling Drive Interferon-β Production by Epidermal Keratinocytes during Skin Injury. *Immunity* **45,** 119–130 (2016).
190. Wildenberg, M. E., van Helden-Meeuwsen, C. G., van de Merwe, J. P., Drexhage, H. A. & Versnel, M. A. Systemic increase in type I interferon activity in Sj??gren's syndrome: A putative role for plasmacytoid dendritic cells. *Eur. J. Immunol.* **38,** 2024–2033 (2008).
191. Wu, M. & Assassi, S. The role of type 1 interferon in systemic sclerosis. *Front. Immunol.* **4,** 1–7 (2013).
192. Wong, D., Kea, B., Pesich, R., Higgs, B. W., Zhu, W., Brown, P., Yao, Y. & Fiorentino, D. Interferon and biologic signatures in dermatomyositis skin: Specificity and heterogeneity across diseases. *PLoS One* **7,** 1–14 (2012).
193. Gall, A., Treuting, P., Elkon, K. B., Loo, Y. M., Gale, M., Barber, G. N. & Stetson, D. B. Autoimmunity Initiates in Nonhematopoietic Cells and Progresses via Lymphocytes in an Interferon-Dependent Autoimmune Disease. *Immunity* **36,** 120–131 (2012).
194. Liu, Y., Jesus, A. a, Marrero, B., Yang, D., Ramsey, S. E., Sanchez, G. a M., Tenbrock, K., Wittkowski, H., Jones, O. Y., Kuehn, H. S., *et al.* Activated STING in a Vascular and Pulmonary Syndrome. *N. Engl. J. Med.* 1–12 (2014). doi:10.1056/NEJMoa1312625
195. Zeng, M., Hu, Z., Shi, X., Li, X., Zhan, X., Li, X.-D., Wang, J., Choi, J. H., Wang, K., Purrington, T., *et al.* MAVS, cGAS, and endogenous retroviruses in T-independent B cell responses. *Science* **346,** 1486–92 (2014).
196. Stetson, D. B., Ko, J. S., Heidmann, T. & Medzhitov, R. Trex1 Prevents Cell-Intrinsic Initiation of Autoimmunity. 587–598 (2008). doi:10.1016/j.cell.2008.06.032
197. Buskiewicz, I. A., Montgomery, T., Yasewicz, E. C., Huber, S. A., Murphy, M. P.,

Hartley, R. C., Kelly, R., Crow, M. K., Perl, A., Budd, R. C., *et al.* Reactive oxygen species induce virus-independent MAVS oligomerization in systemic lupus erythematosus. **115,** 1–18 (2016).
198. Baccala, R., Gonzalez-Quintial, R., Schreiber, R. D., Lawson, B. R., Kono, D. H. & Theofilopoulos, A. N. Anti-IFN- / Receptor Antibody Treatment Ameliorates Disease in Lupus-Predisposed Mice. *J. Immunol.* **189,** 5976–5984 (2012).
199. O'Shea, J. J., Schwartz, D. M., Villarino, A. V., Gadina, M., McInnes, I. B. & Laurence, A. The JAK-STAT Pathway: Impact on Human Disease and Therapeutic Intervention*. *Annu. Rev. Med.* **66,** 311–328 (2015).
200. Byskosh, P. V & Reder, A. T. Interferon beta-1b effects on cytokine mRNA in peripheral mononuclear cells in multiple sclerosis. *Mult. Scler.* **1,** 262–9 (1996).
201. Feng, X., Petraglia, A. L., Chen, M., Byskosh, P. V., Boos, M. D. & Reder, A. T. Low expression of interferon-stimulated genes in active multiple sclerosis is linked to subnormal phosphorylation of STAT1. *J. Neuroimmunol.* **129,** 205–215 (2002).
202. Reder, A. T. & Feng, X. Aberrant type I interferon regulation in autoimmunity: Opposite directions in MS and SLE, shaped by evolution and body ecology. *Front. Immunol.* **4,** 1–13 (2013).
203. Cargnello, M. & Roux, P. P. Activation and Function of the MAPKs and Their Substrates, the MAPK-Activated Protein Kinases. *Microbiol. Mol. Biol. Rev.* **75,** 50–83 (2011).
204. Arthur, J. S. C. & Ley, S. C. Mitogen-activated protein kinases in innate immunity. *Nat. Rev. Immunol.* **13,** 679–92 (2013).
205. K Sater, A. TAK1: Kinase at the Crossroads. *Biochem. Anal. Biochem.* **01,** 1–2 (2012).
206. Adhikari, A., Xu, M. & Chen, Z. J. Ubiquitin-mediated activation of TAK1 and IKK. *Oncogene* **26,** 3214–3226 (2007).
207. Erhardt, P., Schremser, E. J. & Cooper, G. M. B-Raf inhibits programmed cell death downstream of cytochrome c release from mitochondria by activating the MEK/Erk pathway. *Mol. Cell. Biol.* **19,** 5308–5315 (1999).
208. Shonai, T., Adachi, M., Sakata, K., Takekawa, M., Endo, T., Imai, K. & Hareyama, M. MEK/ERK pathway protects ionizing radiation-induced loss of mitochondrial membrane potential and cell death in lymphocytic leukemia cells. *Cell Death Differ.* **9,** 963–971 (2002).
209. Jaco, I., Annibaldi, A., Lalaoui, N., Wilson, R., Tenev, T., Laurien, L., Kim, C., Jamal, K., Wicky John, S., Liccardi, G., *et al.* MK2 Phosphorylates RIPK1 to Prevent TNF-Induced Cell Death. *Mol. Cell* **66,** 698-710.e5 (2017).
210. Geng, J., Ito, Y., Shi, L., Amin, P., Chu, J., Ouchida, A. T., Mookhtiar, A. K., Zhao, H., Xu, D., Shan, B., *et al.* Regulation of RIPK1 activation by TAK1-mediated phosphorylation dictates apoptosis and necroptosis. *Nat. Commun.* **8,** 359 (2017).
211. Menon, M. B., Gropengießer, J., Fischer, J., Novikova, L., Deuretzbacher, A., Lafera, J., Schimmeck, H., Czymmeck, N., Ronkina, N., Kotlyarov, A., *et al.* p38MAPK/MK2-dependent phosphorylation controls cytotoxic RIPK1 signalling in inflammation and infection. *Nat. Cell Biol.* **19,** 1248–1259 (2017).
212. Dondelinger, Y., Delanghe, T., Rojas-Rivera, D., Priem, D., Delvaeye, T., Bruggeman, I., Van Herreweghe, F., Vandenabeele, P. & Bertrand, M. J. M. MK2

phosphorylation of RIPK1 regulates TNF-mediated cell death. *Nat. Cell Biol.* **19,** 1237–1247 (2017).
213. Mihaly, S. R., Ninomiya-Tsuji, J. & Morioka, S. TAK1 control of cell death. *Cell Death Differ.* **21,** 1667–1676 (2014).
214. Sato, S., Sanjo, H., Takeda, K., Ninomiya-Tsuji, J., Yamamoto, M., Kawai, T., Matsumoto, K., Takeuchi, O. & Akira, S. Essential function for the kinase TAK1 in innate and adaptive immune responses. *Nat. Immunol.* **6,** 1087–1095 (2005).
215. Tang, M., Wei, X., Guo, Y., Breslin, P., Zhang, S., Zhang, S., Wei, W., Xia, Z., Diaz, M., Akira, S., *et al.* TAK1 is required for the survival of hematopoietic cells and hepatocytes in mice. *J. Exp. Med.* **205,** 1611–9 (2008).
216. Vink, P. M., Smout, W. M., Driessen-Engels, L. J., de Bruin, A. M., Delsing, D., Krajnc-Franken, M. A., Jansen, A. J., Rovers, E. F., van Puijenbroek, A. A., Kaptein, A., *et al.* In Vivo Knockdown of TAK1 Accelerates Bone Marrow Proliferation/Differentiation and Induces Systemic Inflammation. *PLoS One* **8,** (2013).
217. Omori, E., Morioka, S., Matsumoto, K. & Ninomiya-Tsuji, J. TAK1 regulates reactive oxygen species and cell death in keratinocytes, which is essential for skin integrity. *J. Biol. Chem.* **283,** 26161–26168 (2008).
218. Malireddi, R. K. S., Gurung, P., Mavuluri, J., Dasari, T. K., Klco, J. M. & Chi, H. TAK1 restricts spontaneous NLRP3 activation and cell death to control myeloid proliferation. 1–12 (2018).
219. Lamothe, B., Lai, Y., Xie, M., Schneider, M. D. & Darnay, B. G. TAK1 is essential for osteoclast differentiation and is an important modulator of cell death by apoptosis and necroptosis. *Mol. Cell. Biol.* **33,** 582–95 (2013).
220. Morioka, S., Broglie, P., Omori, E., Ikeda, Y., Takaesu, G., Matsumoto, K. & Ninomiya-Tsuji, J. TAK1 kinase switches cell fate from apoptosis to necrosis following TNF stimulation. *J. Cell Biol.* **204,** 607–623 (2014).
221. Guo, X., Yin, H., Chen, Y., Li, L., Li, J. & Liu, Q. TAK1 regulates caspase 8 activation and necroptotic signaling via multiple cell death checkpoints. *Cell Death Dis.* **7,** e2381 (2016).
222. Lluis, J. M., Nachbur, U., Cook, W. D., Gentle, I. E., Moujalled, D., Moulin, M., Wong, W. W. L., Khan, N., Chau, D., Callus, B. A., *et al.* TAK1 is required for survival of mouse fibroblasts treated with TRAIL, and does so by NF-??B dependent induction of cFLIPL. *PLoS One* **5,** (2010).
223. Sakurai, H. Targeting of TAK1 in inflammatory disorders and cancer. *Trends Pharmacol. Sci.* **33,** 522–530 (2012).
224. Wu, J., Powell, F., Larsen, N. A., Lai, Z., Byth, K. F., Read, J., Gu, R., Roth, M., Toader, D., Saeh, J. C., *et al.* Mechanism and In Vitro Pharmacology of TAK1 Inhibition by (5 Z) - 7- Oxozeaenol. (2013).
225. Mowafy, S., Lauffenburger, D. A., Jenney, A., Sorger, P. K., Gray, N. S., Gurbani, D., Weisberg, E. L., Jones, D. S., Singer, W. D., Bernard, F. M., *et al.* Studies of TAK1-centered polypharmacology with novel covalent TAK1 inhibitors. *Bioorganic Med. Chem.* **25,** 1320–1328 (2017).
226. Tan, L., Gurbani, D., Weisberg, E. L., Hunter, J. C., Li, L., Jones, D. S., Ficarro, S. B., Mowafy, S., Tam, C.-P., Rao, S., *et al.* Structure-guided development of covalent TAK1 inhibitors. *Bioorg. Med. Chem.* **25,** 838–846 (2017).

227. Guan, S., Lu, J., Zhao, Y., Woodfield, S. E. & Zhang, H. TAK1 inhibitor 5Z-7-oxozeaenol sensitizes cervical cancer to doxorubicin-induced apoptosis. **8,** 33666–33675 (2017).
228. Totzke, J., Gurbani, D., Raphemot, R., Hughes, P. F., Bodoor, K., Carlson, D. A., Loiselle, D. R., Bera, A. K., Eibschutz, L. S., Perkins, M. M., *et al.* Takinib, a Selective TAK1 Inhibitor, Broadens the Therapeutic Efficacy of TNF-α Inhibition for Cancer and Autoimmune Disease. *Cell Chem. Biol.* **24,** 1029-1039.e7 (2017).
229. Wang, Z., Zheng, H., Shi, M., Yu, Y., Wang, H., Cao, W. M., Zhao, Y. & Zhang, H. TAK1 inhibitor NG25 enhances doxorubicin-mediated apoptosis in breast cancer cells. *Sci. Rep.* **6,** 1–10 (2016).
230. Li, J., Liang, C., Zhang, Z. K., Pan, X., Peng, S., Lee, W. S., Lu, A., Lin, Z., Zhang, G., Leung, W. N., *et al.* TAK1 inhibition attenuates both inflammation and fibrosis in experimental pneumoconiosis. *Cell Discov.* **3,** 1–21 (2017).
231. Zietz, B. P. & Dunkelberg, H. The history of the plague and the research on the causative agent Yersinia pestis. *Int. J. Hyg. Environ. Health* **207,** 165–78 (2004).
232. Yang, R. Plague: Recognition, Treatment, and Prevention. *J. Clin. Microbiol.* **56,** 293–312 (2018).
233. Yue, R. P. H., Lee, H. F. & Wu, C. Y. H. Trade routes and plague transmission in pre-industrial Europe. *Sci. Rep.* **7,** 1–10 (2017).
234. Nikiforov, V. V, Gao, H., Zhou, L. & Anisimov, A. Yersinia pestis: Retrospective and Perspective. **918,** 293–312 (2016).
235. Welch, T. J., Fricke, W. F., McDermott, P. F., White, D. G., Rosso, M. L., Rasko, D. A., Mammel, M. K., Eppinger, M., Rosovitz, M. J., Wagner, D., *et al.* Multiple antimicrobial resistance in plague: An emerging public health risk. *PLoS One* **2,** (2007).
236. Riedel, S. Plague: from natural disease to bioterrorism. *Proc. (Bayl. Univ. Med. Cent).* **18,** 116–24 (2005).
237. Galindo, C. L., Rosenzweig, J. A., Kirtley, M. L. & Chopra, A. K. Pathogenesis of Y. enterocolitica and Y. pseudotuberculosis in Human Yersiniosis. *J. Pathog.* **2011,** 182051 (2011).
238. Vergez, L. M., Land, M. L., Motin, V. L., Brubaker, R. R., Fowler, J., Hinnebusch, J., Marceau, M., Medigue, C., Simonet, M., Souza, B., *et al.* Insights into the evolution of Yersinia pestis through whole-genome comparison with Yersinia pseudotuberculosis. **101,** (2004).
239. Knirel, Y. A. & Anisimov, A. P. Lipopolysaccharide of Yersinia pestis , the Cause of Plague : Structure , Genetics , Biological Properties. **4,** 46–58 (2012).
240. Montminy, S. W., Khan, N., Mcgrath, S., Walkowicz, M. J., Sharp, F., Conlon, J. E., Fukase, K., Kusumoto, S., Sweet, C., Miyake, K., *et al.* Virulence factors of Yersinia pestis are overcome by a strong lipopolysaccharide response. **7,** 1066–1073 (2006).
241. Viboud, G. I. & Bliska, J. B. Yersinia outer proteins: role in modulation of host cell signaling responses and pathogenesis. *Annu. Rev. Microbiol.* **59,** 69–89 (2005).
242. Paquette, N., Conlon, J., Sweet, C., Rus, F., Wilson, L., Pereira, A., Rosadini, C. V, Goutagny, N., Weber, A. N. R., Lane, W. S., *et al.* Serine/threonine acetylation of TGFβ-activated kinase (TAK1) by Yersinia pestis YopJ inhibits innate immune

signaling. *Proc. Natl. Acad. Sci. U. S. A.* **109,** 12710–5 (2012).
243. Monack, D. M., Mecsas, J., Ghori, N. & Falkow, S. Yersinia signals macrophages to undergo apoptosis and YopJ is necessary for this cell death. *Proc. Natl. Acad. Sci.* **94,** 10385–10390 (1997).
244. Philip, N. H., Dillon, C. P., Snyder, A. G., Fitzgerald, P., Wynosky-Dolfi, M. A., Zwack, E. E., Hu, B., Fitzgerald, L., Mauldin, E. A., Copenhaver, A. M., *et al.* Caspase-8 mediates caspase-1 processing and innate immune defense in response to bacterial blockade of NF- B and MAPK signaling. *Proc. Natl. Acad. Sci.* **111,** 7385–90 (2014).
245. Weng, D., Marty-Roix, R., Ganesan, S., Proulx, M. K., Vladimer, G. I., Kaiser, W. J., Mocarski, E. S., Pouliot, K., Chan, F. K.-M., Kelliher, M. a, *et al.* Caspase-8 and RIP kinases regulate bacteria-induced innate immune responses and cell death. *Proc. Natl. Acad. Sci. U. S. A.* **111,** 7391–6 (2014).
246. Peterson, L. W., Philip, N. H., Delaney, A., Dolfi, M. A. W., Asklof, K., Gray, F., Choa, R., Bjanes, E., Buza, E. L., Hu, B., *et al.* RIPK1-dependent apoptosis bypasses pathogen blockade of innate signaling to promote immune defense. 1–17 (2017).
247. Park, J. M. Macrophage Apoptosis by Anthrax Lethal Factor Through p38 MAP Kinase Inhibition. *Science (80-.).* **297,** 2048–2051 (2002).
248. Ali, S. R., Timmer, A. M., Bilgrami, S., Park, E. J., Eckmann, L., Nizet, V. & Karin, M. Article Anthrax Toxin Induces Macrophage Death by p38 MAPK Inhibition but Leads to Inflammasome Activation via ATP Leakage. *Immunity* **35,** 34–44 (2011).
249. Sarhan, J., Liu, B. C., Muendlein, H. I., Weindel, C. G., Smirnova, I., Tang, A. Y., Ilyukha, V., Sorokin, M., Buzdin, A., Fitzgerald, K. A., *et al.* Constitutive interferon signaling maintains critical threshold of MLKL expression to license necroptosis. *Cell Death Differ.* (2018). doi:10.1038/s41418-018-0122-7
250. Cai, Z., Jitkaew, S., Zhao, J., Chiang, H.-C., Choksi, S., Liu, J., Ward, Y., Wu, L. & Liu, Z.-G. Plasma membrane translocation of trimerized MLKL protein is required for TNF-induced necroptosis. *Nat. Cell Biol.* **16,** 55–65 (2013).
251. Rodriguez, D. A., Weinlich, R., Brown, S., Guy, C., Fitzgerald, P., Dillon, C. P., Oberst, A., Quarato, G., Low, J., Cripps, J. G., *et al.* Characterization of RIPK3-mediated phosphorylation of the activation loop of MLKL during necroptosis. *Cell Death Differ.* **23,** 76–88 (2016).
252. Wang, H., Sun, L., Su, L., Rizo, J., Liu, L., Wang, L. F., Wang, F. S. & Wang, X. Mixed Lineage Kinase Domain-like Protein MLKL Causes Necrotic Membrane Disruption upon Phosphorylation by RIP3. *Mol. Cell* **54,** 133–146 (2014).
253. He, S., Liang, Y., Shao, F. & Wang, X. Toll-like receptors activate programmed necrosis in macrophages through a receptor-interacting kinase-3-mediated pathway. *Proc. Natl. Acad. Sci.* **108,** 20054–20059 (2011).
254. Kaiser, W. J., Upton, J. W. & Mocarski, E. S. Receptor-interacting protein homotypic interaction motif-dependent control of NF-kappa B activation via the DNA-dependent activator of IFN regulatory factors. *J. Immunol.* **181,** 6427–34 (2008).
255. Kaiser, W. J., Sridharan, H., Huang, C., Mandal, P., Upton, J. W., Gough, P. J., Sehon, C. A., Marquis, R. W., Bertin, J. & Mocarski, E. S. Toll-like receptor 3-

mediated necrosis via TRIF, RIP3, and MLKL. *J. Biol. Chem.* **288,** 31268–31279 (2013).
256. Sato, S., Sugiyama, M., Yamamoto, M., Watanabe, Y., Kawai, T., Takeda, K. & Akira, S. Toll/IL-1 receptor domain-containing adaptor inducing IFN- (TRIF) associates with TNF receptor-associated factor 6 and TANK-binding kinase 1, and activates two distinct transcription factors, NF-κB and IFN-regulatory factor-3, in the Toll-like receptor si. *J. Immunol.* **171,** 4304–4310 (2003).
257. McComb, S., Cessford, E., Alturki, N. a., Joseph, J., Shutinoski, B., Startek, J. B., Gamero, a. M., Mossman, K. L. & Sad, S. Type-I interferon signaling through ISGF3 complex is required for sustained Rip3 activation and necroptosis in macrophages. *Proc. Natl. Acad. Sci.* **111,** E3206–E3213 (2014).
258. Robinson, N., McComb, S., Mulligan, R., Dudani, R., Krishnan, L. & Sad, S. Type I interferon induces necroptosis in macrophages during infection with Salmonella enterica serovar Typhimurium. *Nat. Immunol.* **13,** 954–962 (2012).
259. Dupuis, S., Jouanguy, E., Al-Hajjar, S., Fieschi, C., Al-Mohsen, I. Z., Al-Jumaah, S., Yang, K., Chapgier, A., Eidenschenk, C., Eid, P., *et al.* Impaired response to interferon-alpha/beta and lethal viral disease in human STAT1 deficiency. *Nat. Genet.* **33,** 388–91 (2003).
260. Ofengeim, D., Ito, Y., Trapp, B., Yuan, J., Ofengeim, D., Ito, Y., Najafov, A., Zhang, Y., Shan, B., Dewitt, J. P., *et al.* Activation of Necroptosis in Multiple Sclerosis. *CellReports* **10,** 1–14 (2015).
261. O'Donnell, J. A., Lehman, J., Roderick, J. E., Martinez-Marin, D., Zelic, M., Doran, C., Hermance, N., Lyle, S., Pasparakis, M., Fitzgerald, K. A., *et al.* Dendritic Cell RIPK1 Maintains Immune Homeostasis by Preventing Inflammation and Autoimmunity. *J. Immunol.* **200,** 737–748 (2018).
262. Legarda, D., Justus, S. J., Ang, R. L., Rikhi, N., Li, W., Moran, T. M., Zhang, J., Mizoguchi, E., Zelic, M., Kelliher, M. A., *et al.* CYLD Proteolysis Protects Macrophages from TNF-Mediated Auto-necroptosis Induced by LPS and Licensed by Type I IFN. *Cell Rep.* **15,** 2449–2461 (2016).
263. Härtlova, A., Erttmann, S. F., Raffi, F. A., Schmalz, A. M., Resch, U., Anugula, S., Lienenklaus, S., Nilsson, L. M., Kröger, A., Nilsson, J. A., *et al.* DNA Damage Primes the Type I Interferon System via the Cytosolic DNA Sensor STING to Promote Anti-Microbial Innate Immunity. *Immunity* **42,** 332–343 (2015).
264. Rongvaux, A., Jackson, R., Harman, C. C. D., Li, T., West, A. P., De Zoete, M. R., Wu, Y., Yordy, B., Lakhani, S. A., Kuan, C. Y., *et al.* Apoptotic caspases prevent the induction of type i interferons by mitochondrial DNA. *Cell* **159,** 1563–1577 (2014).
265. Hasan, M., Koch, J., Rakheja, D., Pattnaik, A. K., Brugarolas, J., Dozmorov, I., Levine, B., Wakeland, E. K., Lee-Kirsch, M. A. & Yan, N. Trex1 regulates lysosomal biogenesis and interferon-independent activation of antiviral genes. *Nat. Immunol.* **14,** 61–71 (2013).
266. Hata, N., Sato, M., Takaoka, a, Asagiri, M., Tanaka, N. & Taniguchi, T. Constitutive IFN-alpha/beta signal for efficient IFN-alpha/beta gene induction by virus. *Biochem. Biophys. Res. Commun.* **285,** 518–525 (2001).
267. Schworer, S. a., Smirnova, I. I., Kurbatova, I., Bagina, U., Churova, M., Fowler, T., Roy, A. L., Degterev, A. & Poltorak, A. Toll-like receptor-mediated down-

regulation of the deubiquitinase cylindromatosis (CYLD) protects macrophages from necroptosis in wild-derived mice. *J. Biol. Chem.* **289,** 14422–14433 (2014).
268. Surpris, G., Chan, J., Thompson, M., Ilyukha, V., Liu, B. C., Atianand, M., Sharma, S., Volkova, T., Smirnova, I., Fitzgerald, K. A., *et al.* Cutting Edge: Novel Tmem173 Allele Reveals Importance of STING N Terminus in Trafficking and Type I IFN Production. *J. Immunol.* **196,** 547–552 (2016).
269. Wu, X.-N., Yang, Z.-H., Wang, X.-K., Zhang, Y., Wan, H., Song, Y., Chen, X., Shao, J. & Han, J. Distinct roles of RIP1-RIP3 hetero- and RIP3-RIP3 homo-interaction in mediating necroptosis. *Cell Death Differ.* 1–12 (2014). doi:10.1038/cdd.2014.77
270. Najjar, M., Saleh, D., Zelic, M., Nogusa, S., Shah, S., Tai, A., Finger, J. N., Polykratis, A., Gough, P. J., Bertin, J., *et al.* RIPK1 and RIPK3 Kinases Promote Cell-Death-Independent Inflammation by Toll-like Receptor 4. *Immunity* 1–14 (2016). doi:10.1016/j.immuni.2016.06.007
271. Chen, W., Wu, J., Li, L., Zhang, Z., Ren, J., Liang, Y., Chen, F., Yang, C., Zhou, Z., Su, S. S., *et al.* Ppm1b negatively regulates necroptosis through dephosphorylating Rip3. *Nat. Cell Biol.* **17,** 434–44 (2015).
272. Petersen, S. L., Chen, T. T., Lawrence, D. A., Marsters, S. A., Gonzalvez, F. & Ashkenazi, A. TRAF2 is a biologically important necroptosis suppressor. 1–12 (2015). doi:10.1038/cdd.2015.35
273. Seo, J., Lee, E.-W., Sung, H., Seong, D., Dondelinger, Y., Shin, J., Jeong, M., Lee, H.-K., Kim, J.-H., Han, S. Y., *et al.* CHIP controls necroptosis through ubiquitylation- and lysosome-dependent degradation of RIPK3. *Nat. Cell Biol.* **18,** (2016).
274. Gong, Y., Guy, C., Olauson, H., Becker, J. U., Yang, M., Fitzgerald, P., Linkermann, A. & Green, D. R. ESCRT-III Acts Downstream of MLKL to Regulate Necroptotic Cell Death and Its Consequences. *Cell* **169,** 286-300.e16 (2017).
275. Berghe, T. Vanden & Kaiser, W. J. RIPK1 prevents aberrant ZBP1-initiated necroptosis. **8,** 1–2 (2017).
276. Newton, K., Wickliffe, K. E., Maltzman, A., Dugger, D. L., Strasser, A., Pham, V. C., Lill, J. R., Roose-Girma, M., Warming, S., Solon, M., *et al.* RIPK1 inhibits ZBP1-driven necroptosis during development. *Nature* **54o,** 1–18 (2016).
277. Kuriakose, T., Ming Man, S., Subbarao Malireddi, R. K., Karki, R., Kesavardhana, S., Place, D. E., Neale, G., Vogel, P. & Kanneganti, T. D. ZBP1/DAI is an innate sensor of influenza virus triggering the NLRP3 inflammasome and programmed cell death pathways. *Sci. Immunol.* **1,** ssg2045 (2016).
278. Takaoka, A., Wang, Z., Choi, M. K., Yanai, H., Negishi, H., Ban, T., Lu, Y., Miyagishi, M., Kodama, T., Ohba, Y., *et al.* LETTERS DAI (DLM-1 / ZBP1) is a cytosolic DNA sensor and an activator of innate immune response. **448,** 501–506 (2007).
279. Pisitkun, P., Deane, J. A., Difilippantonio, M. J., Tarasenko, T., Satterthwaite, A. B. & Bolland, S. Autoreactive B cell responses to RNA-related antigens due to TLR7 gene duplication. *Science* **312,** 1669–72 (2006).
280. White, M. J., McArthur, K., Metcalf, D., Lane, R. M., Cambier, J. C., Herold, M. J., Van Delft, M. F., Bedoui, S., Lessene, G., Ritchie, M. E., *et al.* Apoptotic

caspases suppress mtDNA-induced STING-mediated type i IFN production. *Cell* **159,** 1549–1562 (2014).
281. West, A. P., Khoury-Hanold, W., Staron, M., Tal, M. C., Pineda, C. M., Lang, S. M., Bestwick, M., Duguay, B. A., Raimundo, N., MacDuff, D. A., *et al.* Mitochondrial DNA stress primes the antiviral innate immune response. *Nature* **520,** 553–7 (2015).
282. Magna, M. & Pisetsky, D. S. The Role of Cell Death in the Pathogenesis of SLE: Is Pyroptosis the Missing Link? *Scand. J. Immunol.* **82,** 218–224 (2015).
283. Lau, A., Wang, S., Jiang, J., Haig, A., Pavlosky, A., Linkermann, A., Zhang, Z.-X. & Jevnikar, A. M. RIPK3-Mediated Necroptosis Promotes Donor Kidney Inflammatory Injury and Reduces Allograft Survival. *Am. J. Transplant.* **13,** 2805–2818 (2013).
284. Contreras, G., Mattiazzi, A., Guerra, G., Ortega, L. M., Tozman, E. C., Li, H., Tamariz, L., Carvalho, C., Kupin, W., Ladino, M., *et al.* Recurrence of lupus nephritis after kidney transplantation. *J. Am. Soc. Nephrol.* **21,** 1200–1207 (2010).
285. Lionaki, S. Kidney transplantation in patients with systemic lupus erythematosus. *World J. Transplant.* **4,** 176 (2014).
286. Case, C. L., Kohler, L. J., Lima, J. B., Strowig, T., de Zoete, M. R., Flavell, R. A., Zamboni, D. S. & Roy, C. R. Caspase-11 stimulates rapid flagellin-independent pyroptosis in response to Legionella pneumophila. *Proc. Natl. Acad. Sci. U. S. A.* **110,** 1851–1856 (2013).
287. Dillon, C. P., Weinlich, R., Rodriguez, D. A., Cripps, J. G., Quarato, G., Gurung, P., Verbist, K. C., Brewer, T. L., Llambi, F., Gong, Y. N., *et al.* RIPK1 blocks early postnatal lethality mediated by caspase-8 and RIPK3. *Cell* **157,** 1189–1202 (2014).
288. Murphy, J. M., Czabotar, P. E., Hildebrand, J. M., Lucet, I. S., Zhang, J.-G., Alvarez-Diaz, S., Lewis, R., Lalaoui, N., Metcalf, D., Webb, A. I., *et al.* The pseudokinase MLKL mediates necroptosis via a molecular switch mechanism. *Immunity* **39,** 443–53 (2013).
289. Ishii, K. J., Kawagoe, T., Koyama, S., Matsui, K., Kumar, H., Kawai, T., Uematsu, S., Takeuchi, O., Takeshita, F., Coban, C., *et al.* TANK-binding kinase-1 delineates innate and adaptive immune responses to DNA vaccines. **451,** 725–730 (2008).
290. Moriwaki, K., Balaji, S., Bertin, J., Gough, P. J. & Chan, F. K. Distinct Kinase-Independent Role of RIPK3 in CD11c(+) Mononuclear Phagocytes in Cytokine-Induced Tissue Repair. *Cell Rep.* **18,** 2441–2451 (2017).
291. Lehtonen, A., Ahlfors, H., Veckman, V., Miettinen, M., Lahesmaa, R. & Julkunen, I. Gene expression profiling during differentiation of human monocytes to macrophages or dendritic cells. *J. Leukoc. Biol.* **82,** 710–20 (2007).
292. Thomas, K. E., Galligan, C. L., Newman, R. D., Fish, E. N. & Vogel, S. N. Contribution of interferon-β to the murine macrophage response to the toll-like receptor 4 agonist, lipopolysaccharide. *J. Biol. Chem.* **281,** 31119–31130 (2006).
293. Sarhan, J., Liu, B. C., Muendlein, H. I., Li, P., Nilson, R., Tang, A. Y., Rongvaux, A., Bunnell, S. C., Shao, F., Green, D. R., *et al.* Caspase-8 induces cleavage of gasdermin D to elicit pyroptosis during Yersinia infection. *Proc. Natl. Acad. Sci. U. S. A.* **115,** E10888–E10897 (2018).

294. Takeuchi, O. & Akira, S. Pattern recognition receptors and inflammation. *Cell* **140,** 805–20 (2010).
295. Reddick, L. E. & Alto, N. M. Bacteria fighting back: How pathogens target and subvert the host innate immune system. *Mol. Cell* **54,** 321–328 (2014).
296. Krachler, A. M., Woolery, A. R. & Orth, K. Manipulation of kinase signaling by bacterial pathogens. *J. Cell Biol.* **195,** 1083–1092 (2011).
297. Park, J. M., Greten, F. R., Wong, A., Westrick, R. J., Arthur, J. S. C., Otsu, K., Hoffmann, A., Montminy, M. & Karin, M. Signaling pathways and genes that inhibit pathogen-induced macrophage apoptosis - CREB and NF-κB as key regulators. *Immunity* **23,** 319–329 (2005).
298. Feltham, R., Vince, J. E. & Lawlor, K. E. Caspase-8: not so silently deadly. *Clin. Transl. Immunol.* **6,** e124 (2017).
299. Omori, E., Inagaki, M., Mishina, Y., Matsumoto, K. & Ninomiya-Tsuji, J. Epithelial transforming growth factor -activated kinase 1 (TAK1) is activated through two independent mechanisms and regulates reactive oxygen species. *Proc. Natl. Acad. Sci.* **109,** 3365–3370 (2012).
300. Rajput, A., Kovalenko, A., Bogdanov, K., Yang, S.-H., Kang, T.-B., Kim, J.-C., Du, J. & Wallach, D. RIG-I RNA helicase activation of IRF3 transcription factor is negatively regulated by caspase-8-mediated cleavage of the RIP1 protein. *Immunity* **34,** 340–51 (2011).
301. Ratner, D., Orning, M. P. A., Starheim, K. K., Marty-Roix, R., Proulx, M. K., Goguen, J. D. & Lien, E. Manipulation of Interleukin-1β and Interleukin-18 Production by Yersinia pestis Effectors YopJ and YopM and Redundant Impact on Virulence. *J. Biol. Chem.* **291,** 9894–905 (2016).
302. Sutterwala, F. S., Haasken, S. & Cassel, S. L. Mechanism of NLRP3 inflammasome activation. *Ann. N. Y. Acad. Sci.* **1319,** 82–95 (2014).
303. Lawlor, K. E. & Vince, J. E. Ambiguities in NLRP3 inflammasome regulation: Is there a role for mitochondria? *Biochim. Biophys. Acta - Gen. Subj.* **1840,** 1433–1440 (2014).
304. Kroemer, G., Galluzzi, L., Vandenabeele, P., Abrams, J., Alnemri, E. S., Baehrecke, E. H., Blagosklonny, M. V, El-Deiry, W. S., Golstein, P., Green, D. R., *et al.* Classification of cell death: recommendations of the Nomenclature Committee on Cell Death 2009. *Cell Death Differ.* **16,** 3–11 (2009).
305. Aglietti, R. A., Estevez, A., Gupta, A., Ramirez, M. G., Liu, P. S., Kayagaki, N., Ciferri, C., Dixit, V. M. & Dueber, E. C. GsdmD p30 elicited by caspase-11 during pyroptosis forms pores in membranes. *Proc. Natl. Acad. Sci. U. S. A.* **113,** 7858–63 (2016).
306. Xie, T., Peng, W., Liu, Y., Yan, C., Maki, J., Degterev, A., Yuan, J. & Shi, Y. Structural basis of RIP1 inhibition by necrostatins. *Structure* **21,** 493–499 (2013).
307. Degterev, A., Hitomi, J., Germscheid, M., Ch'en, I. L., Korkina, O., Teng, X., Abbott, D., Cuny, G. D., Yuan, C., Wagner, G., *et al.* Identification of RIP1 kinase as a specific cellular target of necrostatins. *Nat. Chem. Biol.* **4,** 313–321 (2008).
308. Cho, Y. S., Challa, S., Moquin, D., Genga, R., Ray, T. D., Guildford, M. & Chan, F. K. M. Phosphorylation-Driven Assembly of the RIP1-RIP3 Complex Regulates Programmed Necrosis and Virus-Induced Inflammation. *Cell* **137,** 1112–1123 (2009).

309. Tenev, T., Bianchi, K., Darding, M., Broemer, M., Langlais, C., Wallberg, F., Zachariou, A., Lopez, J., MacFarlane, M., Cain, K., *et al.* The Ripoptosome, a Signaling Platform that Assembles in Response to Genotoxic Stress and Loss of IAPs. *Mol. Cell* **43,** 432–448 (2011).
310. Micheau, O. & Tschopp, J. Induction of TNF receptor I-mediated apoptosis via two sequential signaling complexes. *Cell* **114,** 181–190 (2003).
311. Taylor, R. C., Cullen, S. P. & Martin, S. J. Apoptosis: controlled demolition at the cellular level. *Nat. Rev. Mol. Cell Biol.* **9,** 231–241 (2008).
312. Palchaudhuri, R., Lambrecht, M. J., Botham, R. C., Partlow, K. C., van Ham, T. J., Putt, K. S., Nguyen, L. T., Kim, S. H., Peterson, R. T., Fan, T. M., *et al.* A Small Molecule that Induces Intrinsic Pathway Apoptosis with Unparalleled Speed. *Cell Rep.* **13,** 2027–2036 (2015).
313. Hande, K. R. Etoposide: Four decades of development of a topoisomerase II inhibitor. *Eur. J. Cancer* **34,** 1514–1521 (1998).
314. Sborgi, L., Rühl, S., Mulvihill, E., Pipercevic, J., Heilig, R., Stahlberg, H., Farady, C. J., Müller, D. J., Broz, P. & Hiller, S. GSDMD membrane pore formation constitutes the mechanism of pyroptotic cell death. *EMBO J.* **35,** 1766–78 (2016).
315. Taabazuing, C. Y., Okondo, M. C. & Bachovchin, D. A. Pyroptosis and Apoptosis Pathways Engage in Bidirectional Crosstalk in Monocytes and Macrophages. *Cell Chem. Biol.* **24,** 507-514.e4 (2017).
316. Wang, J., Wu, D., Huang, D. & Lin, W. TAK1 inhibition-induced RIP1-dependent apoptosis in murine macrophages relies on constitutive TNF-α signaling and ROS production. *J. Biomed. Sci.* **22,** 1–13 (2015).
317. Chen, M., Guerrero, A. D., Huang, L., Shabier, Z., Pan, M., Tan, T. H. & Wang, J. Caspase-9-induced mitochondrial disruption through cleavage of anti-apoptotic BCL-2 family members. *J. Biol. Chem.* **282,** 33888–33895 (2007).
318. Wallach, D., Kang, T.-B., Dillon, C. P. & Green, D. R. Programmed necrosis in inflammation: Toward identification of the effector molecules. *Science* **352,** aaf2154 (2016).
319. Peterson, L. W., Philip, N. H., Dillon, C. P., Bertin, J., Gough, P. J., Green, D. R. & Brodsky, I. E. Cell-Extrinsic TNF Collaborates with TRIF Signaling To Promote *Yersinia* -Induced Apoptosis. *J. Immunol.* **197,** 4110–4117 (2016).
320. Eddy, J. L., Gielda, L. M., Caulfield, A. J., Rangel, S. M. & Lathem, W. W. Production of outer membrane vesicles by the plague pathogen Yersinia pestis. *PLoS One* **9,** 1–11 (2014).
321. Cecil, J. D., O'Brien-Simpson, N. M., Lenzo, J. C., Holden, J. A., Singleton, W., Perez-Gonzalez, A., Mansell, A. & Reynolds, E. C. Outer membrane vesicles prime and activate macrophage inflammasomes and cytokine secretion in vitro and in vivo. *Front. Immunol.* **8,** 1–22 (2017).
322. Jung, A. L., Herkt, C. E., Schulz, C., Bolte, K., Seidel, K., Scheller, N., Sittka-Stark, A., Bertrams, W. & Schmeck, B. Legionella pneumophila infection activates bystander cells differentially by bacterial and host cell vesicles. *Sci. Rep.* **7,** 6301 (2017).
323. Franklin, B. S., Bossaller, L., De Nardo, D., Ratter, J. M., Stutz, A., Engels, G., Brenker, C., Nordhoff, M., Mirandola, S. R., Al-Amoudi, A., *et al.* The adaptor ASC has extracellular and 'prionoid' activities that propagate inflammation. *Nat.*

Immunol. **15,** 727–37 (2014).
324. Baroja-Mazo, A., Martín-Sánchez, F., Gomez, A. I., Martínez, C. M., Amores-Iniesta, J., Compan, V., Barberà-Cremades, M., Yagüe, J., Ruiz-Ortiz, E., Antón, J., *et al.* The NLRP3 inflammasome is released as a particulate danger signal that amplifies the inflammatory response. *Nat. Immunol.* **15 VN-r,** 738–748 (2014).
325. Zanoni, I., Tan, Y., Gioia, M. Di, Broggi, A., Ruan, J., Shi, J., Donado, C. A., Shao, F., Wu, H., Springstead, J. R., *et al.* An endogenous caspase-11 ligand elicits interleukin-1 release from living dendritic cells. *Science (80-.).* **3036,** 1–9 (2016).
326. Zanoni, I., Tan, Y., Di Gioia, M., Springstead, J. R. & Kagan, J. C. By Capturing Inflammatory Lipids Released from Dying Cells, the Receptor CD14 Induces Inflammasome-Dependent Phagocyte Hyperactivation. *Immunity* **47,** 697–709 (2017).
327. Jorgensen, I., Zhang, Y., Krantz, B. A. & Miao, E. A. Pyroptosis triggers pore-induced intracellular traps (PITs) that capture bacteria and lead to their clearance by efferocytosis. *J. Exp. Med.* **213,** 2113–2128 (2016).
328. Case, C. L., Shin, S. & Roy, C. R. Asc and Ipaf Inflammasomes direct distinct pathways for caspase-1 activation in response to Legionella pneumophila. *Infect. Immun.* **77,** 1981–91 (2009).
329. Shenoy, A. R., Wellington, D. A., Kumar, P., Kassa, H., Booth, C. J., Cresswell, P. & MacMicking, J. D. GBP5 promotes NLRP3 inflammasome assembly and immunity in mammals. *Science (80-.).* **336,** 481–485 (2012).
330. Man, S. M., Karki, R., Sasai, M., Place, D. E., Kesavardhana, S., Temirov, J., Frase, S., Zhu, Q., Malireddi, R. K. S., Kuriakose, T., *et al.* IRGB10 Liberates Bacterial Ligands for Sensing by the AIM2 and Caspase-11-NLRP3 Inflammasomes. *Cell* 1–15 (2016). doi:10.1016/j.cell.2016.09.012
331. Meunier, E., Wallet, P., Dreier, R. F., Costanzo, S., Anton, L., Rühl, S., Dussurgey, S., Dick, M. S., Kistner, A., Rigard, M., *et al.* Guanylate-binding proteins promote activation of the AIM2 inflammasome during infection with Francisella novicida. *Nat. Immunol.* **16,** 476–84 (2015).
332. Miao, E. a, Leaf, I. a, Treuting, P. M., Mao, D. P., Dors, M., Sarkar, A., Warren, S. E., Wewers, M. D. & Aderem, A. Caspase-1-induced pyroptosis is an innate immune effector mechanism against intracellular bacteria. *Nat. Immunol.* **11,** 1136–42 (2010).
333. Peterson, L. W., Philip, N. H., Dillon, C. P., Bertin, J., Gough, P. J., Green, D. R. & Brodsky, I. E. Cell-Extrinsic TNF Collaborates with TRIF Signaling To Promote *Yersinia* -Induced Apoptosis. *J. Immunol.* **197,** 4110–4117 (2016).
334. Martin, C. J., Peters, K. N. & Behar, S. M. Macrophages clean up: Efferocytosis and microbial control. *Curr. Opin. Microbiol.* **17,** 17–23 (2014).
335. Kolb, J. P., Oguin, T. H., Oberst, A. & Martinez, J. Programmed Cell Death and Inflammation: Winter Is Coming. *Trends Immunol.* **38,** 705–718 (2017).
336. Golenbock, D. T., Hampton, R. Y., Qureshi, N., Takayama, K. & Raetz, C. R. H. Lipid A-like Molecules That Antagonize the Effects of Endotoxins on Human Monocytes. *J. Biol. Chem.* **266,** 19490–19496 (1991).
337. Upton, J. W., Kaiser, W. J. & Mocarski, E. S. DAI/ZBP1/DLM-1 complexes with RIP3 to mediate virus-induced programmed necrosis that is targeted by murine cytomegalovirus vIRA. *Cell Host Microbe* **11,** 290–297 (2012).

338. Vanlangenakker, N., Vanden Berghe, T., Bogaert, P., Laukens, B., Zobel, K., Deshayes, K., Vucic, D., Fulda, S., Vandenabeele, P. & Bertrand, M. J. M. cIAP1 and TAK1 protect cells from TNF-induced necrosis by preventing RIP1/RIP3-dependent reactive oxygen species production. *Cell Death Differ.* **18,** 656–665 (2010).
339. Newton, K., Sun, X. & Dixit, V. M. Kinase RIP3 is dispensable for normal NF-kappa Bs, signaling by the B-cell and T-cell receptors, tumor necrosis factor receptor 1, and Toll-like receptors 2 and 4. *Mol. Cell. Biol.* **24,** 1464–1469 (2004).
340. Berger, S. B., Kasparcova, V., Hoffman, S., Swift, B., Dare, L., Schaeffer, M., Capriotti, C., Cook, M., Finger, J., Hughes-Earle, A., *et al.* Cutting Edge: RIP1 Kinase Activity Is Dispensable for Normal Development but Is a Key Regulator of Inflammation in SHARPIN-Deficient Mice. *J. Immunol.* **192,** 5476–5480 (2014).
341. Mandal, P., Berger, S. B., Pillay, S., Moriwaki, K., Huang, C., Guo, H., Lich, J. D., Finger, J., Kasparcova, V., Votta, B., *et al.* RIP3 Induces Apoptosis Independent of Pronecrotic Kinase Activity. *Mol. Cell* **56,** 481–495 (2014).
342. Auerbuch, V., Golenbock, D. T. & Isberg, R. R. Innate immune recognition of Yersinia pseudotuberculosis type III secretion. *PLoS Pathog.* **5,** (2009).
343. Jaguin, M., Houlbert, N., Fardel, O. & Lecureur, V. Polarization profiles of human M-CSF-generated macrophages and comparison of M1-markers in classically activated macrophages from GM-CSF and M-CSF origin. *Cell. Immunol.* **281,** 51–61 (2013).
344. Davies, J. Q. & Gordon, S. in *Basic Cell Culture Protocols* (eds. Helgason, C. D. & Miller, C. L.) **290,** 105–116 (Humana Press, 2005).
345. Logue, S. E., Elgendy, M. & Martin, S. J. Expression, purification and use of recombinant annexin V for the detection of apoptotic cells. *Nat. Protoc.* **4,** 1383–1395 (2009).
346. Brumatti, G., Sheridan, C. & Martin, S. J. Expression and purification of recombinant annexin V for the detection of membrane alterations on apoptotic cells. *Methods* **44,** 235–240 (2008).
347. Sadler, A. J. & Williams, B. R. G. Interferon-inducible antiviral effectors. *Nat. Rev. Immunol.* **8,** 559–568 (2008).
348. Sergeev, Y. V., Dolinska, M. B. & Wingfield, P. T. in *Current Protocols in Protein Science* **43,** 20.13.1-20.13.15 (John Wiley & Sons, Inc., 2014).
349. Quarato, G., Guy, C. S., Grace, C. R., Llambi, F., Nourse, A., Rodriguez, D. A., Wakefield, R., Frase, S., Moldoveanu, T. & Green, D. R. Sequential Engagement of Distinct MLKL Phosphatidylinositol-Binding Sites Executes Necroptosis. *Mol. Cell* **61,** 589–601 (2016).
350. Hildebrand, J. M., Tanzer, M. C., Lucet, I. S., Young, S. N., Spall, S. K., Sharma, P., Pierotti, C., Garnier, J.-M., Dobson, R. C. J., Webb, A. I., *et al.* Activation of the pseudokinase MLKL unleashes the four-helix bundle domain to induce membrane localization and necroptotic cell death. *Proc. Natl. Acad. Sci.* **111,** 15072–15077 (2014).
351. Tanzer, M. C., Matti, I., Hildebrand, J. M., Young, S. N., Wardak, A., Tripaydonis, A., Petrie, E. J., Mildenhall, A. L., Vaux, D. L., Vince, J. E., *et al.* Evolutionary divergence of the necroptosis effector MLKL. *Cell Death Differ.* **23,** 1185–1197 (2016).

352. Chen, X., Li, W., Ren, J., Huang, D., He, W.-T., Song, Y., Yang, C., Li, W., Zheng, X., Chen, P., *et al.* Translocation of mixed lineage kinase domain-like protein to plasma membrane leads to necrotic cell death. *Cell Res.* **24,** 105–21 (2014).
353. Dondelinger, Y., Declercq, W., Montessuit, S., Roelandt, R., Goncalves, A., Bruggeman, I., Hulpiau, P., Weber, K., Sehon, C. A., Marquis, R. W., *et al.* MLKL Compromises Plasma Membrane Integrity by Binding to Phosphatidylinositol Phosphates. *Cell Rep.* **7,** 971–981 (2014).
354. Hildebrand, J. M., Tanzer, M. C., Lucet, I. S., Young, S. N., Spall, S. K., Sharma, P., Pierotti, C., Garnier, J.-M., Dobson, R. C. J., Webb, a. I., *et al.* Activation of the pseudokinase MLKL unleashes the four-helix bundle domain to induce membrane localization and necroptotic cell death. *Proc. Natl. Acad. Sci.* **111,** 15072–15077 (2014).
355. Tanzer, M. C., Tripaydonis, A., Webb, A. I., Young, S. N., Varghese, L. N., Hall, C., Alexander, W. S., Hildebrand, J. M., Silke, J. & Murphy, J. M. Necroptosis signalling is tuned by phosphorylation of MLKL residues outside the pseudokinase domain activation loop. *Biochem. J.* **471,** 255–265 (2015).
356. Aldridge, B. B., Gaudet, S., Lauffenburger, D. a & Sorger, P. K. Lyapunov exponents and phase diagrams reveal multi-factorial control over TRAIL-induced apoptosis. *Mol. Syst. Biol.* **7,** 1–21 (2011).
357. Flusberg, D. A. & Sorger, P. K. Surviving apoptosis: Life-death signaling in single cells. *Trends Cell Biol.* **25,** 446–458 (2015).
358. Reynoso, E., Liu, H., Li, L., Yuan, A. L., Chen, S. & Wang, Z. Thioredoxin-1 actively maintains the pseudokinase MLKL in a reduced state to suppress disulfide bond-dependent MLKL polymer formation and necroptosis. *J. Biol. Chem.* jbc.M117.799353 (2017). doi:10.1074/jbc.M117.799353
359. Parnas, O., Jovanovic, M., Eisenhaure, T. M., Herbst, R. H., Dixit, A., Ye, C. J., Przybylski, D., Platt, R. J., Tirosh, I., Sanjana, N. E., *et al.* A Genome-wide CRISPR Screen in Primary Immune Cells to Dissect Regulatory Networks. *Cell* **162,** 1–12 (2015).
360. Jaitin, D. A., Weiner, A., Yofe, I., Lara-Astiaso, D., Keren-Shaul, H., David, E., Salame, T. M., Tanay, A., van Oudenaarden, A. & Amit, I. Dissecting Immune Circuits by Linking CRISPR-Pooled Screens with Single-Cell RNA-Seq. *Cell* **167,** 1883-1896.e15 (2016).
361. Chu, V. T., Graf, R., Wirtz, T., Weber, T., Favret, J., Li, X., Petsch, K., Tran, N. T., Sieweke, M. H., Berek, C., *et al.* Efficient CRISPR-mediated mutagenesis in primary immune cells using CrispRGold and a C57BL/6 Cas9 transgenic mouse line. *Proc. Natl. Acad. Sci.* **113,** 12514–12519 (2016).
362. Martinez, J., Huang, X. & Yang, Y. Toll-like receptor 8-mediated activation of murine plasmacytoid dendritic cells by vaccinia viral DNA. *Proc. Natl. Acad. Sci. U. S. A.* **107,** 6442–6447 (2010).
363. Madisen, L., Zwingman, T. A., Sunkin, S. M., Oh, S. W., Zariwala, H. A., Gu, H., Ng, L. L., Palmiter, R. D., Hawrylycz, M. J., Jones, A. R., *et al.* A robust and high-throughput Cre reporting and characterization system for the whole mouse brain. *Nat. Neurosci.* **13,** 133–40 (2010).
364. Scheu, S., Dresing, P. & Locksley, R. M. Visualization of IFNbeta production by

plasmacytoid versus conventional dendritic cells under specific stimulation conditions in vivo. *Proc. Natl. Acad. Sci. U. S. A.* **105,** 20416–21 (2008).
365. Lienenklaus, S., Cornitescu, M., Zietara, N., Łyszkiewicz, M., Gekara, N., Jabłónska, J., Edenhofer, F., Rajewsky, K., Bruder, D., Hafner, M., *et al.* Novel reporter mouse reveals constitutive and inflammatory expression of IFN-beta in vivo. *J. Immunol.* **183,** 3229–36 (2009).
366. Liu, J., Mcclary, B., Zinshteyn, B., Meyer, M., Jouanneau, M., Pellegrino, S., Yusupova, G., Schuller, A., Reyes, J., Lu, J., *et al.* EDHS-206, an exquisitely selective inhibitor of TAK1, targets pro survival TNFα- dependent signaling, inducing apoptosis in rheumatoid arthritis and breast cancer models. *Cell Chem. Biol. (under Rev.*
367. Madrigal, A. G., Barth, K., Papadopoulos, G. & Genco, C. A. Pathogen-mediated proteolysis of the cell death regulator RIPK1 and the host defense modulator RIPK2 in human aortic endothelial cells. *PLoS Pathog.* **8,** (2012).
368. Barth, K. & Genco, C. A. Microbial Degradation of Cellular Kinases Impairs Innate Immune Signaling and Paracrine TNFα Responses. *Sci. Rep.* **6,** 34656 (2016).
369. Park, J. M., Greten, F. R., Wong, A., Westrick, R. J., Arthur, J. S. C., Otsu, K., Hoffmann, A., Montminy, M. & Karin, M. Signaling pathways and genes that inhibit pathogen-induced macrophage apoptosis--CREB and NF-kappaB as key regulators. *Immunity* **23,** 319–29 (2005).
370. Hsu, L.-C., Park, J. M., Zhang, K., Luo, J.-L., Maeda, S., Kaufman, R. J., Eckmann, L., Guiney, D. G. & Karin, M. The protein kinase PKR is required for macrophage apoptosis after activation of Toll-like receptor 4. *Nature* **428,** 341–5 (2004).
371. Larkin, B., Ilyukha, V., Sorokin, M., Buzdin, A., Vannier, E. & Poltorak, A. Cutting Edge: Activation of STING in T Cells Induces Type I IFN Responses and Cell Death. *J. Immunol.* **199,** 397–402 (2017).